STUDY OF DIFFERENT ATMOSPHERIC ENVIRONMENTS ASSOCIATED TO STORMS DEVELOPMENT IN THE MADEIRA ISLAND

Flavio Tiago do Couto

ORIENTADORES: *Rui Paulo Vasco Salgado*
Maria João Tavares da Costa
Véronique Ducrocq

ÉVORA, JULHO 2016

INSTITUTO DE INVESTIGAÇÃO E FORMAÇÃO AVANÇADA

To my parents

SUMMARY

The study aims to improve the understanding about different atmospheric environments leading to the development of storms associated with heavy precipitation in Madeira Island. For this purpose, four main goals have been considered: 1) To document the synoptic and mesoscale environments associated with heavy precipitation. 2) To characterize surface precipitation patterns that affected the island during some periods of significant accumulated precipitation using numerical modelling. 3) To study the relationship between surface precipitation patterns and mesoscale environments. 4) To highlight how the PhD findings obtained in the first three goals can be translated into an operational forecast context. Concerning the large scale environment, precipitation over the island was favoured by weather systems (e.g, mesoscale convective systems and low pressure systems), as well as by the meridional transport of high amount of moisture from a structure denominated as "Atmospheric River". The tropical origin of this moisture is underscored, however, their impact on the precipitation in Madeira was not so high during the 10 winter seasons [2002 – 2012] studied. The main factor triggering heavy precipitation events over the island is related to the local orography. The steep terrain favours orographically-induced stationary precipitation over the highlands, although maximum of precipitation at coastal region may be produced by localized blocking effect. These orographic precipitating systems presented different structures, associated with shallow and deep convection. Essentially, the study shows that the combination of airflow dynamics, moist content, and orography is the major mechanism that produces precipitation over the island. These factors together with the event duration act to define the regions of excessive precipitation. Finally, the study highlights two useful points for the operational sector, regarding the meridional water vapour transport and local effects causing significant precipitation over the island.

RESUMO

Estudo de diferentes ambientes atmosféricos associados ao desenvolvimento de tempestades na ilha da Madeira

O estudo procura melhorar o entendimento sobre os diferentes ambientes atmosféricos que favorecem o desenvolvimento de tempestades associadas com precipitação intensa na ilha da Madeira. Nesse sentido foram definidos quatro objetivos: 1) Documentar os ambientes sinópticos e de mesoescala associados com precipitação intensa; 2) Caracterizar padrões de precipitação na superfície, em eventos de elevada precipitação acumulada, utilizando modelação numérica; 3) Estudar as relações entre os padrões de precipitação e ambientes de mesoescala; 4) Mostrar como tais resultados podem ser utilizados num contexto operacional de previsão do tempo. Em relação a ambientes de larga escala, verificou-se que a ocorrência de eventos de precipitação intensa sobre a ilha foi favorecida por sistemas meteorológicos, assim como pelo transporte meridional de humidade por meio de estruturas atualmente denominadas Rios atmosféricos. Neste último caso é de destacar a origem tropical de humidade, no entanto, o seu impacto na precipitação sobre a Madeira durante os 10 invernos estudados [2002-2012] não foi tão elevada. O principal fator que favorece os eventos de precipitação intensa está relacionado com a orografia local. O terreno complexo da ilha favorece a ocorrência de precipitação estacionária induzida orograficamente sobre as terras mais altas, embora a precipitação nas zonas costeiras possa ser produzida por um efeito localizado de bloqueio. Estes sistemas orográficos precipitantes apresentaram diferentes estruturas, associados a convecção pouco profunda e profunda. O estudo mostra que a combinação entre as características do escoamento, a quantidade de humidade, e a orografia são os condimentos essenciais para o desenvolvimento da precipitação sobre a ilha, atuando de maneira a definir as regiões de precipitação excessiva. Por fim, o estudo destaca dois pontos que podem ser úteis na previsão do tempo operacional, ligados a larga escala e aos efeitos locais, os quais podem levar ao desenvolvimento de tempestades e precipitação intensa sobre a ilha.

ACKNOWLEDGEMENTS

CONTENTS

LIST OF PAPERS

This thesis includes the following articles:

Couto FT, Salgado R, Costa MJ, Prior V. 2015. Precipitation in the Madeira Island over a 10-year period and the meridional water vapour transport during the winter seasons. *International Journal of Climatology*. **35**: 3748-3759. DOI: 10.1002/joc.4243.

Couto FT, Ducrocq V, Salgado R, Costa MJ. 2016. Numerical simulations of significant orographic precipitation in Madeira Island. *Atmospheric Research*. **169**: 102-112. DOI: 10.1016/j.atmosres.2015.10.002.

Couto FT, Ducrocq V, Salgado R, Costa MJ. Understanding significant precipitation in Madeira island using high-resolution numerical simulations of real cases. *Submitted to Quarterly Journal of the Royal Meteorological Society*.

x

LIST OF FIGURES

LIST OF TABLES

CHAPTER 1 – INTRODUCTION

1.1 STATE OF THE ART

The huge impact of heavy precipitation events (HPE) is observed worldwide and depends, in large part, on factors linked to the surface and atmospheric conditions. The latter is related to weather and climate dynamic. On a regional as well as on a global scale, these events have an important role in the hydrological cycle and water resources.

The physical processes occurring in the atmosphere are observed and documented since the ancients, from the Greeks and Romans, but they have been better understood after the middle age (Strangeways, 2006). The rapid improvement of the measurement techniques and modelling capacities, specifically during the last two decades, brought a significant improvement in the knowledge about these processes in the atmosphere, as well as its behaviour. In parallel to the advancement of the technologies, the economic growth, rapid urbanization, and thus increase of the population density, many regions around the world became more vulnerable to HPE occurrences. In addition, the widespread improper planning, allowing constructions over water courses make some areas more susceptible to disasters.

The HPE are generally associated with thunderstorms occurring in a short period, however, they may persist for a long period. Both situations can lead to flash floods or floods with several damages and casualties. Storms, or thunderstorms, can produce different hazards (e.g., strong winds, hail, and lightning), but only heavy precipitation with potential for flash floods have been considered in this work. Although the general environments causing heavy precipitation are well documented for different regions, the increase of the knowledge on specific regions is still needed, for example, over small mountainous regions. Overall, the initiation and development of HPE over complex terrain remains a challenging problem worldwide.

In the last years, the Madeira Island showed to be an unexplored place in the matter of HPE. The attentions were directed to the island after a disaster induced by a HPE, and several studies were developed to explain the event. The study of Couto et al. (2012), highlighted the main atmospheric conditions of HPE in Madeira during the 2009/2010 winter, however, some questions kept without an answer when considered from a general point of view.

Over the island, the surface precipitation is observed with a network of few surface rain gauges (considering the very complex orography), which have difficulties to capture the high spatial variability of the precipitation associated with thunderstorms. The island is not covered by weather radar, and thus the studies of precipitating systems in the region should rely in techniques, such as remote sensing from satellite observations and numerical modelling. The latter, requires a configuration with very high-resolution in order to obtain more realistic results, in view of the fact that the Madeira has a very steep orography.

The Madeira Archipelago is located in the Macaronesian region, which is formed by other volcanic archipelagos in the North Atlantic Ocean. The archipelago is a group of Portuguese islands and formed by two main inhabited islands, Madeira and Porto Santo. To the south-east, the Archipelago continues along the Desertas and Selvagens, both composed of three islands.

Madeira (32°75'N and 17°00'W) is the largest island of the archipelago with approximately 740 km² and 250 thousand inhabitants. The island is completely formed by volcanic materials and consists of an enormous east-west oriented barrier with a very complex relief cut by deep valleys (e.g., Prada and Silva, 2001). The central mountain chain presents regions above of 1400 m (Paúl da Serra region) to westward, and the highest peaks to eastward (Pico do Areeiro and Pico Ruivo, both above of 1800 m). These geographical aspects contribute to the great variety of micro-climates in Madeira, with mild summer and winter, except for the elevated regions where the lowest temperatures are observed (e.g., Borges et al., 2008).

The mountainous terrain favours the development of orographic fogs in Madeira's highlands throughout the year, inducing dense vegetation as well. This natural vegetation is essential for the groundwater recharge, which is dependent on precipitation and cloud water interception, and have been extensively studied in the last years (Prada et al., 2005, 2009, 2012). Additionally, Prada et al. (2015) showed the important role of the cloud water interception as groundwater resource, and pointed out the necessity for conservation of the local vegetation. Although these areas are currently maintained, new strategies for improving its preservation are still in discussion (Fernandes et al., 2015).

Using historical data, Baioni (2011) found that flash floods followed by landslide events are the natural hazards with greater impact and causing the worst damages. Most

of these events take place in the period from November to April, when almost all annual rainfall occurs in Madeira. In addition, this author's findings suggested that there is a relationship between landslide occurrences and the human activities over the island. This point is highlighted since Madeira became an important tourist destination and the development of tourist infrastructures modified the landscapes in some regions, in addition to the increase of agriculture.

There are two disastrous floods marking the Madeira history. The first dramatic event was on October 1803. According to the description of the disaster published by John Driver in 1838, the event was preceded by several months without precipitation. The torrential rain began in the evening and swept away bridges and several houses, leading to an estimate of above 300 deaths (Driver, 1838). The second natural disaster episode showed the vulnerability of the island to extreme precipitation events. The disaster on 20 February 2010 was marked by a huge economic damage, estimated in millions of Euros, and more than 40 deaths. The catastrophe raised several questions about the occurrence of events with such socio-economic impact. The episode altered the island's landscape and, in order to improve the capacity to adapt to changes, some projects have been developed increasing the landscape resilience (Bonati, 2014; Bonati and Mendes, 2014).

Before the disaster, there were not many studies about precipitation over the island, which were highly motivated after 2010. Recent papers indicate the growing interest in providing an understanding about HPE over the island. The analysis of the disaster in 2010 using different methods and meteorological data represents an important step towards achieving this goal. The studies found that an anomalous wet winter and several rainfall events during the season contributed to the catastrophe (e.g., Couto et al., 2012; Fragoso et al., 2012). The greatest impact was observed in the southern region, where flash floods induced shallow, small, and numerous landslides (Lira et al., 2013).

The high amount of moisture in the lower troposphere was associated with a frontal system that reached the island on 20 February 2010 (Luna et al., 2011). The tropical origin of this moisture was underscored by Couto et al. (2012) and linked to a structure denominated as Atmospheric River (AR), due to its filamentary structure and moisture amount. Basically, this structure represents the meridional transport of moisture and contributed to other heavy precipitation events in Madeira during the 2009/2010 winter (Couto et al., 2012). According to Fragoso et al. (2012), the wet winter was strongly

connected to a negative North Atlantic Oscillation phase. The effect of multi-scale and orographic factors inducing elevated seasonal precipitation was also verified in the Philippines by Pullen et al. (2015).

Besides the numerical studies showing the important role of the local orography for the maximums of accumulated precipitation over the island (Luna et al., 2011; Couto et al., 2012; Dasari and Salgado, 2015, among others), Levizzani et al. (2013) confirmed this feature of the Madeira using passive microwave sounders, pointing out the usefulness of a high-resolution satellite rainfall estimation algorithm for monitoring localized precipitation. They found that the rainfall over the island during the disaster originated in shallow convection reaching an altitude of around 5 km.

There is no doubt that orographic precipitation is one of the strongest evidences of interaction between the surface and the atmosphere, and that mountains are responsible for modulating the weather and climate in several regions. The orographic mechanisms producing precipitation are well described in the literature, demonstrating how orographic precipitation may occur, depending on the orographic and on the atmospheric conditions, including size/shape of the mountain, moisture content, air stability, and large scale disturbances (e.g. Smith, 1979; Houze, 1993; Roe, 2005; Lin, 2007; Houze, 2012). In short, mountains may deflect air near the surface in different directions depending on its physical structure, inducing flow upward, downward, or around the mountain. If the atmospheric conditions are favourable to induce the saturation as the air is forced to lift, clouds may form and produce precipitation. The basic mechanisms creating upward motion and producing clouds and precipitation over mountains are shown in Figure 1.1. They can be associated with stable ascending air, enhancement of a pre-existing orographic precipitation, or convection (Houze, 1993). The first is observed when saturated air is forced to ascend over the mountain (Figure 1.1a); the second is known as seeder-feeder mechanism and causes the amplification of an already formed orographic precipitation from the rainfall associated to large scale disturbances (Figure 1.1b); the third mechanism is associated to convection triggered from instabilities of the flow, also divided into three mechanisms. 1) Upslope or upstream triggering: the orographic lifting occurs and upstream blocking trigger convection producing precipitation on the windward slope (Figure 1.1c and 1.1d); 2) Thermal triggering: the daytime heating produce an elevate heat source with local convergence near the top of the mountain (Figure 1.1e); and 3) Lee-side triggering or enhancement of deep convection: in the first

case (Figure 1.1f), low Froude number flowing around the mountain leads to convergence in the lee side of the mountain, whereas in the second (Figure 1.1g), the flow across a mountain converges with low-level thermally induced upslope flow.
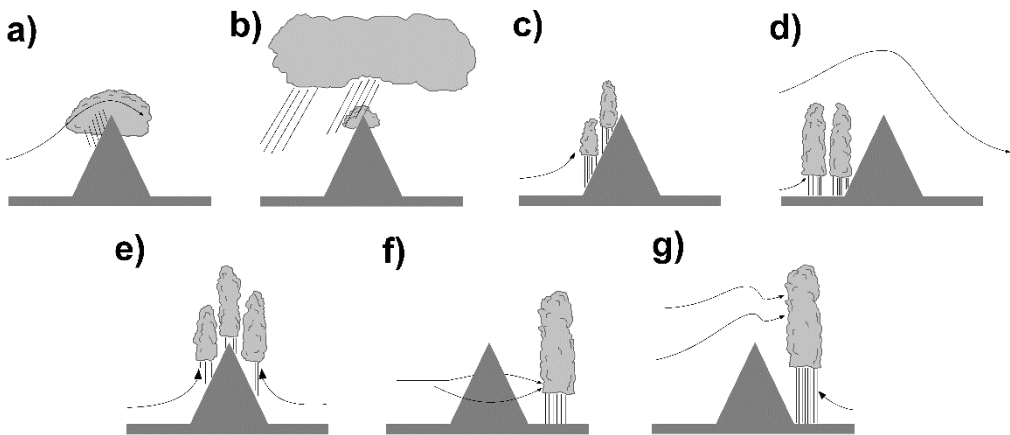
Figure 1.1 *Orographic mechanisms producing orographic precipitation. Adapted from Houze (1993).*

In the light of these orographic effect findings, the formation of precipitation over mountainous islands has been studied worldwide. The orographic effects in the distribution and intensification of rainfall over the Dominica Island (Caribbean Sea) have been highlighted thanks to idealized simulations mainly (e.g. Kirshbaum and Smith, 2009; Smith et al., 2009a; Smith et al., 2009b). During the drier season, purely orographic precipitation may be observed, and the mechanisms triggering convection (mechanical or thermodynamical), as well as associated precipitation (strong or little) depends basically on the speeds of the trade winds (Smith et al., 2012).

Taiwan is another place where the orographic effects in rainfall distribution have been widely studied (e.g. Yeh and Chen, 1998). Wang et al. (2014), analysing two HPE over Taiwan, showed that the synoptic circulation was dominant over the diurnal effects, and the steep topography of Taiwan was essential to increase the rainfall amount over and near Taiwan. Heavy precipitation events may be induced by several different orographic effects. Chen et al. (2010, 2011) identified that orographic lifting and convergence at low-levels caused by the flow deflection due the local orography was related to other precipitation events over Taiwan.

5

The inducing of convergence zones or the intensification of convective cells by orographic blocking in the lee side of an island are other mechanisms favouring heavy precipitation, as concluded in studies about precipitation over the quasi elliptical Jeju island (Lee et al., 2010, 2014). In general, the real cases of HPE in Jeju island, or the idealized studies conducted in the tropical island of Dominica show how precipitation may develop in small mountainous islands.

Lin et al. (2001) summarized some common synoptic and mesoscale environments responsible for heavy orographic precipitation in United States, European Alps, and East Asia. They found that the main environments are connected with a conditionally unstable air and a very moist low level jet. Most of the studies about orographic precipitation have been developed for regions located in mid-latitudes, for example, under the Mesoscale Alpine Programme (MAP; e.g., Bougeault et al., 2001), the Convective and Orographically induced Precipitation Study (COPS; e.g., Barthlott et al., 2011; Richard et al., 2011), and more recently, the Hydrological cycle in Mediterranean Experiment (HyMEX; e.g., Ducrocq et al., 2014). In the latter, efforts have been devoted to the observation and study of precipitating systems in the Mediterranean region.

Zhu and Newell (1998) found that most middle-latitude moisture flux occurs in filamentary features as revealed by the satellite data, called atmospheric rivers, and that the area of the globe they cover is 10 percent or less. They are generally directed poleward and their water vapour content mostly derives from evaporation from the sea, playing an important role in the rapid development of frontal cyclones (Zhu and Newell, 1994), also described as "warm conveyor belts". According to Ralph et al. (2004), the warm conveyor belt is an integral component of extratropical cyclones that plays a key role in transporting sensible and latent heat poleward, balancing the equatorward transport of relatively cool, dry air in other branches of the extratropical cyclone's circulation. In a maritime environment, a deep corridor of concentrated water vapour transport is often found in cyclone warm sectors, which are referred to as atmospheric rivers (Neiman et al., 2008b). In fact, ARs play an important role in tropical and extra-tropical interaction. When these strong water vapour fluxes encounter a mountainous coastal region, water vapour content is drastically reduced while rainfall greatly increases (e.g. Houze, 2012; Neiman et al., 2008a). The great impact of ARs in producing significant precipitation due to orographic effects, followed by floods and landslides, has been well documented in studies for the west coast of the USA (e.g. Ralph et al., 2004; Ralph et al., 2006; Neiman et al., 2008b).

Dettinger et al. (2011) investigating meteorological aspects of the connection between floods and water resources in California, observed that atmospheric rivers are a primary meteorological factor in flood generation of many California rivers, as well as a primary source of precipitation and water resources in the state.

Concerning the ARs occurrence over North Atlantic Ocean, Stohl et al. (2008) analysed an extreme precipitation event on the Norwegian southwest coast, which produced flooding and landslides. They found that it was triggered by the transport of (sub) tropical moisture through an atmospheric river rooted in the tropical western North Atlantic. The steep topography of the Norwegian coast caused strong orographic enhancement of the precipitation associated with the river. Lavers et al. (2011) pointed out that ARs transported moisture influencing the 10 largest winter flood events since 1970 in a range of British basins, demonstrating that this mechanism is of critical relevance for extreme winter floods in the UK and implementing an algorithm for the study of ARs and flooding in UK (Lavers et al., 2012).

Couto et al. (2012) also highlighted the occurrence of ARs in the North Atlantic Ocean favouring intense precipitation in Madeira. They found that, besides orographic forcing, the large amounts of rainfall observed in Madeira's highlands recorded during the 2009/2010 winter were favoured by the passage of weather systems such as low pressure and cold fronts. Coupled to the frontal systems, the presence of ARs was identified, which together with orographic lifting induced the formation of denser clouds, although their vertical development was relatively weak. In short, the study showed the role of ARs in six out of the seven cases of heavy precipitation over the island, providing significant amount of water vapour from the tropics for the triggering or enhancement of precipitation by the island terrain.

1.2 MOTIVATION

The Madeira island was chosen as study region after the disaster on February 20, 2010. The disaster is the most tragic event in terms of HPE in recent history of the island and presented high impact at the surface. As mentioned, the island suffered significant socio-economic losses. This study have been directed toward the advance of understanding about HPE affecting the island, and motivated by the possibility of improving the forecast of precipitation over the Madeira island.

1.3 GOALS

The overarching thesis's goal is to improve the understanding of heavy precipitation in Madeira Island associated with various atmospheric environments leading to the development of storms. The PhD is divided into the following specific goals:

1) To document the synoptic and mesoscale environments associated with heavy precipitation:

➢ What is the distribution of the daily accumulated precipitation on the highlands of Madeira for a 10-year period?

➢ What are the characteristics of the meridional transport of water vapour affecting the island, and which is its role in the precipitation enhancement during the winter seasons?

2) To characterize surface precipitation patterns that affected the island during some periods of significant accumulated precipitation using numerical modelling:

➢ What is the performance of high-resolution simulations against available observations?

➢ How the precipitation patterns are sensitive to the model resolution by comparing 500 m and 2.5 km horizontal resolution simulations?

➢ What is the partition between orographic precipitation and precipitation due to systems initially formed over the ocean?

3) To study the relationship between surface precipitation patterns and mesoscale environments:

➢ What are the factors that may cause HPE on the island, disentangling atmospheric environment factors and orographic effects?

➢ What is the role of mesoscale circulations triggering convection and the concentration of precipitation in distinct regions over the island?

➢ What is the microphysical structure of the cloudiness from the simulations, as well as their triggering mechanisms?

4) To highlight how the PhD findings obtained in the first three goals can be translated into an operational forecast context.

1.4 THESIS'S STRUCTURE

The thesis is structured as followed:

Chapter 1 – Introduction: The chapter introduces the thesis from the state of the art, motivation and goals of the study.

Chapter 2 – Precipitation in the Madeira Island over a 10-year period and the meridional water vapour transport during the winter seasons: The chapter consists in the precipitation analysis in Madeira's highlands during a 10-year period and the visual analysis of large scale from the total precipitable water obtained from the Atmospheric Infrared Sounder (AIRS), over an observational period of 10 winter periods. The relationship between atmospheric rivers and significant precipitation recorded in Madeira is also showed, and followed by a summary of the results. This chapter is transcription of the article:

> Couto FT, Salgado R, Costa MJ, Prior V. 2015. Precipitation in the Madeira Island over a 10-year period and the meridional water vapour transport during the winter seasons. International Journal of Climatology. 35: 3748-3759. DOI: 10.1002/joc.4243.

Chapter 3 – Numerical simulations of significant orographic precipitation in Madeira island: Numerical simulations are presented aiming to show the main features associated with all significant accumulated precipitation events in Madeira during the second wettest period identified in Chapter 2. The simulations with 2.5 km and 0.5 km horizontal resolution are shown, as well as the synoptic configuration associated with each period. This chapter is transcription of the article:

> Couto FT, Ducrocq V, Salgado R, Costa MJ. 2016. Numerical simulations of significant orographic precipitation in Madeira Island. Atmospheric Research. 169: 102-112. DOI: 10.1016/j.atmosres.2015.10.002.

Chapter 4 – Understanding significant precipitation in Madeira island using high-resolution numerical simulations of real cases: The atmospheric environments associated with four precipitation periods identified in Chapter 3 are described in order to explain how significant precipitation occurred over the island. The causes for the spatial variability of the accumulated precipitation are studied from the identification of orographic effects and microphysical structure of clouds, closely related to the mixing

ratio for water substance (e.g., cloud droplets, rain, graupel, snow and ice crystals). This chapter is transcription of the article:

> Couto FT, Ducrocq V, Salgado R, Costa MJ. Understanding significant precipitation in Madeira island using high-resolution numerical simulations of real cases. Submitted to Quarterly Journal of the Royal Meteorological Society.

Chapter 5 – Brief notes on the weather forecast of HPE in Madeira: Some results found in the previous chapters are highlighted considering their importance for the operational sector.

Chapter 6 – Conclusions: The conclusions are summarized in this chapter, jointly with some suggestions for future studies in order to help the predictability of HPE over the Madeira island. Essentially, the importance of the study is underscored from the advancement in the knowledge about precipitation development in Madeira after 5 years of the historical disaster on February 2010.

REFERENCES

Baioni D. 2011. Human activity and damaging landslides and floods on Madeira Island. *Natural Hazards and Earth System Sciences*. **11**: 3035-3046.

Barthlott C, Burton R, Kirshbaum D, Hanley K, Richard E, Chaboureau J-P, Trentmann J, Kern B, Bauer H-S, Schwitalla T, Keil C, Seity Y, Gadian A, Blyth A, Mobbs S, Flamant C, Handwerker J. 2011. Initiation of deep convection at marginal instability in an ensemble of mesoscale models: A case-study from COPS. *Quarterly Journal of the Royal Meteorological Society*. **137**: 118-136.

Bonati S. 2014. Resilientscapes: Perception and Resilience to Reduce Vulnerability in the Island of Madeira. *Procedia Economics and Finance*. **18**: 513-520.

Bonati S, Mendes MP. 2014. Building Participation to Reduce Vulnerability: How Can Local Educational Strategies Promote Global Resilience? A Case Study in Funchal? Madeira Island. *Procedia Economics and Finance*. **18**: 165-172.

Borges PAV, Abreu C, Aguiar AMF, Carvalho P, Fontinha S, Jardim R, Melo I, Oliveira P, Sequeira MM, Sérgio C, Serrano ARM, Sim-Sim M, Vieira P. 2008. Terrestrial and freshwater biodiversity of the Madeira and Selvagens archipelagos. In: Borges, P.A.V., Abreu, C., Aguiar, A.M.F., Carvalho, P., Jardim, R., Melo, I., Oliveira, P., Sérgio, C., Serrano, A.R.M. & Vieira, P. (eds.). A list of the terrestrial fungi, flora and fauna of Madeira and Selvagens archipelagos. pp. 13-26, Direcção Regional do Ambiente da Madeira and Universidade dos Açores, Funchal and Angra do Heroísmo.

Bougeault P, Binder P, Buzzi A, Dirks R, Kuettner J, Houze R, Smith RB, Steinacker R, Volkert H. 2001. The MAP Special Observing Period. *Bulletin of the American Meteorological Society*. **82**: 433-462.

Chen C-S, Lin Y-L, Peng W-C, Liu C-L. 2010. Investigation of a heavy rainfall event over southwestern Taiwan associated with a subsynoptic cyclone during the 2003 Mei-Yu season. *Atmospheric Research*. **95**: 235–254.

Chen C-S, Lin Y-L, Hsu N-N, Liu C-L, Chen C-Y. 2011. Orographic effects on localized heavy rainfall events over southwestern Taiwan on 27 and 28 during the Post-Mei-Yu season. *Atmospheric Research*. **101**: 595–610.

Couto FT, Salgado R, Costa MJ. 2012. Analysis of intense rainfall events on Madeira Island during the 2009/2010 winter. *Natural Hazards and Earth System Sciences*. **12**: 2225-2240.

Dasari HP, Salgado R. 2015. Numerical modelling of heavy rainfall event over Madeira Island in Portugal: sensitivity to different micro physical processes. *Meteorological Applications*. **22**: 113-127.

Dettinger MD, Ralph FM, Das T, Neiman PJ, Cayan DR. 2011. Atmospheric Rivers, Floods and the Water Resources of California. *Water*. **3(2)**: 445-478.

Driver J. 1838. Letters from Madeira in 1834: with an appendix, illustrative of the history of the island, climate, wines, and other information up to the year 1838. By John Driver, London: Longman & Co. Liverpool; J. F. Cannell, Castle street. Available on 12 Feb. 2016: http://purl.pt/17099.

Ducrocq V, Braud I, Davolio S, Ferretti R, Flamant C, Jansa A, Kalthoff N, Richard E, Taupier-Letage I, Ayral P-A, Belamari S, Berne A, Borga M, Boudevillain B, Bock O, Boichard J-L, Bouin M-N, Bousquet O, Bouvier C, Chiggiato J, Cimini D, Corsmeier U, Coppola L, Cocquerez P, Defer E, Delanoë J, Di Girolamo P, Doerenbecher A, Drobinski P, Dufournet Y, Fourrié N, Gourley JJ, Labatut L, Lambert D, Le Coz J, Marzano FS, Molinié G, Montani A, Nord G, Nuret M, Ramage K, Rison B, Roussot O, Said F, Schwarzenboeck A, Testor P, Van Baelen J, Vincendon B, Aran M, Tamayo J. 2014. HyMeX-SOP1, the field campaign dedicated to heavy precipitation and flash flooding in the northwestern Mediterranean. *Bulletin of the American Meteorological Society*. **95**: 1083–1100.

Fernandes JP, Guiomar N, Gil A. 2015. Strategies for conservation planning and management of terrestrial ecosystems in small islands (exemplified for the Macaronesian islands). *Environmental Science & Policy*. **51**: 1-22.

Fragoso M, Trigo RM, Pinto JG, Lopes S, Lopes A, Ulbrich S, Magro C. 2012. The 20 February 2010 Madeira flash-floods: synoptic analysis and extreme rainfall assessment. *Natural Hazards and Earth System Sciences*. **12**: 715-730.

Houze Jr. RA. 1993. Cloud dynamics. Academic Press. 573 pages.

Houze Jr. RA. 2012. Orographic effects on precipitating clouds. *Reviews of Geophysics.* **50**: RG1001.

Kirshbaum JD, Smith RB. 2009. Orographic Precipitation in the Tropics: Large-Eddy Simulations and Theory. *Journal of the Atmospheric Sciences.* **66**: 2559–2578.

Lavers DA, Allan RP, Wood EF, Villarini G, Brayshaw DJ, Wade AJ. 2011. Winter floods in Britain are connected to atmospheric rivers. *Geophysical Research Letters.* **38**: L23803.

Lavers DA, Villarini G, Allan RP, Wood EF, Wade AJ. 2012. The detection of atmospheric rivers in atmospheric reanalyses and their links to British winter floods and the large-scale climatic circulation. *Journal of Geophysical Research.* **117**: D20106.

Lee K-O, Shimizu S, Maki M, You C-H, Uyeda H, Lee D-I. 2010. Enhancement mechanism of the 30 June 2006 precipitation system observed over the northwestern slope of Mt. Halla, Jeju Island, Korea. *Atmospheric Research.* **97(3)**: 343-358.

Lee K-O, Uyeda H, Lee D-I. 2014. Microphysical structures associated with enhancement of convective cells over Mt. Halla, Jeju Island, Korea on 6 July 2007. *Atmospheric Research.* 135–136, 76–90.

Levizzani V, Laviola S, Cattani E, Costa MJ. 2013. Extreme precipitation on the Island of Madeira on 20 February 2010 as seen by satellite passive microwave sounders. *European Journal of Remote Sensing.* **46**: 475-489.

Lin Y-L, Chiao S, Wang T-A, Kaplan ML, Weglarz RP. 2001. Some Common Ingredients for Heavy Orographic Rainfall. *Weather Forecasting.* **16**: 633–660.

Lin Y-L. 2007. Mesoscale dynamics. Cambridge University Press. Cambridge. 630pp.

Lira C, Lousada M, Falcão AP, Gonçalves AB, Heleno S, Matias M, Pereira MJ, Pina P, Sousa AJ, Oliveira R, Almeida AB. 2013. The 20 February 2010 Madeira Island flash-floods: VHR satellite imagery processing in support of landslide inventory and sediment budget assessment. *Natural Hazards and Earth System Sciences.* **13**: 709-719.

Luna T, Rocha A, Carvalho AC, Ferreira JA, Sousa J. 2011. Modelling the extreme precipitation event over Madeira Island on 20 February 2010. *Natural Hazards and Earth System Sciences.* **11**: 2437-2452.

Neiman PJ, Ralph FM, Wick GA, Kuo Y-H, Wee T-K, Ma Z, Taylor GH, Dettinger MD. 2008a. Diagnosis of an intense atmospheric river impacting the Pacific Northwest: Storm summary and offshore vertical structure observed with COSMIC satellite retrievals. *Monthly Weather Review.* **136**: 4398-4420.

Neiman PJ, Ralph FM, Wick GA, Lundquist J, Dettinger MD. 2008b. Meteorological characteristics and overland precipitation impacts of atmospheric rivers affecting

the West Coast of North America based on eight years of SSM/I satellite observations. *Journal of Hydrometeorology*. **9**: 22-47.

Prada S, Silva MO. 2001. Fog precipitation on the island of Madeira (Portugal). *Environmental Geology.* **41**: 384-389.

Prada S, Silva MO, Cruz JV. 2005. Groundwater behaviour in Madeira, volcanic island (Portugal). *Hydrogeology Journal*. **13**: 800-812.

Prada S, de Sequeira MM, Figueira C, Silva MO. 2009. Fog precipitation and rainfall interception in the natural forests of Madeira Island (Portugal). *Agricultural and Forest Meteorology*. **149**: 1179-1187.

Prada S, de Sequeira MM, Figueira C, Vasconcelos R. 2012. Cloud water interception in the high altitude tree heath forest (Erica arborea L.) of Paul da Serra Massif (Madeira, Portugal). *Hydrological Processes*. **26**: 202-212.

Prada S, Figueira C, Aguiar N, Cruz JV. 2015. Stable isotopes in rain and cloud water in Madeira: contribution for the hydrogeologic framework of a volcanic island. *Environmental Earth Sciences*. **73**: 2733-2747.

Pullen J, Gordon AL, Flatau M, Doyle JD, Villanoy C, Cabrera O. 2015. Multiscale influences on extreme winter rainfall in the Philippines. *Journal of Geophysical Research: Atmospheres*. **120**: 3292–3309.

Ralph FM, Neiman PJ, Wick GA. 2004. Satellite and CALJET aircraft observations of atmospheric rivers over the eastern North-Pacific Ocean during the winter of 1997/98. *Monthly Weather Review*. **132**: 1721-1745.

Ralph FM, Neiman PJ, Wick GA, Gutman SI, Dettinger MD, Cayan DR, White AB. 2006. Flooding on California's Russian River: Role of atmospheric rivers. *Geophysical Research Letters*. **33**: L13801.

Richard E, Chaboureau J-P, Flamant C, Champollion C, Hagen M, Schmidt K, Kiemle C, Corsmeier U, Barthlott C, Di Girolamo P. 2011. Forecasting summer convection over the Black Forest: A case study from the Convective and Orographically induced Precipitation Study (COPS) experiment. *Quarterly Journal of the Royal Meteorological Society*. **137**: 101-117.

Roe GH. 2005. Orographic Precipitation. *Annual Review of Earth and Planetary Sciences*. **33**: 645-671.

Smith RB. 1979. The influence of mountains on the atmosphere. *Advances in Geophysics*. **21**: 87-230.

Smith RB, Schafer P, Kirshbaum D, Regina E. 2009a. Orographic Precipitation in the Tropics: Experiments in Dominica. *Journal of the Atmospheric Sciences*. **66**: 1698–1716.

Smith RB, Schafer P, Kirshbaum D, Regina E. 2009b. Orographic Enhancement of Precipitation inside Hurricane Dean. *Journal of Hydrometeorology*. **10**: 820-831.

Smith RB, Minder JR, Nugent AD, Storelvmo T, Kirshbaum DJ, Warren R, Lareau N, Palany P, James A, French J. 2012. Orographic Precipitation in the Tropics: The Dominica Experiment. *Bulletin of the American Meteorological Society*. **93**: 1567-1579.

Stohl A, Forster C, Sodemann H. 2008. Remote sources of water vapor forming precipitation on the Norwegian west coast at 60°N – A tale of hurricanes and an atmospheric river. *Journal of Geophysical Research*. **113**: 13 pp., D05102.

Strangeways I. 2006. Precipitation: Theory, Measurement and Distribution. Cambridge: Cambridge University Press. 302 pages.

Wang C-C, Hsu J C-S, Chen G T-J, Lee D-I. 2014. A Study of Two Propagating Heavy-Rainfall Episodes near Taiwan during SoWMEX/TiMREX IOP-8 in June 2008. Part II: Sensitivity Tests on the Roles of Synoptic Conditions and Topographic Effects. *Monthly Weather Review*. **142**: 2644-2664.

Yeh HC, Chen Y L. 1998. Characteristics of rainfall distributions over Taiwan during the Taiwan Area Mesoscale Experiment (TAMEX). *Journal of Applied Meteorology*. **37**: 1457-1469.

Zhu Y, Newell RE. 1994. Atmospheric Rivers and bombs. *Geophysical Research Letters*. **21**: 1999-2002.

Zhu Y, Newell RE. 1998. A proposed algorithm for moisture fluxes from atmospheric rivers. *Monthly Weather Review*. **126**: 725-735.

CHAPTER 2 – PRECIPITATION IN THE MADEIRA ISLAND OVER A 10-YEAR PERIOD AND THE MERIDIONAL WATER VAPOUR TRANSPORT DURING THE WINTER SEASONS*

Abstract

In this paper, a 10-year daily accumulated precipitation analysis of Madeira highland is presented, as well as the relationship between meridional water vapour transport during 10 winter seasons and the precipitation recorded in the island during the same period. Here, the meridional water vapour transport is considered as occurring in narrow corridors known as atmospheric rivers – ARs – which were visually identified in the total precipitable water vapour field extracted from Atmospheric Infrared Sounder (AIRS) data within a domain covering the North Atlantic Ocean. European Centre for Medium-range Weather Forecasts (ECMWF) analysis was also used when necessary. Daily precipitation during the period covered by the study evidenced generally dry summers, whereas the highest values for daily accumulated precipitation were recorded mainly during the winter and also during the autumn and spring. Image analysis shows that moist air originating mainly in the Caribbean Sea flows northward or eastward, intersecting, on some occasions, the island during the winter season, often during a stage of dissipation. The orientation of the flow and the amount of water vapour transported to the island are important features, contributing to the occurrence of significant precipitation events. In fact, the moist environment created by ARs may favour the occurrence of precipitation, but this is not the sole factor favouring high rainfall over Madeira.

2.1. INTRODUCTION

Located in the North Atlantic Ocean (32°75'N and 17°00'W), Madeira is an island which forms part of Portugal and has an area of approximately 740 km^2. A salient feature of its physical geography is the east-west oriented barrier (with a length of 58 km and a width of 23 km), which is made up of volcanic material and has a mountainous ridge that extends mainly along the central part of the island, with the highest peak reaching a maximum of 1862 m (Pico Ruivo). Since mountains may induce precipitation through a number of mechanisms (e.g. Houze, 2012), or contribute to the intensification of pre-existing precipitation, Madeira's highlands directly affect cloud formation and consequent precipitation at the surface, mainly during the passage of weather systems over the region. This kind of environment sometimes favours large amounts of rainfall, with consequent floods and landslides. Using historical data from 1611 to the present, Baioni (2011) pointed out that hazardous events that have had the greatest impact and produced the worst damage are flash floods, followed by landslide events, and that most of these events take place in the period from November to April, when almost all annual rainfall occurs in Madeira. Overall, this author's findings suggested that there is a geographical correspondence between the incidence of landslides and floods and the human activity, through modifications of the landscape in response to the recent human development.

Madeira experienced an event of extreme precipitation on 20 February 2010, which was the severest event in its recent history, causing more than 40 deaths and damage estimated at millions of euros. Following the disaster, a number of papers have been produced, reflecting a growing interest in providing an understanding of the main mechanisms and atmospheric conditions that may be relevant for the establishment of extreme rainfall, and consequently flash flood occurrences in Madeira. The analysis of this event using different methods and meteorological data represents an important step towards achieving this goal. For example, Lira et al. (2013) pointed out the importance of the use of high resolution multispectral satellite images for identifying landslides that occur, as observed in the above-mentioned disaster: in this case they were numerous, mostly small in size, dispersed and shallow in depth. Fragoso et al. (2012) showed that the episode was preceded by anomalously wet conditions during the winter of 2010, and that large-scale atmospheric forcing was of crucial importance in inducing deep convection, due to the passage of a frontal cyclone. The main process responsible for

converting the high moisture content of the southern flow associated with the passage of a frontal system was the orographic lifting imposed by Madeira's topography (Luna et al., 2011).

More recently, in order to provide an improved representation of the event which occurred on 20th February 2010, using the WRF model, Dasari and Salgado (2013) tested different microphysics schemes available by the model, while Teixeira et al. (2014) studied the impact of the use of different topographies and land use data on the evolution of the episode, considering the lower boundary. Levizzani et al. (2013) using passive microwave sounders, pointed out the usefulness of a high-resolution satellite rainfall estimation algorithm for monitoring very localised precipitation, and also showed that the rainfall over the island during the episode originated in shallow convection reaching an altitude of around 5 km.

Couto et al. (2012) highlighted another point regarding intense precipitation events in Madeira, stressing the occurrence of atmospheric rivers (ARs) in the North Atlantic Ocean. They found that, besides orographic forcing, the large amounts of rainfall observed in Madeira's highlands recorded during the winter of 2009-2010 were favoured by the passage of weather systems such as low pressure and cold fronts. Coupled with these frontal systems, the presence of ARs was identified, which together with orographic lifting induced the formation of denser clouds, although their vertical development was relatively weak.

Zhu and Newell (1998) showed that most middle-latitude moisture flux occurs in filamentary features called atmospheric rivers, and that the area of the globe they cover is 10% or less. They are generally directed poleward and their water vapour content mostly derives from evaporation from the sea, playing an important role in the rapid development of frontal cyclones (Zhu and Newell, 1994), and they are often found in the warm sector of these systems, also described as "warm conveyor belts" (WCB; Carlson, 1991). According to Houze (2012), ARs are closely associated with the pre-frontal low level jet that keeps a cold front in semigeostrophic balance. Moreover, the filamentary structure associated with an atmospheric river is apparently a result of the kinematic deformation of the flow field just ahead of the front, with higher water vapour content from lower latitudes.

In fact, ARs play an important role in tropical and extra-tropical interaction, and when these strong water vapour fluxes encounter a mountainous coastal region, water vapour content is drastically reduced while rainfall greatly increases (e.g. Neiman et al., 2008a; Houze, 2012). The great impact of ARs in producing significant precipitation due to orographic effects, followed by floods and landslides, has been well documented in recent years in studies of the west coast of the USA (e.g. Ralph et al., 2004; Ralph et al., 2006; Neiman et al., 2008b; Kim et al., 2012). According to Guan et al. (2010), ARs also provide an important contribution to total seasonal snow accumulation in the Sierra Nevada, accounting for a relatively large percentage of such (approximately 30 – 40 %).

Although few studies have been produced for the North Atlantic Ocean, Lavers et al. (2011) showed that ARs transported moisture influencing the 10 largest winter flood events since 1970 in a range of British basins, demonstrating that this mechanism is of critical relevance for extreme winter floods in the UK. Lavers et al. (2012) introduced an algorithm for the study of ARs and flooding in UK. Besides orographic effects on rainfall enhancement, they found that the frequency of persistent winter ARs was linked to the Scandinavian Pattern (SCP), with the high frequency of ARs associated with lower SCP values. Considering climate change scenarios, Lavers et al. (2013) showed that the strongest ARs are projected to become more intense and frequent and may be associated with more frequent and more serious winter flood episodes in the UK.

The aim of this paper is to analyse the distribution of daily accumulated precipitation in Madeira's highlands over a period of 10 years, followed by a discussion of the main characteristics associated with meridional water vapour transport by means of ARs during the 10 winter seasons considered, and their impact on rainfall amounts recorded over the island during the same period. The paper is organized as follows: the data and methodology are presented in Section 2.2. In Section 2.3, the analysis and a discussion of the results are presented. The conclusions and recommendations for future research appear in Section 2.4.

2.2. DATA AND METHODOLOGY

2.2.1 Rain gauge data

The Weather Network in Madeira is dependent on the Instituto Português do Mar e Atmosfera – the IPMA and provides the observations required for weather surveillance

purposes, also being used for climate monitoring and scientific research. Conventional in situ observations have been made at the Funchal station since 1865, and the Madeira network currently comprises 18 automatic surface weather stations distributed throughout the island at different altitudes (Figure 2.1). For example, in the southern part of the island, observations are made at 50 m, 1000 m, 1500 m, and 1800 m. All stations are equipped with 200-cm^2 rain gauges (8 LAMBRECHT and 10 RM YOUNG), and data are recorded every 10 min.

For the winter of 2009-2010, Couto et al. (2012) showed that, as expected, precipitation tends to be concentrated in mountainous areas of the island. This study focuses on rainfall distribution at the Areeiro station, located near the mountain crest in the south-eastern part of the island, at an altitude of 1590 m. The 10-year period from September 2002 to November 2012 is considered for analysis in this study. However, during February, November, and December 2006, there are at least 15 days in each month missing in the rainfall measurements of Areeiro station, which significantly influences analysis for this period.

Figure 2.1 *The automatic weather stations network of the Madeira's Archipelago.*

2.2.2 Satellite Data

In this study, meridional water vapour transport by means of ARs was identified on the basis of the total precipitable water vapour field (unit: kg m^{-2}) extracted from Level 2 (AIRX2RET), version 005, of Atmospheric Infrared Sounder (AIRS) data products. The

AIRS was launched on 4 May 2002 into a sun-synchronous orbit at an altitude of 705 km on board the Aqua satellite, which is part of the Earth Observing System, with global coverage twice a day. The AIRS, together with the Advanced Microwave Sounding Unit (AMSU-A), and the Humidity Sounder for Brazil (HSB), form the sounding system on board the Aqua satellite; however, the HSB ceased operating in February 2003.

The data products provided by AIRS/AMSU-A/HSB measurements are divided into two groups: Level 1b, including calibrated and geolocated radiances from AIRS/AMSU-A/HSB; and Level 2, including cloud-cleared infrared radiances, sea and land surface temperatures, temperature and humidity profiles, total precipitable water vapour, fractional cloud cover, cloud top height, and cloud top temperature. Calibrated radiance (also referred to above as Level 1b products) is obtained at the instrument footprint size of 13.5 km, 40 km, and 13.5 km, for AIRS, AMSU-A, and HSB, respectively. Retrieved geographical products, also referred to as Level 2 products, including cloud-cleared radiances, are based on the combined AIRS/AMSU-A/HSB 40 km scale. AIRS Products are often the result of calculations involving AMSU-A and/or HSB data, as well as AIRS data (Aumann et al., 2003; Olsen et al., 2007). In general, the AIRS instrument is a high-resolution infrared sounder, simultaneously measuring in 2378 spectral channels in the $3.74 - 15.4\,\mu m$ spectral range (the spatial resolution in the infrared is 13.5 km at nadir), and the spectral resolution ($\lambda/\Delta\lambda$) is nominally 1200. The instrument also provides four visible/near-infrared (VIS/NIR) channels ($0.4 - 1.0\,\mu m$) for characterising cloud and surface properties. Spatial resolution in the VIS/NIR is 2.3 km at nadir (Parkinson et al., 2006). In this paper, AIRS observations are used for the 10 winter periods from September 2002 to November 2012, totalling 903 days. However, for the 2009-10 winter, there are 16 days in January 2010 for which there are no AIRS observations. The data were downloaded for the domain that covers the North Atlantic Ocean, shown in Figure 2.2, and correspond to the latitudes between 10° and 60° N and longitudes between 5° E and 100° W.

2.2.3 ECMWF Analysis

The precipitable water vapour field (unit: mm) from European Centre for Medium-range Weather Forecasts (ECMWF) analyses was used to support AIRS data, for example, when there was no satellite information for the island. The data were downloaded in

gridded binary (GRIB) format, and obtained from the ECMWF Meteorological Archive and Retrieval System. Analyses were updated every 6 h, for the same domain used for AIRS observations (Figure 2.2), with 0.125º of resolution, for a period of 10 winters, similar to AIRS data.

Figure 2.2 *Location of Madeira Island (MI), and domain for the identification of atmospheric rivers over the North Atlantic Ocean (NAO). The rectangle covers the NAO, with the latitudes between 10°N and 60°N and longitudes between 5°E and 100°W. Source: AIRS's website.*

2.2.4 Methodology

The methodology adopted for conducting this study consists of three steps: (1) analysing 10 years of Areeiro station precipitation data for Madeira's highlands; (2) identifying days during the 10-winter period when there were ARs over Madeira; and (3) comparing the results of the first two steps for winter cases in order to verify the role of meridional transport in the accumulated precipitation in Madeira's highlands.

In this study, meridional water vapour transport is considered as occurring in narrow corridors known as atmospheric rivers. A methodology for AR detection was first proposed by Ralph et al. (2004) for studying the main features of narrow bands with strong horizontal water vapour flux, associated with polar fronts that occurred over the eastern North Pacific Ocean. They defined an atmospheric river as an elongated moisture plume with precipitable water vapour (PW) > 2 cm, which is < 1000 km wide and > 2000 km long. Regions with high levels of water vapour transport, with maximum PW values

exceeding 4 cm, represented a pre-cold-frontal Low Level Jet, and consequently, strong winds were associated with them. On the basis of eight hydrological years, Neiman et al. (2008b) added to the initial criterion the observation that PW plumes intersected the west coast of the North America between 32.5° and 52.5°N latitudes and, in addition to the 2-cm threshold described above, they also considered an additional class of strong wintertime PW plumes with coherent regions of PW > 3 cm within 1000 km of the coast. More recently, in order to study atmospheric rivers in a climatological context for different regions, Wick et al. (2013) presented an Atmospheric River detection tool for the northern Pacific area, which was developed, implemented, and validated on the basis of the initial criteria for AR identification used by Ralph et al. (2004).

For ARs occurring in the North Atlantic Ocean that favoured the strongest floods occurring in the UK since 1970, Lavers et al. (2012) introduced an AR detection algorithm, based on Integrated Vapour Transport (IVT). They considered IVT distribution at grid points spanning 50° to 60°N along 4°W, and IVT values equivalent to those used by Ralph et al. (2004).

The identification of atmospheric rivers that intersected Madeira during the 10 winter periods considered in this study was carried out using total precipitable water vapour image analysis obtained from AIRS observations. The large domain presented in Figure 2.2 was used not only to identify the narrow bands of high moisture content over Madeira, but also to identify the source of moisture contained in the rivers that reached the island. This point is considered in accordance with the results obtained by Couto et al. (2012), who observed that these narrow bands with high precipitable water vapour levels originated in the tropics, particularly in the Caribbean Sea region. Unfortunately, sometimes there were no satellite observations over the island, and AR identification was conducted using the precipitable water field from ECMWF analysis, with a view to confirming possible AR episodes identified in AIRS images. For example, on 30 December 2008, the two AIRS observations were not sufficient to verify that the transport of water vapour from the tropical region reached Madeira. In the first image at 0853 UTC (Figure 2.3a), the absence of observations all over the island is clear, while in the second (not shown here), the transport of moisture to the island is not clear. Therefore, ECMWF Analysis at 1200 UTC (Figure 2.3b) helped to identify and confirm the presence of moisture transport from lower latitudes.
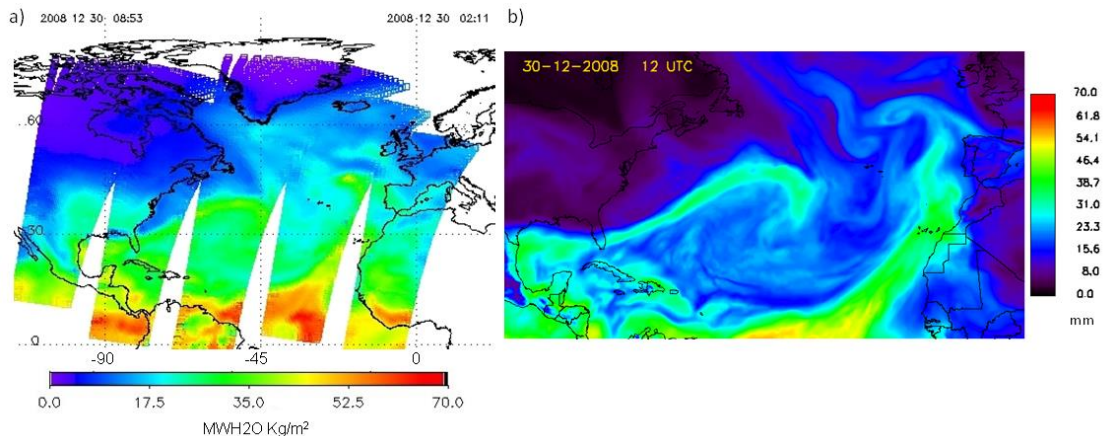
Figure 2.3 *Precipitable water vapour field on 30 December 2008 for (a) AIRS observation (unit: kg/m²) at 0853 UTC, and (b) ECMWF Analysis (unit: mm) at 1200 UTC.*

Because Madeira is located at a lower latitude than other regions which have been the object of atmospheric river studies (e.g. the UK and the state of California), higher values for precipitable water vapour may be observed. Therefore, no threshold is considered here for the amount of precipitable water vapour associated with ARs, which are visually identified as filamentary structures when their length is several times larger than their width. This feature is clearly discernible in the precipitable water field on the basis of significant values of precipitable water and presents a horizontal gradient.

2.3. RESULTS AND DISCUSSION

In this section, the analysis of rainfall from the Areeiro station and AIRS precipitable water vapour observations are presented, as well as a discussion about the relationships between atmospheric rivers and the precipitation accumulated over Madeira during 10 winter seasons.

2.3.1 Precipitation at surface level

Daily precipitation at Areeiro is analysed for the period from September 2002 to November 2012, and the distribution during the period, as well as the seasonal average calculated from the total accumulated precipitation in the entire period for each season, are shown in Figure 2.4. In Figure 2.4.a, seasonal accumulated precipitation shows maximum values normally occurring during autumn and winter. However, sometimes a

drier winter is followed by a wetter spring, as with the 2008 spring and possibly also in 2007 (the lack of data in December 2006 does not enable this to be confirmed; see Section 2.2.1), when seasonal accumulated precipitation was higher than in previous winters. In the same figure, the high precipitation levels during the winter of 2009-2010 and the autumn of 2012, the two wettest periods in recent years, should be noted, with accumulated values of 2701.9 mm and 2051.7 mm, respectively. Another period of significant accumulated rainfall was the winter of 2010-2011, with a total of 1780.5 mm. It should also be noted that the summer (301.3 mm) and autumn (944.5 mm) of 2009 were very wet, as compared with the same periods in previous years. Overall, these values show that in recent years there were three seasons with accumulated maximums which were clearly greater than those observed in previous years and significantly above the seasonal average for these periods. For the other winters, the seasonal accumulated precipitation was near or lower than the average (Figure 2.4a).

Daily precipitation was classified in classes according to the total of accumulated precipitation in 24 hours (AP) as follows: low (25 mm < AP < 50 mm; green), medium (50 mm < AP < 100 mm; yellow), high (100 mm < AP < 200 mm; red), and extreme (AP > 200 mm; blue). The number of days with precipitation observed within these accumulation classes for each season is presented in Figure 2.4b.

Regarding warm seasons, it is clear that there were not many days with significant precipitation during summers, i.e. with daily accumulated precipitation above 25 mm. One day during the summer of 2006 shows moderate accumulated precipitation (73.6 mm), and 1 day during the summer of 2007 presents low accumulated precipitation (26.9 mm). Nevertheless, the summer of 2009 was marked by 3 days with daily accumulated precipitation of 50 – 100 mm. All these summer cases occurred in June, as can be seen in Figure 2.4c.

Regarding wet seasons, Figure 2.4b shows the occurrence of five extreme precipitation events (> 200 mm) during the period as whole, all in the final years. These cases are shown in blue, and refer to one case in the spring of 2008, two during the winter of 2009-2010, one in the winter of 2010-2011, and one in the autumn of 2012. They can be clearly identified in Figure 2.4c. The episodes occurred on 8 April 2008 (264.3 mm), in February 2010 (02: 284.8 mm; and 20: 387.1 mm), on 25 January 2011 (297.2 mm), and on 30 October 2012 (295 mm). Overall, three of the five episodes of extreme precipitation occurred in winter. For the other classes, high levels of precipitation (100 –

200 mm day^{-1}) were recorded on 36 days (14 in autumn, 17 in winter, and 5 in spring), while moderate and low accumulated rainfall were observed on a total of 90 days (37 in autumn, 34 in winter, 15 in spring, 4 in summer), and 96 days (31 in autumn, 42 in winter, 21 in spring, and 2 in summer), respectively. Rainfall events with a daily precipitation of 100 – 200 mm occurring with a high frequency were identified during the 2009-2010 winter, totalling 7 days throughout the season (Figure 2.4b), contributing to making the winter of 2009-2010 the wettest winter during the study period as a whole. It should be noted that the three wettest periods with seasonal accumulated values of above 1500 mm are the winters of 2009-2010 and 2010-2011, and the autumn of 2012. The relationships between precipitation at Areeiro and the passage of atmospheric rivers over the island during the winter periods will be discussed in Sub-section 2.3.3.

2.3.2 AIRS observations and meridional water vapour transport

In a previous study it was observed that the organized meridional transport of moisture from the tropical regions to the mid-latitudes, especially to the European continent, may pass over the Madeira archipelago, leading to a high level of precipitation in Madeira, through the formation or by the intensification of a pre-existing precipitation (Couto et al., 2012). Now the precipitable water vapour fields for 10 winter seasons are analysed.

The visual analysis of AIRS satellite images confirms the fact that sometimes Madeira is located in the path of atmospheric rivers, which transport a significant amount of precipitable water vapour. They were identified and classified as such because their length was greater than their width, and they clearly accounted for the transport of large amounts of moisture from the tropical regions to higher latitudes. In accordance with the criteria for AR selection described in Section 2.2, for the 10 winter periods considered, 56 days were selected when this type of structure was found over the island or close by. From the images, it was verified that many rivers pass over the island in a stage of dissipation, when their filamentary structure is no longer well defined.

On 37 of the 56 days, ARs were considered as being well configured before and during their passage over the island. These 37 days accounted for 32 atmospheric river episodes because five ARs were observed passing during 2 days. Episodes are shown in Table 2.1 together with the values of total AIRS precipitable water vapour in the Madeira region.
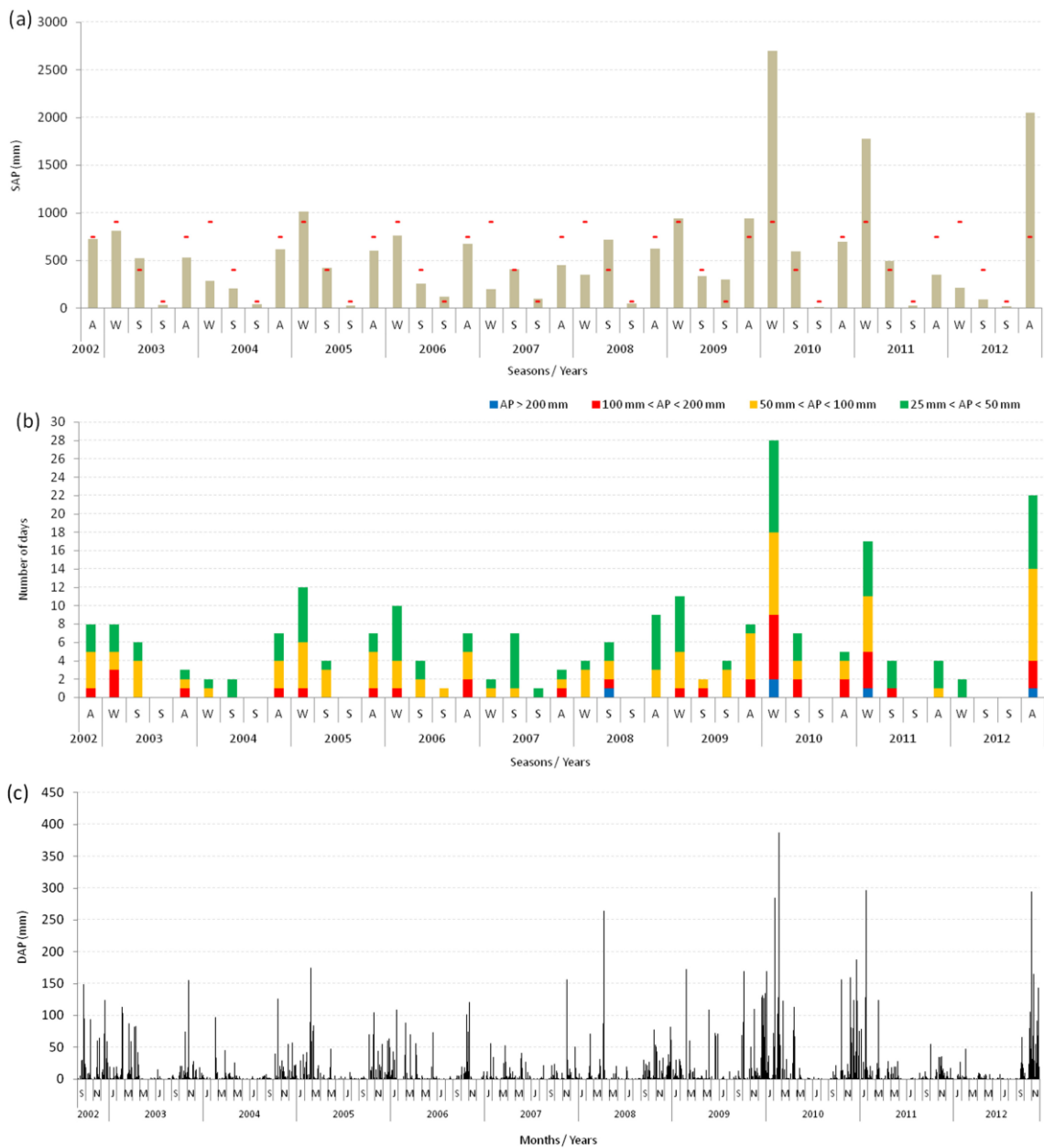
Figure 2.4 Rain gauge data for Areeiro station during the period between September 2002 and November 2012: (a) seasonal accumulated precipitation (SAP) and the seasonal average, (b) number of days with low (25 mm < AP < 50 mm), medium (50 mm < AP < 100 mm), high (100 mm < AP < 200 mm), or extreme (AP > 200 mm) daily accumulated precipitation, and (c) daily accumulated precipitation (DAP) recorded along the entire period.

In some cases, observation of only one of the two daily satellite images is sufficient to verify the presence of ARs over the island. However, in 3 of 32 episodes, ECMWF analysis was required in order to verify AIRS observations, confirming the transport of water vapour to the island. For the first six winters analysed, it can be observed in Table 2.1 that the filamentary transport of water vapour to the island was a significantly frequent

occurrence, with five episodes in the winter of 2002-2003, followed by a period of low frequency, with occurrences not exceeding four episodes in 2005-2006, three cases during the winter of 2006-2007, and no occurrences in the winters of 2003-2004, 2004-2005, and 2007-2008. On the other hand, in the final years, the meridional transport of water vapour over Madeira by means of atmospheric rivers, was a more frequent occurrence, with 5 episodes in the winter of 2008-2009, 10 in that of 2009-2010, and 5 in that of 2010-2011. Finally, in the winter of 2011-2012, no atmospheric rivers were identified passing directly over the island. The fact that no ARs were identified passing over the island during these periods means that this type of meridional transport was not observed reaching the island, while it does not mean that there were no atmospheric rivers over the Atlantic. As mentioned earlier, many atmospheric rivers pass over Madeira in a stage of dissipation, which eliminated some cases.

Another point associated with the occurrence of ARs is the amount of precipitable water vapour that must be identified or transported to the island, during the wintertime, in order to induce an episode with the magnitude of the disaster of 20 February 2010. In Table 2.1, it may be noted that the majority of the atmospheric rivers contain a total of precipitable water vapour of around 35 kg m^{-2}. However, filamentary structures with amounts of nearly 25 kg m^{-2} or above 50 kg m^{-2} were identified. It should be noted that besides occurring more frequently, during the winter of 2009-2010 atmospheric rivers were also more intense, showing the highest values of precipitable water vapour, with episodes presenting amounts above 40 kg m^{-2} and even higher than 50 kg m^{-2}, as observed on 20 February 2010. In the winter of 2010-2011, despite the significantly frequent occurrence of these structures they were not as intense as that observed during the winter of 2009-2010, with just one episode presenting precipitable water vapour of above 45 kg m^{-2}. The relationship between the passage of atmospheric rivers and accumulated rainfall falling over the island will be presented in the next sub-section.

From the analysis of AIRS observations, certain patterns were identified regarding the orientation of water vapour transport that reached Madeira during the winter seasons studied. As stated above, no threshold was considered, because filamentary structures were observed with precipitable water vapour values ranging from 25 to 50 kg m^{-2}. Figure 2.5 shows the patterns observed in the images. In general, two main types were identified, while one of these may be subdivided into three distinct types. These configurations are described separately below, each along with its main features.

Table 2.1 *Atmospheric river episodes for the winters considered, followed by the date, total precipitable water vapour (PW; unit: kg/m²) observed around the island, the type of structure, use (x) or not (-) of the ECMWF analysis, as well as the precipitation recorded at surface for each case.*

Winter		Atmospheric rivers				Precipitation
		Date	PW	TYPE	ECMWF	
2002/2003	01	2002/12/16	40-45 kg/m²	2	-	124.30 mm
	02	2002/12/22	35-40 kg/m²	1.a		59.80 mm
	03	2003/01/21	35-40 kg/m²	1.b	-	4.50 mm
	04	2003/02/18	30-35 kg/m²	1.a	-	16.20 mm
		2003/02/19	< 25 kg/m²		-	0.00 mm
	05	2003/02/21	40-45 kg/m²	1.a		113.60 mm
2005/2006	06	2005/12/25	35-40 kg/m²	1.a	-	64.30 mm
	07	2006/01/15	25-30 kg/m²	1.c	-	15.80 mm
	08	2006/01/26	35-40 kg/m²	1.c	-	N/A*
	09	2006/02/17	25-30 kg/m²	1.b	x	N/A
2006/2007	10	2006/12/08	30-35 kg/m²	1.b	-	N/A
	11	2007/02/14	25-30 kg/m²	1.a	-	0.00 mm
	12	2007/02/22	25-30 kg/m²	1.b	-	1.00 mm
2008/2009	13	2008/12/30	30-35 kg/m²	2	x	N/A
	14	2009/01/19	30-35 kg/m²	1.b	-	4.70 mm
		2009/01/20	25-30 kg/m²		-	5.90 mm
	15	2009/01/24	30-35 kg/m²	1.b	-	0.30 mm
		2009/01/25	30-35 kg/m²		-	2.70 mm
	16	2009/01/30	35-40 kg/m²	1.a	-	27.00 mm
	17	2009/02/03	25-30 kg/m²	1.a	-	2.30 mm
2009/2010	18	2009/12/11	30-35 kg/m²	1.a	-	33.80 mm
	19	2009/12/15	35-40 kg/m²	1.a	-	129.20 mm
	20	2009/12/17	> 40 kg/m²	1.a	-	131.50 mm
	21	2009/12/22	N/A	1.a	x	127.70 mm
		2009/12/23	45-50 kg/m²		-	N/A
	22	2009/12/28	40-45 kg/m²	1.a	-	135.10 mm
	23	2010/01/02	35-40 kg/m²	1.a	-	169.70 mm
	24	2010/02/07	30-35 kg/m²	1.a	-	7.30 mm
	25	2010/02/14	35-40 kg/m²	1.a	-	103.30 mm
	26	2010/02/20	> 50 kg/m²	1.a	-	387.10 mm
	27	2010/02/26	35-40 kg/m²	1.a	-	53.10 mm
		2010/02/27	35-40 kg/m²		-	N/A
2010/2011	28	2010/12/04	45-50 kg/m²	2	-	80.50 mm
	29	2010/12/27	35-40 kg/m²	1.a	-	37.40 mm
	30	2011/01/06	30-35 kg/m²	1.a	-	79.10 mm
	31	2011/02/13	30-35 kg/m²	1.c	-	4.70 mm
	32	2011/02/19	30-35 kg/m²	1.a	-	13.20 mm

*Not available (N/A)

TYPE 1: Narrow corridors (a few hundred kilometres wide and thousands of kilometres long). Moisture source is identified as being over the Caribbean Sea, and the filamentary structure extended, in some cases, up to latitudes higher than 50°N,

supporting the suggestion of intense water vapour transport from the tropical zone towards the Pole.

This pattern may be divided into three types because of the same configuration (narrow corridors, source in the Caribbean Sea), but with different paths. Pattern TYPE 1a (Figure 2.5a) is characterised by a south-west to north-east orientation over the island, and therefore, a typical south-westerly flow. With the second type identified (TYPE 1b; Figure 2.5b), vapour originating in the Caribbean reaches the island as a westerly flow, established around the latitude of 30°N. Sometimes, the displacement of drier air masses from higher latitudes to the subtropical zones creates a meridional undulation of this narrow westerly flow, also characterized like Type 1b, and creating a type of valley. When this feature is observed, the filamentary structure is observed passing over the island as a south-westerly flow, which is generally weaker than when the transport system is of Type 1a (Figure 2.5a). This configuration represents Type 1c (Figure 2.5c).

TYPE 2: This pattern, unlike the first type, seems to be associated with a cyclonic circulation, centred near the Azores archipelago, north-west of Madeira. In this configuration (Figure 2.5d), the aspect of a WCB is clearer than with the first type, which may be associated with extra-tropical cyclones centred in higher latitudes. Rather than narrow bands, this type of transport system occurs as a structure whose length is greater than its width, which is clearly visible, transporting large amounts of precipitable water vapour from lower latitudes. With this pattern, the source of water vapour is located in the central to eastern part of the Tropical Atlantic Ocean. The atmospheric river also passes over the island as a south to south-westerly flow, moreover, being more latitudinal than meridional.

Each atmospheric river episode presented in Table 2.1 was classified as one of these two types, and the result of this classification is also shown in the table. Analysis highlights the fact that Type 1 occurred more frequently than Type 2, which was identified as reaching the island only three times, while Type 1 was identified as such 29 times, considering all three sub-types.
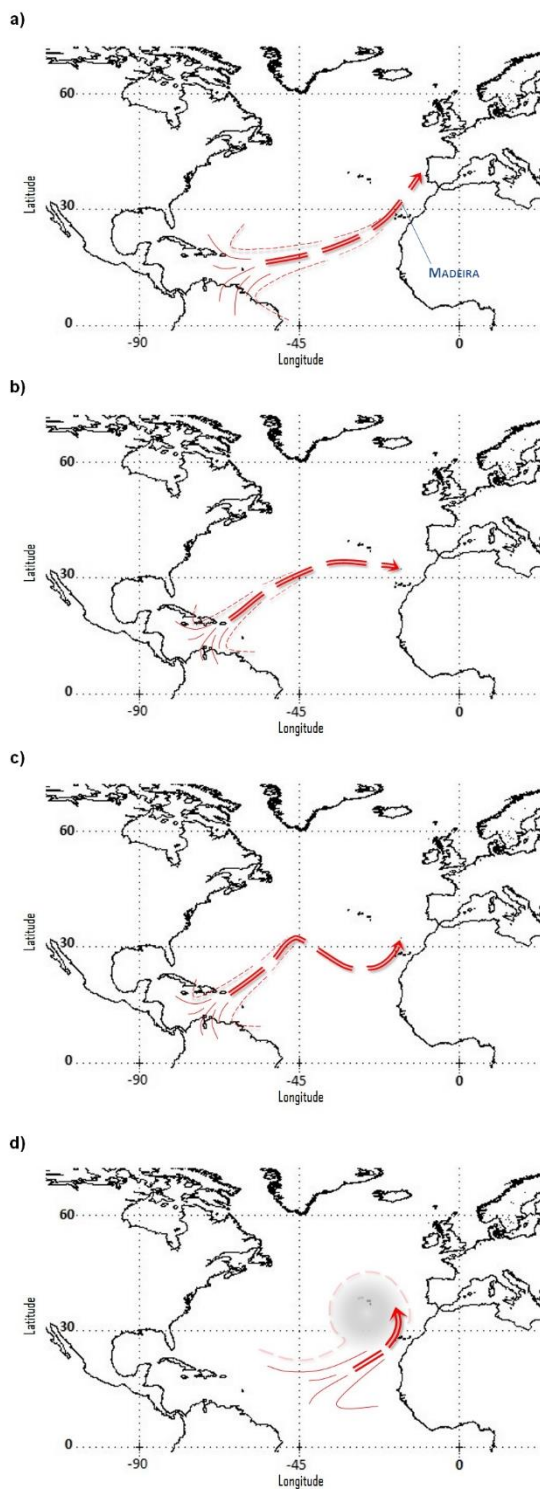
Figure 2.5 *Patterns of the meridional water vapour transport that reached Madeira Island during the winter seasons considered. TYPE 1: Narrow corridors presenting over the island a (a) south-westerly flow – Type 1a, (b) westerly flow – Type 1b, (c) south-westerly flow – Type 1c; TYPE 2: Warm conveyor belt presenting a (d) south or south-westerly flow.*

30

To summarise, the results show that during the winter seasons studied, tropical moisture transported by means of ARs occasionally reaches Madeira, presenting a range of different intensities and orientations. For a transport system occurrence such as Type 1, total precipitable water vapour of $25 - 35$ kg m^{-2} over Madeira is frequently identified. However, sometimes amounts observed are greater, and these filamentary structures present values of greater than 40 kg m^{-2} for central regions (observed mainly for Type 1a). On the other hand, the second type, which occurs less frequently, was associated with total precipitable water vapour values of above 30 kg m^{-2}.

2.3.3 Atmospheric rivers and precipitation in Madeira

The relationship between the AR events over Madeira and accumulated precipitation at Areeiro station is presented in this sub-section.

The daily precipitation recorded on each day with the occurrence of ARs is shown in Table 2.1. Comparing the results obtained in Sub-sections 2.3.1 and 2.3.2, only one of the three winter cases of extreme accumulated precipitation may be associated with meridional water vapour transport from the tropical region. In cases of a high level of daily accumulated precipitation ($100 - 200$ mm), subjective analysis shows that 8 of the 17 episodes were favoured by atmospheric rivers. Apparently, episodes with lower daily accumulated values were not greatly influenced by this means of transport: of 34 episodes with daily precipitation of $50 - 100$ mm, only 5 were related to atmospheric rivers, while only 3 of the 42 cases with daily accumulated values of $25 - 50$ mm were associated with the water vapour transport occurring in the form of ARs during the period. In six cases of the occurrence of ARs over Madeira, precipitation was not measured at the Areeiro station. However, precipitation was recorded in other places on the island on these days. For the rest of AR episodes, daily accumulated precipitation at Areeiro was lower than 25 mm or zero. Overall, these results show that the impact of ARs on accumulated precipitation in the winter season during the 2002-2011 period was not as great as is suggested by occurrences in the winter of 2009-2010, studied by Couto et al. (2012). It should be noted that on days with no AIRS observations (see Section 2.2.2), no significant precipitation was observed at Areeiro.

In order to simplify the results, episodes which were representative of the range of ways in which meridional water vapour can reach Madeira were selected along with their impact on accumulated precipitation.

For the winter of 2009-2010, some cases of ARs were already identified by Couto et al. (2012); however, the 20 February 2010 episode should be highlighted. As already mentioned, the passage of ARs favoured the occurrence of flash floods and landslides in some places on the island. Figure 2.6a shows the configuration of the precipitable water vapour field for this episode, and it can be observed that the transport of water vapour from the Caribbean Sea to Madeira occurred showing values of over 50 kg m^{-2}, the highest values associated with atmospheric rivers identified during the 10-year period, following a south-westerly direction (Type 1a; Figure 2.5a). This AR favoured the occurrence of extreme accumulated precipitation of 387.10 mm at Areeiro, or perhaps even more because the station failed to record data in the evening.

Another case presenting a configuration similar to that of 20 February 2010, but with lower amounts of precipitable water vapour, was identified on 25 December 2005 (Figure 2.6b). The south-westerly flow over the island presenting amounts of 35 – 40 kg m^{-2} favoured daily accumulated precipitation of 64.30 mm.

Two examples of transport of Types 1b and 1c are presented in Figure 2.6c and 2.6d, respectively. Associated with total precipitable water vapour of 35 – 40 kg m^{-2}, the environment created by the passage of the atmospheric river on 21 January 2003 (Figure 2.6c) favoured a very low value of accumulated rainfall at Areeiro (4.50 mm). Similarly, a daily accumulated precipitation of 4.70 mm was observed during the atmospheric river event identified on 13 February 2011 (Figure 2.6d), which contained precipitable water vapour amounts of 30 – 35 kg m^{-2}.

In the last example, Figure 2.6e, the precipitable water vapour field observed on 16 December 2002 clearly shows the presence of a structure of Type 2 (Figure 2.5d). In this case, moisture was transported to Madeira from the central part of the Tropical Atlantic Ocean, and with total precipitable water vapour of 40 kg m^{-2} near Madeira. At surface level, the Areeiro station recorded accumulated rainfall of 124.30 mm. Another example of a Type 2 structure is shown in Figure 2.3. In this case precipitation was not measured at Areeiro, but it was observed in other places on the island (not shown here), indicating that the presence of ARs favoured precipitation in this case as well.
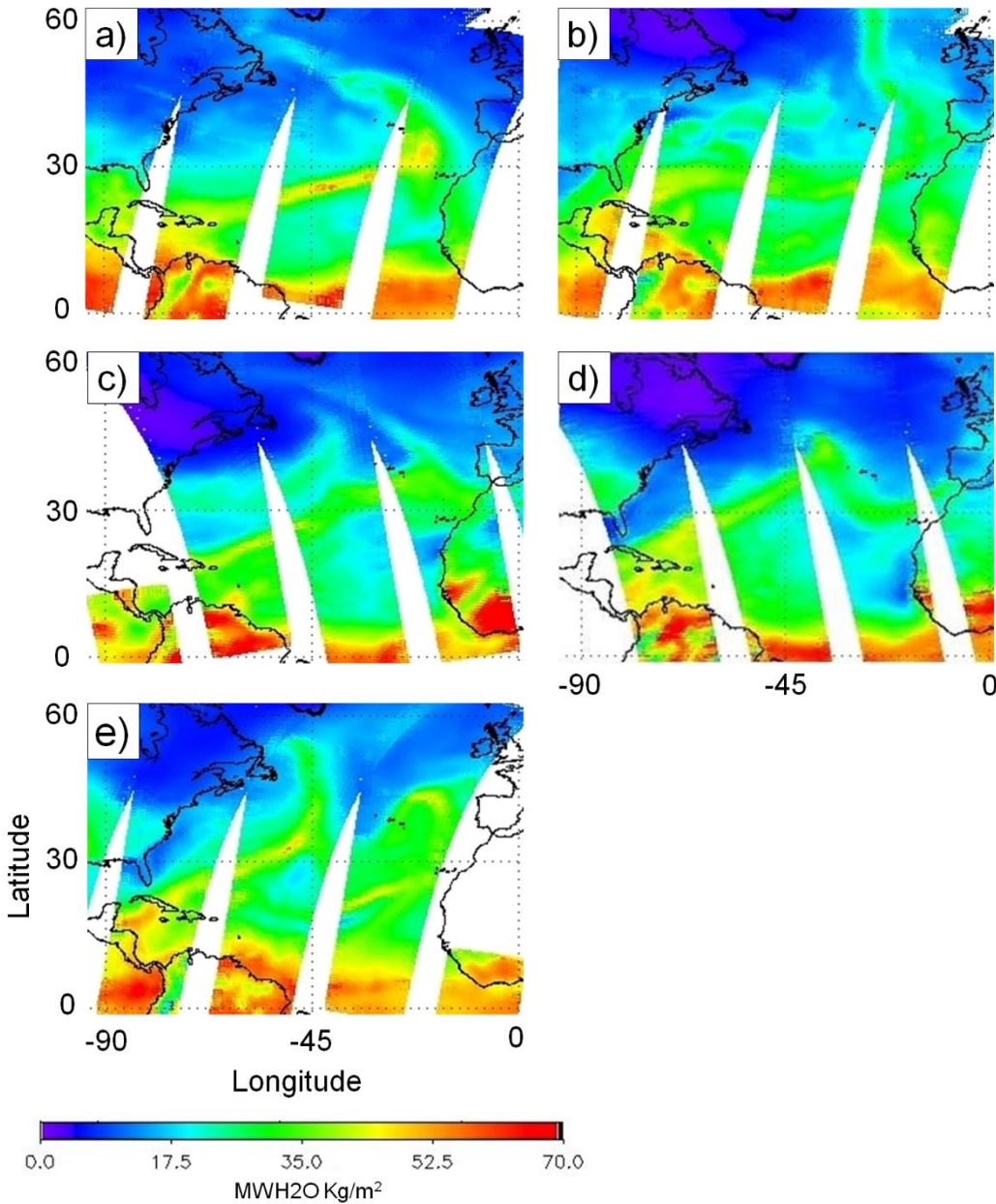
Figure 2.6 *Atmospheric river episodes on (a) 20 February 2010 at 0759 UTC, (b) 25 December 2005 at 0741 UTC, (c) 21 January 2003 at 1859 UTC, (d) 13 February 2011 at 1823 UTC, and (e) 16 December 2002 at 0841 UTC. The satellite images represent the precipitable water vapour (kg/m²) obtained from the Atmospheric Infrared Sounder (Aqua-AIRS).*

The results indicate that the impact of an atmospheric river on precipitation in Madeira depends not only on the amount of water vapour transported to the island but also on the type of AR. From the patterns shown in the Section 2.3.2, it can be seen that AR Type 2 favoured significant precipitation in Madeira's highlands, even if it is less

frequent than Type 1. On the other hand, the patterns associated with Types 1b and 1c were associated with the lowest daily accumulated values, even in cases where the amount of precipitable water vapour was around 35 kg m^{-2}. Type 1a cases with precipitable water vapour amounts of above 40 kg m^{-2} favoured high precipitation events, presenting surface daily accumulated values of 50 – 200 mm. This study suggests that for an atmospheric river to favour significant accumulated precipitation in Madeira during the winter it should contain precipitable water vapour amounts of over 40 kg m^{-2}.

2.4. CONCLUSIONS

This paper analyses the main aspects of the precipitation in the highlands of Madeira over a 10 year period. Features associated with meridional water vapour transport occurring in narrow bands with high levels of precipitable water vapour, also known as atmospheric rivers, and their impact on the precipitation recorded in Madeira during 10 winter periods, are also presented.

Daily accumulated precipitation at surface level shows generally dry summers, while the highest accumulated precipitation are recorded mainly during the winter, although some significant events may occur in the spring and autumn. The winter of 2009-2010 was the wettest season during the period of study, and the wettest autumn was observed in 2012, both showing seasonal accumulated precipitation of over 2000 mm, higher than the seasonal average. The occurrence of these maximums in the last years may be associated with climate variability or change, however, this point deserves more attention in future studies about the precipitation over the island with longer data series.

Meridional water vapour transport was analysed on the basis of AIRS data because atmospheric river structures are easily identifiable from this type of observation. Sometimes water vapour transported by means of AR reaches the island, creating a favourable environment for intense precipitation occurrences, which may lead to episodes with the magnitude of the disaster of 20 February 2010.

Precipitable water vapour field patterns reaching the island as ARs were investigated, and although most ARs reach the island in a stage of dissipation, showing low precipitable water vapour values, some are strong enough to reach Madeira, configured as filamentary structures presenting a large amount of precipitable water vapour. Two main types of AR may be observed carrying a significant amount of water

vapour to the island from the tropics. As presented in Figure 2.5, these two types were classified as narrow corridors, Type 1 (and according to their orientation over the island they were sub-classified as Type 1a, 1b, and 1c), and Type 2, reminiscent of WCB structures. In this study the source of high amounts of precipitable water vapour was identified as being mainly over the Caribbean Sea region (Type 1), although moist air masses from the central part of the Tropical Atlantic were also identified as being transported to the island (Type 2).

From a comparison of daily accumulated precipitation measurements and the presence of atmospheric rivers over the island, it is clear that the larger the amount of water vapour transported by atmospheric rivers, the greater the likelihood of the occurrence of intense to extreme precipitation events over the island. As a result of this study it was found that atmospheric rivers transporting precipitable water vapour levels of at least 40 kg m^{-2} favoured the occurrence of high levels of accumulated precipitation during the winter, especially if they were of Type 1a, with a south-west to north-east orientation over the island. Type 2 ARs were associated with heavy rainfall for all days on which they were identified. Atmospheric rivers with smaller amounts of precipitable water did not favour significant precipitation. Generally, AR Types 1b and 1c pass over the island when they are already in a stage of dissipation and do not favour the occurrence of intense precipitation. In the winter of 2009-2010, moisture transport over Madeira associated with atmospheric rivers was more intense and frequent, and was of crucial importance for the occurrence of significant precipitation over the island, as concluded in a previous study (Couto et al., 2012). However, considering the 10-winter period focused on in this paper, it may be concluded that atmospheric rivers were not the sole factor affecting the onset of intense precipitation events.

Therefore, the results of this study lead to the conclusion that atmospheric rivers, when associated with large amounts of precipitable water vapour over the island of Madeira may provide favourable conditions for the development of precipitation and are sometimes associated with high levels of rainfall. In addition, in accordance with the results of this study and those of previous studies carried out on high precipitation events in Madeira, it is suggested that the wind speed associated with this meridional transport should be the object of further study because the speed at which this flow reaches the island may be very important in triggering certain physical processes at the scale of the island. The efficiency of the topography of the island in converting precipitable water into

precipitation should also be further investigated. It is also suggested that an objective analysis of these structures should be made using an automatic method.

Finally, it was found that many cases of high to extreme levels of accumulated precipitation at surface level were not associated with the AR. This provides a motivation for future research into precipitation in Madeira, which could provide an improved understanding of the environments favouring the occurrence of significant precipitation in the region, looking at other factors besides atmospheric river transport concept. The findings of this study may be of use for future studies of significant precipitation events in Madeira.

REFERENCES

Aumann HH, Chahine MT, Gautier C, Goldberg MD, Kalnay E, McMillin LM, Revercomb H, Rosenkranz PW, Smith WL, Staelin DH, Strow LL, Susskind J. 2003. AIRS/AMSU/HSB on the Aqua mission: design, science objectives, data products and processing system, *IEEE Trans. Geosci. and Remote Sensing*, 41, 253-264.

Baioni D. 2011. Human activity and damaging landslides and floods on Madeira Island, *Nat. Hazards Earth Syst. Sci.*, 11, 3035-3046, doi:10.5194/nhess-11-3035-2011.

Carlson TN. 1991. Mid-latitude Weather Systems. Harper Collins Academic.

Couto FT, Salgado R, Costa MJ. 2012. Analysis of intense rainfall events on Madeira Island during the 2009/2010 winter, *Nat. Hazards Earth Syst. Sci.*, 12, 2225-2240, doi:10.5194/nhess-12-2225-2012.

Dasari HP, Salgado R. Numerical modelling of heavy rainfall event over Madeira Island in Portugal: sensitivity to different micro physical processes. *Met. Apps*, n/a. doi: 10.1002/met.1375.

Fragoso M, Trigo RM, Pinto JG, Lopes S, Lopes A, Ulbrich S, Magro C. 2012. The 20 February 2010 Madeira flash-floods: synoptic analysis and extreme rainfall assessment, *Nat. Hazards Earth Syst. Sci.*, 12, 715-730, doi:10.5194/nhess-12-715-2012.

Guan B, Molotch NP, Waliser DE, Fetzer EJ, Neiman PJ. 2010. Extreme snowfall events linked to atmospheric rivers and surface air temperature via satellite measurements, *Geophys. Res. Lett.*, 37, L20401, doi:10.1029/2010GL044696.

Houze RA Jr. 2012. Orographic effects on precipitating clouds, *Rev. Geophys.*, 50, RG1001, doi:10.1029/2011RG000365.

Kim J, Waliser DE, Neiman PJ, Guan B, Ryoo J-M, Wick GA. 2012. Effects of atmospheric river landfalls on the cold season precipitation in California. *Climate Dynamics*, 40, 465-474, doi: 10.1007/s00382-012-1322-3.

Lavers DA, Allan RP, Wood EF, Villarini G, Brayshaw DJ, Wade AJ. 2011. Winter floods in Britain are connected to atmospheric rivers, *Geophys. Res. Lett.*, 38, L23803, doi:10.1029/2011GL049783.

Lavers DA, Villarini G, Allan RP, Wood EF, Wade AJ. 2012. The detection of atmospheric rivers in atmospheric reanalyses and their links to British winter floods and the large-scale climatic circulation, *J. Geophys. Res.*, 117, D20106, doi:10.1029/2012JD018027.

Lavers DA, Allan RP, Villarini G, Lloyd-Hughes B, Brayshaw DJ, Wade AJ. 2013. Future changes in atmospheric rivers and their implications for winter flooding in Britain, *Environmental Research Letters*, 8 034010 doi:10.1088/1748-9326/8/3/034010.

Levizzani V, Laviola S, Cattani E, Costa MJ. 2013. Extreme precipitation on the Island of Madeira on 20 February 2010 as seen by satellite passive microwave sounders. *European Journal of Remote Sensing*, 46: 475-489, doi: 10.5721/EuJRS20134628.

Lira C, Lousada M, Falcão AP, Gonçalves AB, Heleno S, Matias M, Pereira MJ, Pina P, Sousa AJ, Oliveira R, Almeida AB. 2013. The 20 February 2010 Madeira Island flash-floods: VHR satellite imagery processing in support of landslide inventory and sediment budget assessment, *Nat. Hazards Earth Syst. Sci.*, 13, 709-719, doi:10.5194/nhess-13-709-2013.

Luna T, Rocha A, Carvalho AC, Ferreira JA, Sousa J. 2011. Modelling the extreme precipitation event over Madeira Island on 20 February 2010, *Nat. Hazards Earth Syst. Sci.*, 11, 2437-2452, doi:10.5194/nhess-11-2437-2011.

Neiman PJ, Ralph FM, Wick GA, Kuo Y-H, Wee T-K, Ma Z, Taylor GH, Dettinger MD. 2008a. Diagnosis of an intense atmospheric river impacting the Pacific Northwest: Storm summary and offshore vertical structure observed with COSMIC satellite retrievals. *Mon. Wea. Rev.*, 136, 4398-4420, doi:10.1175/2008MWR2550.1.

Neiman PJ, Ralph FM, Wick GA, Lundquist J, Dettinger MD. 2008b. Meteorological characteristics and overland precipitation impacts of atmospheric rivers affecting the West Coast of North America based on eight years of SSM/I satellite observations. *J. Hydrometeor.*, 9, 22-47, doi:10.1175/2007JHM855.1.

Olsen ET, and Contributors. 2007. AIRS/AMSU/HSB Version 5 data release user guide, Jet Propulsion Laboratory, pp. 68. http://disc.sci.gsfc.nasa.gov/AIRS/documentation.

Parkinson CL, Ward A, King MD, and editors. 2006. Earth Science Reference Handbook: A Guide to NASA's Earth Science Program and Earth Observing Satellite Missions. Washington, D.C.: National Aeronautics and Space Administration.

Ralph FM, Neiman PJ, Wick GA. 2004. Satellite and CALJET aircraft observations of atmospheric rivers over the eastern North-Pacific Ocean during the winter of 1997/98. *Mon. Wea. Rev.*, 132, 1721-1745, doi:10.1175/1520-0493(2004)132<1721:SACAOO>2.0.CO;2.

Ralph FM, Neiman PJ, Wick GA, Gutman SI, Dettinger MD, Cayan DR, White AB, 2006: Flooding on California's Russian River: Role of atmospheric rivers. *Geophys. Res. Lett.*, 33, L13801, doi: 10.1029/2006GL026689.

Teixeira JC, Carvalho AC, Carvalho MJ, Luna T, Rocha A. 2014. Sensitivity of the WRF model to the lower boundary in an extreme precipitation event – Madeira island case study, *Nat. Hazards Earth Syst. Sci.*, 14, 2009-2025, doi:10.5194/nhess-14-2009-2014.

Wick GA, Neiman PJ, Ralph FM. 2013. Description and validation of an automated objective technique for identification and characterization of the integrated water vapor signature of atmospheric rivers. *IEEE Trans. Geosci. Remote Sens.*, 51, 2166–2176.

Zhu Y, Newell RE. 1994. Atmospheric Rivers and bombs. *Geophys. Res. Lett.*, 21, 1999-2002.

Zhu Y, Newell RE. 1998. A proposed algorithm for moisture fluxes from atmospheric rivers. *Mon. Wea. Rev.*, 126, 725-735, doi:10.1175/1520-0493(1998)126<0725:APAFMF>2.0.CO;2.

CHAPTER 3 – NUMERICAL SIMULATIONS OF SIGNIFICANT OROGRAPHIC PRECIPITATION IN MADEIRA ISLAND[†]

Abstract

High-resolution simulations of high precipitation events with the MESO-NH model are presented, and also used to verify that increasing horizontal resolution in zones of complex orography, such as in Madeira island, improve the simulation of the spatial distribution and total precipitation. The simulations succeeded in reproducing the general structure of the cloudy systems over the ocean in the four periods considered of significant accumulated precipitation. The accumulated precipitation over the Madeira was better represented with the 0.5 km horizontal resolution and occurred under four distinct synoptic situations. Different spatial patterns of the rainfall distribution over the Madeira have been identified.

Keywords: MESO-NH model, orographic precipitation, Madeira island.

3.1. INTRODUCTION

Heavy precipitation events are one of the major factors inducing floods, which leads to the constant improvement in numerical models and measurement techniques, also reported from several studies worldwide. Accurately representing precipitation systems in atmospheric models is still however challenging, and better forecasts are mandatory to issue early warnings mainly for urban areas. The general environments causing heavy precipitation are well documented for many regions around the world (e.g. Lin et al., 2001), however, the increase of the knowledge about these heavy events on specific regions is needed, for example, over small mountainous and island regions.

The impact of the orography in the formation or enhancement of the precipitation over mountainous islands have been found dependent of the geographic aspects of the island and synoptic conditions associated to each precipitating event (e.g. Wang et al., 2014a, Smith et al., 2012). For example, Wang et al. (2014b), studying two heavy precipitation events over Taiwan showed that the synoptic circulation was dominant over the diurnal effects, and the steep topography of Taiwan was essential to increase the rainfall amount over and near Taiwan. On the other hand, heavy precipitation events may also be induced by several orographic effects. Chen et al. (2010, 2011) identified that orographic lifting and convergence at low-levels caused by the flow deflection due the local orography was related to other precipitation events over Taiwan. In Jeju island, for example, the orographic blocking inducing convergence zones or the intensification of convective cells in the lee side of the elliptical island were some mechanisms favouring heavy precipitation (Lee et al., 2010, 2014).

More attention has been dedicated to the study of precipitation over the Madeira island, a mountainous Portuguese island located in the mid-latitudes (32°75'N and 17°W), after the disaster on February 20, 2010 (e.g., Luna et al., 2011; Levizzani et al., 2013). It was the most remarkable event in terms of heavy precipitation observed in Madeira, with high impact at the surface. The study of the winter 2009/2010 by Couto et al. (2012) highlighted the role of an atmospheric river in six out of the seven cases of heavy precipitation over the island, providing significant amount of water vapour from the tropics for the triggering or enhancement of precipitation by the island terrain. Couto et al. (2015) further examined the characteristics of the synoptic environment by carrying out a 10-year analysis of precipitation over the island and satellite water vapour fields over the Atlantic Ocean during the winter periods. They found that atmospheric rivers when transporting large amounts of precipitable water, are well correlated with heavy precipitation occurrence over the island. However, there are many other heavy precipitation events over the island that are not favoured by atmospheric rivers, but extra-tropical weather systems. In order to further study heavy precipitation over Madeira associated with extra-tropical weather systems, the same approach as in Couto et al. (2012) is followed by simulating all the heavy precipitation events of autumn 2012, the second wettest season in the 10-year period studied by Couto et al. (2015).

The first aim of this paper is to present these high-resolution simulations and their performance. Contrary to Couto et al. (2012), the convection-permitting simulations are

performed in the present study over large model domains (Figure 3.1) in order not only to describe at high-resolution convection and precipitation enhancement over the Madeira island but also the associated larger-scale cloudy weather systems over the surrounding ocean region.
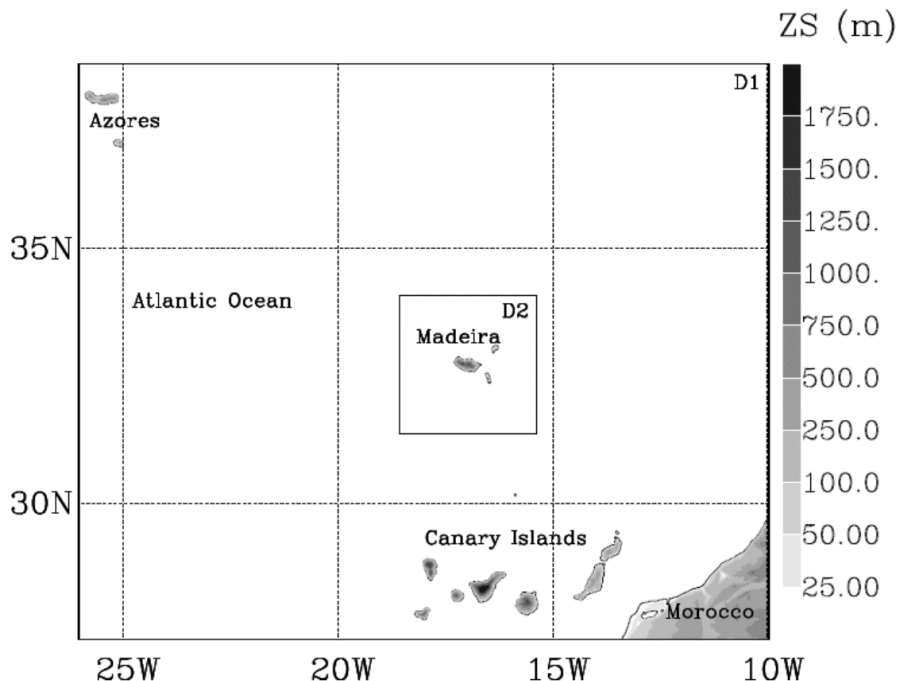
Figure 3.1 *Location of the Madeira island and the MESO-NH configuration. The larger domain (D1) at 2.5 km horizontal resolution, and the inner domain (D2) at 0.5 km grid spacing. The orography was obtained from the SRTM database.*

The Madeira island is a small island (58 km x 23 km), characterized by an east-west mountain chain with peaks above 1800 m. It is thus expected that the simulation of the precipitation distribution over the mountainous island will require a proper horizontal resolution able to describe the main terrain features of the island. The second aim of the study is thus to verify that increasing horizontal resolution in zones of complex orography, such as in Madeira island, improve the simulation of the spatial distribution and total precipitation.

This article is divided into four sections as follows. The data, numerical experiments and methodology are described in Section 3.2, followed by the results and discussion in Section 3.3, and conclusions in Section 3.4.

3.2. DATA, NUMERICAL EXPERIMENTS AND METHODOLOGY

The observed precipitation over the 2012 autumn was characterized using the 12 meteorological stations (Ponta do Sol (986), Quinta Grande (984), Areeiro (973), Santo da Serra (975), Funchal (522), Caniçal (978), Calheta (990), Lombo da terça (980), Bica da Cana (970), São Vicente (967), Santana (965), and Santana/ S. Jorge (960)), and distributed over the island and belonging to the Portuguese Sea and Atmosphere Institute, IPMA (no weather radar covering the island). The Areeiro weather station (see Figure 3.5c), located in the South-eastern part of the island (altitude of 1590 m, close to the maximum height), allowed us to highlight the 2012 seasonal distribution of the daily precipitation, and to select the precipitating periods that have been simulated in this study (Figure 3.2a). The second part of the season was more propitious to heavy precipitation events, with rainfall exceeding 100 mm day^{-1} in four days. These four events have thus been selected for this study, and simulations of the periods encompassing them have been designed. Table 3.1 indicates the start and end of each simulation.

The numerical simulations are performed using the non-hydrostatic research model MESO-NH (Lafore et al., 1998). The initial and boundary conditions are provided by the 6-hourly operational ARPEGE analyses (Courtier et al., 1991). A first series of simulations (called hereafter CTRL) are performed using a 1500 km x 1250 km grid domain (D1) at 2.5 km horizontal resolution. For the second series of simulations (called hereafter EXP) a two-way interactive inner domain (D2) at 500 m horizontal resolution is added prior to the start of the heavy precipitation period (Figure 3.1). In the CTRL simulations, the model terrain is obtained from the GTOPO30 database, whereas in the EXP simulations it is obtained from the SRTM database. The periods simulated are shown in Figure 3.2b-3.2e. The dashed-line rectangles in blue and green represent the simulations with 2.5 km (CTRL and EXPD1) and 0.5 km (EXPD2) resolution, respectively. The inner domain is centered over the Madeira island, covering an area of 300 km x 300 km. The vertical grid is composed of 55 height-based terrain-following levels. With respect to the previous study of Couto et al. (2012), the horizontal resolutions are increased (3km/1km comparing to 2.5km/0.5km here) but the main difference are mostly the larger model domains considered, with about 100 times more grid-points for each domain. More realistic simulations are thus not only expected for precipitation enhanced by the island orography but also for the larger-scale precipitating systems affecting the island.

The physical package is rather similar to the ones successfully used in past studies of heavy precipitation events over complex terrain (e.g. Ducrocq et al., 2008). The model is also able to correctly reproduce the microphysical pattern and dynamical structure of convective systems (e.g., Cohuet et al., 2011; Pujol et al., 2011). The one-moment microphysical scheme predicts the mass mixing ratios of cloud water, rain, graupel, snow, and ice (ICE3; Pinty and Jabouille, 1998). The turbulence scheme is based on a 1.5-order closure (Cuxart et al., 2000). Verrelle et al. (2015) pointed out the necessity to deal with horizontal turbulent fluxes at kilometric resolutions for grid mesh smaller than 2 km. Then, in the inner 500 m resolution domain, the full 3D turbulent fluxes scheme was activated, while in the 2.5 km domain only the vertical fluxes were considered. Shallow convection is parameterized according to Pergaud et al. (2009) for the 2.5-km domain only. The radiation parametrization is based on the Rapid Radiative Transfer Model (Mlawer et al., 1997).

It is well known that the density of raingauge observations is essential in order to achieve a good quantitative evaluation of the model performance to simulate the complex behaviour of the precipitation over a steep terrain. In our case, there are only observations on the island and with poor coverage in its mountainous interior. Nevertheless, the quality of the simulated accumulated precipitation in each event is assessed against raingauge observations qualitatively and quantitatively using correlation (r), Mean Error (ME), Mean Absolute Error (MAE), and Root Mean Square Error (RMSE), Wilks (2006).

Due to the so-called double-penalty effect, point validation sometimes presents high differences between the observed and high resolution simulated precipitation. Couto et al. (2012) compared, point to point, the temporal evolution of the simulated precipitation with observations. Here, besides the point validation, a very simple neighbourhood verification technique is applied. The assumption of this kind of non-traditional verification strategy is, as explained by Mittermaier (2014), that neighbouring forecast values are just (or nearly) as likely to provide the correct value of the single (central) forecast value. By considering a neighbourhood, a distribution of values is available instead of just one. A good review of spatial verification techniques that do not require the forecasts to exactly match the observations at fine scales may be found in Ebert (2008). In the present verification of event accumulated precipitation, square windows surrounding the observation points were considered, and all the gridded precipitation forecasts inside each window are collected and compared with the respective observed

value. The window area corresponds to 3x3 grid points in the 2.5 km resolution domain (CTRL and EXPD1), and 15x15 grid points in the inner domain at 0.5 km resolution (EXPD2). Within this area, the best simulated value ('best point', hereafter), is selected.

Meteosat Second Generation (MSG) Infrared (IR) 10.8 Brightness Temperature (BT) is used to evaluate the realism of the simulation of the larger-scale cloudy weather systems over the Atlantic Ocean. Chaboureau et al. (2008) showed the ability of the MESO-NH in forecasting cloud cover considering precipitation events over southern and northern Europe. The model infrared brightness temperature is simulated from the temperature, water vapour and hydrometeors using the radiative transfer code RTTOV (Radiative Transfer for Tiros Operational Vertical Sounder, Saunders et al., 2005). Finally, the radiosounding launched each day at the Funchal station (located in the southeast of the island) at 12 UTC is used to evaluate the model ambient conditions over the island.

Table 3.1 *Studied periods and time of model integration for each simulation.*

Study periods			Numerical experiments		
Period	Start	End	Time of run		
	Time/date	Time/date	CTRL	EXPD1	EXPD2
PERIOD 1	18 UTC – 21 October	18 UTC – 23 October	48 h	48 h	33 h
PERIOD 2	12 UTC – 29 October	18 UTC – 30 October	30 h	30 h	24 h
PERIOD 3	12 UTC – 04 November	18 UTC – 07 November	78 h	78 h	72 h
PERIOD 4	18 UTC – 23 November	12 UTC – 27 November	90 h	First 42 h	24 h

3.3. RESULTS AND DISCUSSION

In this section the four periods are presented separately, as well as a discussion of the main aspects found in each one.

3.3.1. Periods

3.3.1.1. Period 1 (21-23 October 2012): The synoptic situation is characterized by an upper-level cut-off deepening and progressing southward, toward the Azores archipelago, from 21 to 23 October (Figure 3.3a). Ahead, the frontal system extends from 50°N to 30°N with embedded deep convection triggered during the afternoon on 22 October and the day after (Figure 3.4a). The precipitation over the Madeira during this period is

associated with the passage of the frontal cloudy system over the island. The observed precipitation over the island was continuous along the entire period, with a weak to moderate rain rate, not exceeding 25 mm h^{-1} (Figure 3.2b).
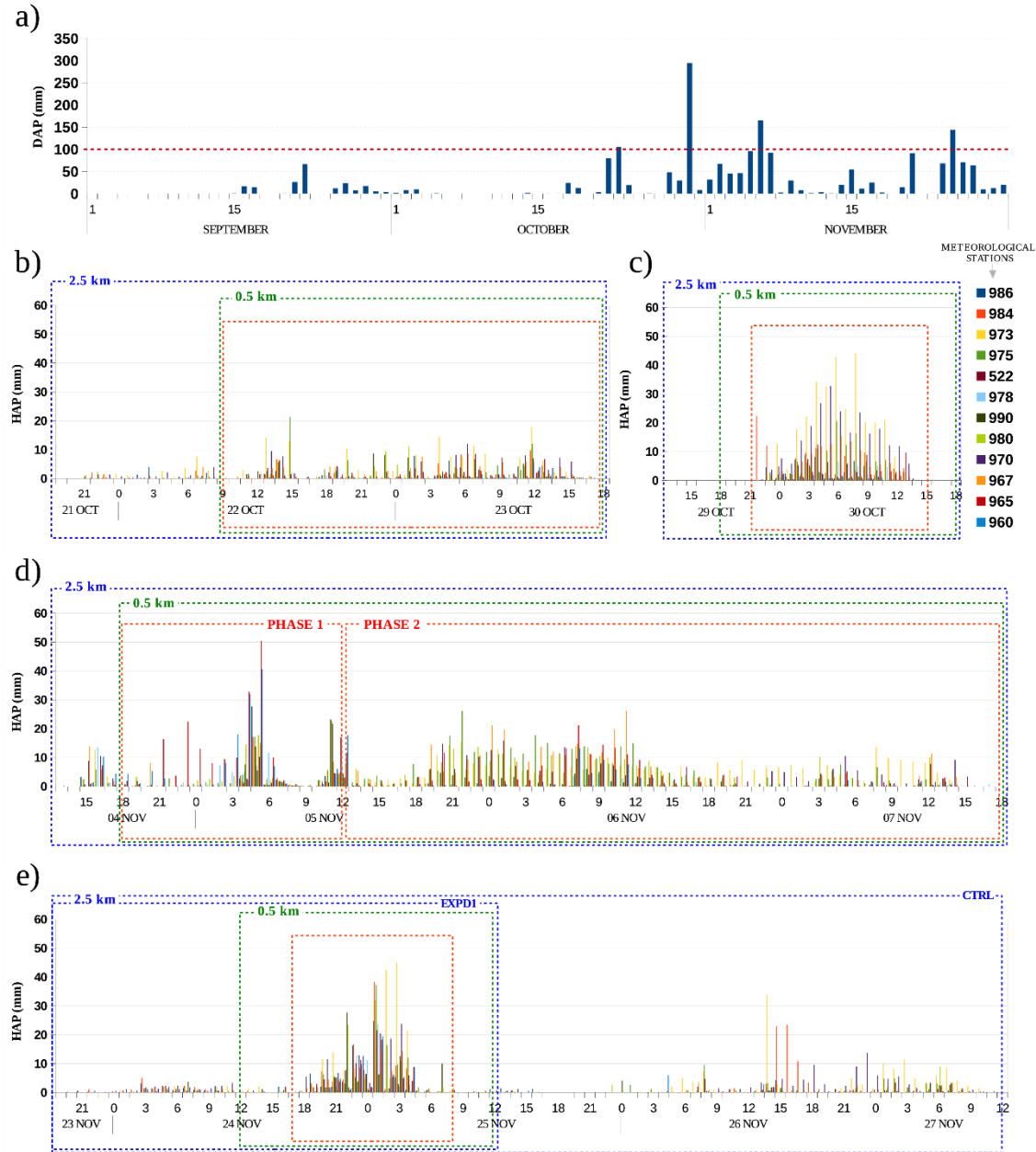
Figure 3.2 *Raingauge observations: (a) daily accumulated precipitation at Areeiro station during the autumn 2012; hourly accumulated precipitation at the meteorological stations (see text) during the (b) period 1, (c) period 2, (d) period 3, and (e) period 4. The simulated periods as described in Table 3.1 are represented as dashed-line blue and dashed-line green boxes for the 2.5-km and 0.5-km model domains, respectively. The dashed-line red boxes delineate the periods used for accumulated precipitation presented in Figure 3.5.*

45
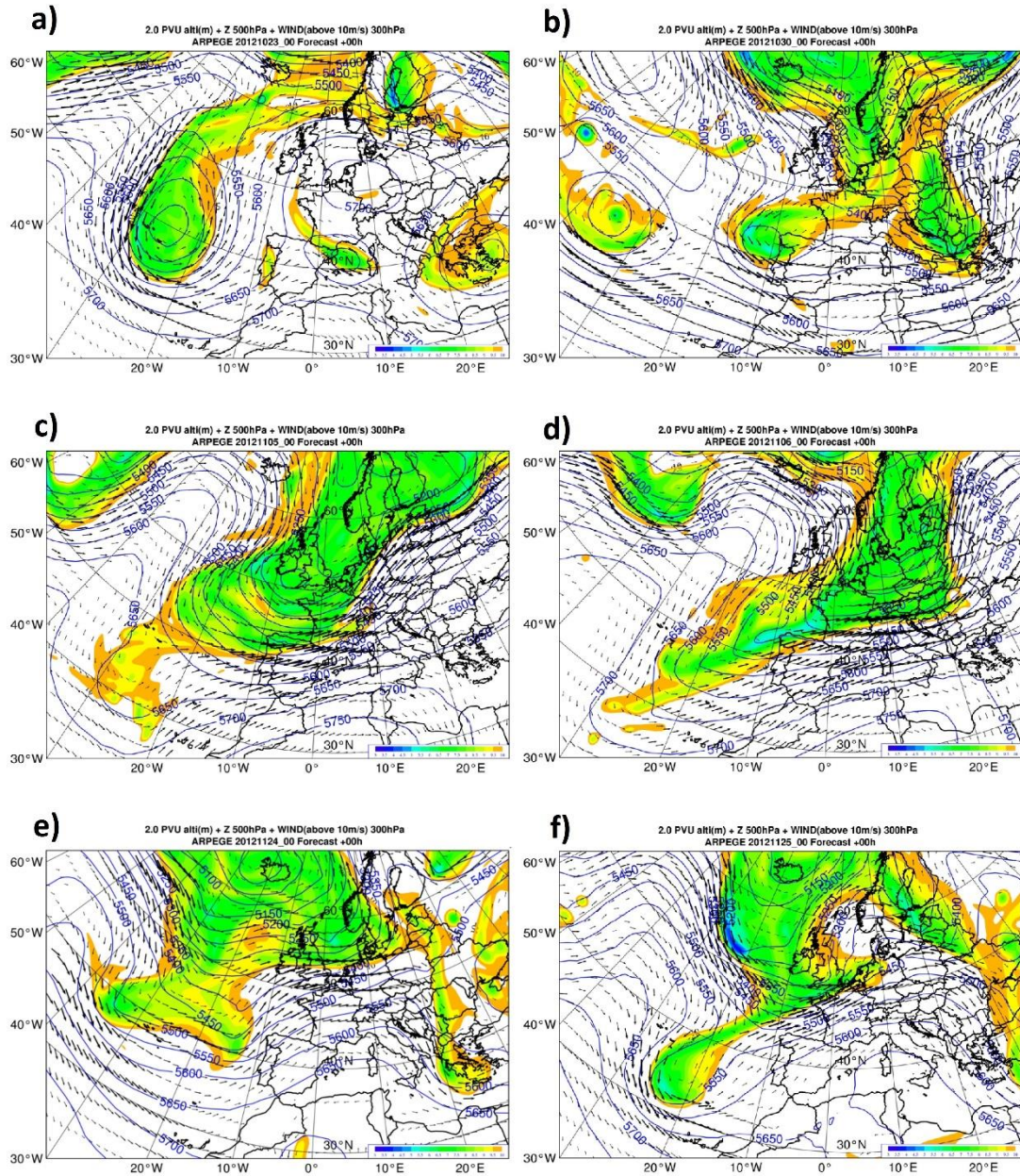
Figure 3.3 *Operational ARPEGE analyses at 0000 UTC with 2.0 PVU surface (shaded), geopotential height at 500 hPa (blue solid lines) and wind (arrows; above 10 m s⁻¹) at 300 hPa: (a) 23 Oct. 2012 (period 1); (b) 30 Oct. 2012 (period 2); (c) 05 Nov. 2012 (period 3 – PHASE 1); (d) 06 Nov. 2012 (period 3 – PHASE 2); (e) 24 Nov. 2012 (period 4); and (f) 25 Nov. 2012 (period 4).*

The CTRL and EXP simulations represent quite well the time evolution of the frontal system passage over the island. Figure 3.4a, b, and c show the observed and simulated IR brightness temperature when the front with embedded convection is over the island. The simulations represent the main patterns of the cloudy system, with slightly lesser post-frontal clouds.

Figure 3.5a, b, and c display the 33-h accumulated surface precipitation over the time-window indicated by the dashed-line red rectangle in Figure 3.2b. The impact of the terrain island on the simulated accumulated precipitation from CTRL and EXP is clearly evidenced, with precipitation totals above 100 mm for terrain height above 1000 m, also in agreement with the raingauge observations (Figure 3.5c). The EXP simulation and in a lesser extend the CTRL experiment globally overestimate the observed precipitation.

3.3.1.2. Period 2 (29-30 October 2012): This period was characterized by diffluent flow at 300 hPa over the Madeira island, associated with an upper level cut-off low centred 35°W/35°N (Figure 3.3b). A large disturbance is associated with the pressure low. The precipitation over the Madeira island is produced by the southern part of the disturbance which progressed eastward while broking away from the main frontal system. The comparison between the model and observed IR brightness temperature shows that both EXP and CTRL represent well the time evolution and extent of the disturbance (not shown).

The high amount of moisture in the lower troposphere was well simulated by the model when compared with the sounding at 12 UTC (Figure 3.6a). However, above about 2 km, the tropospheric moisture is underestimated in both CTRL and EXP simulations.

The heavy precipitation over the Madeira island occurred in less than 18 hours with records above 30 or even 40 mm h^{-1} in the highest stations (dashed-line red rectangle, Figure 3.2c). Both CTRL and EXP successfully captured the short extreme rainfall event with maxima over two distinct regions over the central mountains, more specifically over the southern slopes (Figure 3.5d, e, f). The maximum above 300 mm at Areeiro station was underestimated (eastern top, Figure 3.5f). The EXP simulation represented the precipitation better than CTRL over the eastern coast. Also, EXP simulates less weak precipitation over the Atlantic Ocean, which seems more in agreement with the raingauge observations along the northern coasts having recorded rain lesser than 25 mm.

3.3.1.3. Period 3 (04-07 November 2012): For this event, two phases are defined. The first phase corresponds to heavy precipitation in North/North-eastern (NE) regions of the island between 2000 UTC on 4 Nov. and 0700 UTC on 5 Nov. (Figure 3.2d), and from

0300 to 0500 UTC on 5 Nov. for other stations. The maximum intensities recorded at Santana stations are larger than 40 mm h^{-1} (0500 UTC – 05 Nov.). Another convective precipitation period occurred also between 1100 and 1200 UTC. The second phase is characterized by continuous precipitation over the island, more intense between 1800 UTC on 5 Nov. and 1200 UTC on 6 Nov., remaining relatively weak until the end of the period (7 Nov. 1800 UTC). Floods were observed on the northeastern side of the Madeira island. The analysis of the numerical results was performed according to this two phases called PHASE 1 and PHASE 2 hereafter (dashed-line red rectangles, Figure 3.2d).
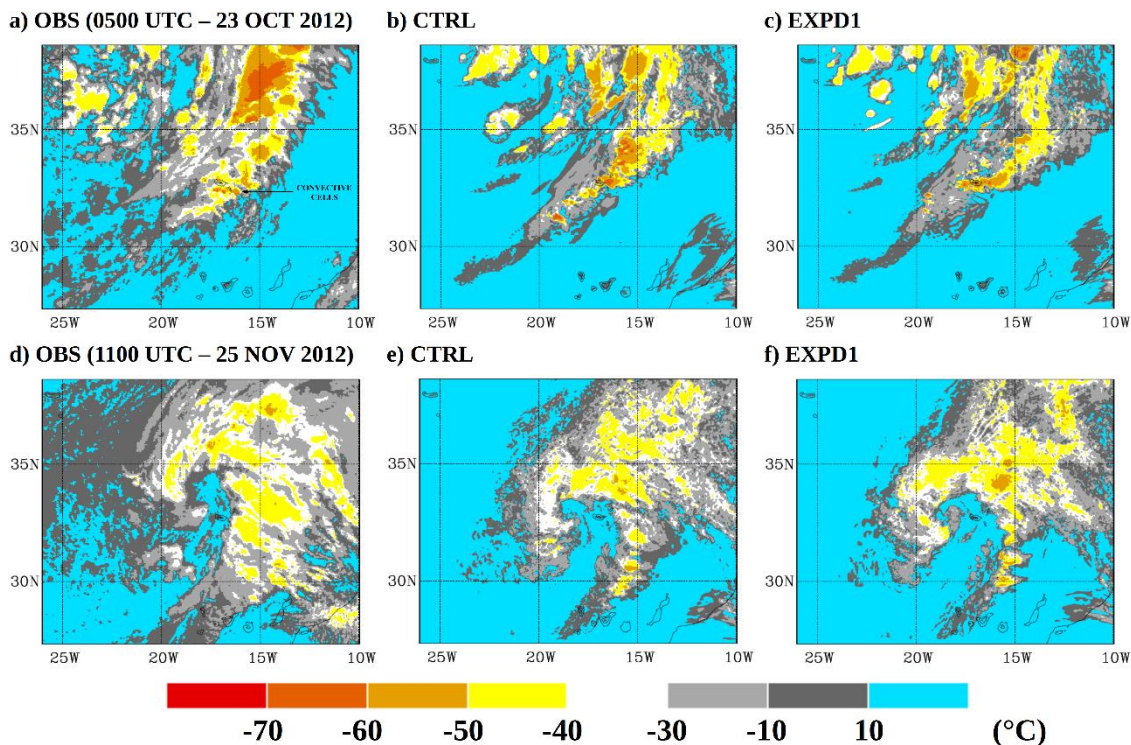
Figure 3.4 Infrared 10.8 µm brightness temperature (°C) obtained from the Meteosat Second Generation observation (left column), and simulated by CTRL (middle column) and EXP- domain D1 (right column) at 0500 UTC, 23 October 2012: (a), (b), and (c); at 1100 UTC, 25 November 2012: (d), (e) and (f).

The synoptic situation was characterized by an upper-level trough extending from Northern Europe to west of the Canary Islands (Figure 3.3c-d). Deep convection formed within the southern part of the cloud belt extending along the right side of the trough axis. The development of deep convection occurred over the ocean and sometimes, transported by the southwesterly flow, reached the island during PHASE 1, but not in PHASE 2. The

comparison between observed and simulated IR brightness temperature shows that the simulations capture well the two phases with a T-shape cloud cluster with embedded deep convection during PHASE 1 and elongated cloud systems, some of them being convective, during PHASE 2 (not shown).

The comparison with the radiosoundings shows a very good agreement between the simulations and observations for the moisture content during PHASE 2 (Figure 3.6c). During PHASE 1, the simulations underestimate the vapour mixing ratio at all levels (Figure 3.6b).

In PHASE 1 (Figure 3.5g, h, i), the very localised heavy precipitation in the NE of the island was simulated in both experiments, also coherent with the region where flood was reported in the late morning on 05 November. Unfortunately, there are no observations to evaluate the model performance for the maximum in the North-western region, but considering the NE maximum and most of the stations, the values measured and simulated are in good agreement (Figure 3.5i). For this event, the EXPD2 rainfall pattern evidences the usefulness of a better representation of the local orography for a more realistic result of the spatial distribution of the precipitation. The maximums between 200 and 300 mm are observed over the terrain slopes and in large part below a height of 500 m. This feature is not so well represented in the 2.5 km domains by CTRL, which underestimates the extent of precipitation over the island.

In PHASE 2 (Figure 3.5j, k, l), large amounts of accumulated precipitation were recorded during 54 hours and simulated over the central region of the island and extending northward over the ocean in the EXP simulations. The distribution of precipitation over the island as deduced from the observations is globally overestimated by the model, and in larger extend by the EXP simulation. It is worth mentioning that the simulations perform well although the long integration period (total of 78 h).

3.3.1.4. Period 4 (23-27 November 2012): It comprises a total of 90 hours (Figure 3.2e). However, we focus in this study on the period between 1700 UTC on 24 Nov. to 0800 UTC on 25 Nov. (dashed-line red rectangle, Figure 3.2e), when heavy rainfall was recorded with maxima above 30 mm h^{-1}, in some cases even 40 mm h^{-1}.
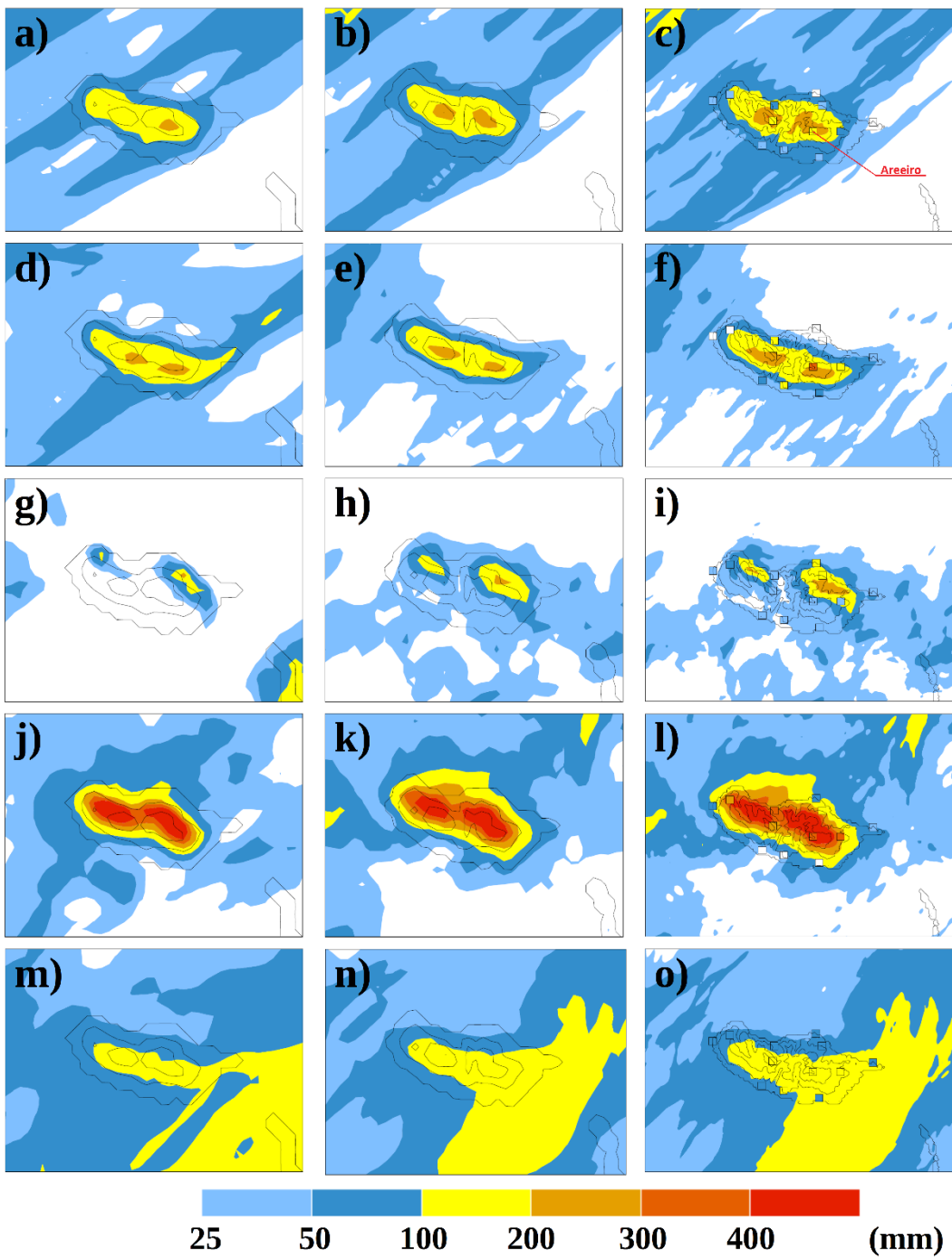
Figure 3.5 *Accumulated precipitation from MESO-NH (coloured areas) CTRL (left column), EXP- domain D1 (middle column), and EXP- domain D2 (right column) simulations during the periods highlighted in Figure 3.2b-3.2e (dashed-line red boxes): period 1: (a), (b), and (c); period 2: (d), (e), and (f); period 3: (g), (h), and (i) for PHASE 1, and (j), (k), and (l) for PHASE 2; and period 4: (m), (n) and (o). The squares in the right column represent the accumulated precipitation at the meteorological stations. The solid lines represent the model terrain (isoline interval: 500 m) obtained from the GTOPO30 database for CTRL (2.5 km resolution) and SRTM database for EXP (D1, 2.5 km resolution; D2, 0.5 km resolution).*

The convective clouds developed on the right side of an upper-level short wave trough associated to stratospheric air intrusion into the troposphere (Figure 3.3e-f), few hours before the clouds start to curve cyclonically. Figure 3.4d clearly shows the dry air intrusion and cloud presenting a spiral configuration in the centre of the cyclonic circulation. This structure is well represented in both simulations (Figure 3.4e-f), but more quickly developed in the EXPD1. The system had a rapid deepening and in the subsequent hours the cyclonic circulation throughout the troposphere was observed, with the cut-off low centred to the southward of the Madeira. The system moved to South-eastward, and dissipated toward the Canary archipelago.

The moisture content in the troposphere was well simulated on 24 Nov. (Figure 3.6d) and 25 Nov. (Figure 3.6e). However, in the latter the CTRL simulation overestimates the amounts at lower levels.
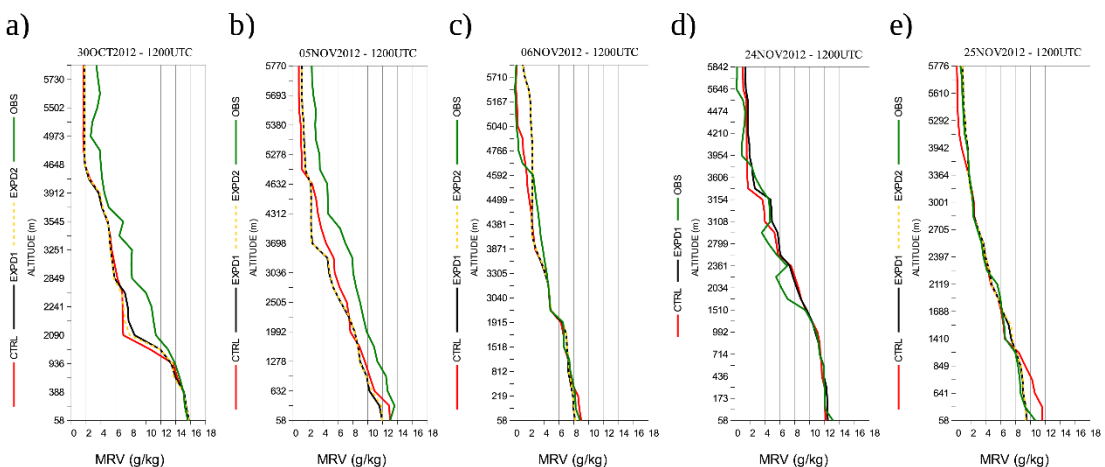
Figure 3.6 *Water vapour mixing ratio from the radiosoundings (OBS, green line) and simulations (CTRL, red line; EXPD1, blue line; EXPD2, yellow dashed-line) at 1200 UTC for (a) period 2 (30 Oct. 2012); (b) period 3, PHASE 1 (05 Nov. 2012); (c) period 3, PHASE 2 (06 Nov. 2012); (d) period 4 (24 Nov. 2012); and (e) period 4 (25 Nov. 2012).*

The simulations represent very well the rainfall pattern over the Madeira island with the higher precipitation over the highlands, except for the two eastern stations (Figure 3.5m, n, o). From these two stations, it may be inferred that the simulations overestimate the large area of heavy precipitation to east of the island, although no observations are available to confirm it. EXPD2 provides details in the precipitation field over the island that agree better with the raingauge values than CTRL.

3.3.1.5 Model performance

Figure 3.7 shows the comparison between the total accumulated precipitation in the meteorological stations and in each simulation for the periods highlighted in Figure 3.2 from the dashed-line red rectangle.

Figure 3.7 *Comparison between the accumulated precipitation at the meteorological stations and those simulated for the nearest grid-point (left column), and for the "best point" in the neighbourhood of the station (right column). The periods of accumulated precipitation are the same showed from the dashed-line red rectangle in the Figure 3.2.*

When comparing the raingauge observations with the simulations at the nearest grid point (left column), some differences may be observed, with overestimation (Figure 3.7a and 3.7g), or underestimation (Figure 3.7c) by the model. The right column of Figure 3.7 shows the results obtained when the "best point" in the neighbour area surrounding the observation site (see Section 3.2) is selected. The differences are significantly reduced, indicating that even with a punctual slight under- or overestimation, the model well simulated quantitatively the accumulated precipitation at least at some point near the station, i.e. no more than 3.75 km away in each axis direction.

Table 3.2 Scores for the accumulated precipitation in each period. Pearson correlation (r), Mean Error (ME), Mean Absolute Error (MAE), and Root Mean Squared Error (RMSE) for the nearest grid-point, and for the "best point" in the neighbourhood of the station.

Period	Simulation	Nearest grid-point				"Best point" in the neighbourhood			
		r	ME	MAE	RMSE	r	ME	MAE	RMSE
1	CTRL	0,94	26,93	28,30	38,91	0,99	0,60	4,45	5,74
	EXPD1	0,86	39,13	39,21	51,64	0,96	15,29	16,73	20,95
	EXPD2	0,88	52,78	52,78	67,06	0,98	8,23	8,23	12,26
2	CTRL	0,85	-5,33	39,68	53,26	0,99	-1,97	13,40	20,30
	EXPD1	0,93	-16,45	33,10	43,03	0,97	1,08	15,03	24,62
	EXPD2	0,90	-10,04	30,08	41,47	0,99	0,43	6,75	13,69
3 – PH1	CTRL	0,73	-42,92	47,75	54,99	0,89	-23,31	24,34	32,20
	EXPD1	0,77	-9,90	24,97	33,03	0,99	0,83	5,45	8,20
	EXPD2	0,71	-5,51	26,08	35,66	1,00	-0,98	1,34	2,81
3 – PH2	CTRL	0,77	12,92	71,52	88,80	0,99	16,47	18,27	21,35
	EXPD1	0,87	47,50	68,48	83,85	0,99	12,58	17,11	20,81
	EXPD2	0,90	67,43	76,93	100,86	1,00	7,47	7,85	13,81
4	CTRL	0,74	-3,41	17,54	25,54	0,94	-2,10	8,05	15,96
	EXPD1	0,75	9,72	21,12	29,00	0,86	8,08	12,92	20,73
	EXPD2	0,75	13,85	24,35	30,82	0,92	6,52	8,43	15,94

The same feature is observed in the errors between the simulated and observed accumulated precipitation, presented in Table 3.2. In general, a high positive correlation is verified, with values close to 1 when the "best point" near the station is considered. In the case of the other scores, for the station nearest grid points, considerable differences (positive or negative) also indicate that the model tends to under or overestimate the total accumulated precipitation at these exact locations. For the RMSE, as an example, the PHASE 2 of period 3 (3-PH2 in Table 3.2) presents the largest differences between the model and observation, as a consequence of the overestimation showed in Figure 3.7g. For the best point near the station, these errors are also greatly reduced and, in general, they are lesser for the simulation at 0.5 km resolution (EXPD2). Therefore, the model successfully captured the totals of accumulated precipitation, despite some horizontal displacement.

3.3.2. Discussion

Considering the results for the four periods, it is shown that the significant accumulated precipitation over the Madeira occurred under different synoptic environments. The general structure of the cloudy systems over the ocean associated to these synoptic situations was well reproduced by MESO-NH. The rainfall periods clearly express the spatial-temporal variability of how heavy rainfall occurred over the island. For example, weak and continuous precipitation occurred during 48 hours, extreme precipitation during approximately 18 hours, heavy precipitation in just a few hours and in high amount resulting from a persistent moderate precipitation for several hours. The MESO-NH also reproduces successfully the spatial distribution of the precipitation over the island, better at 500 m horizontal resolution. The most interesting result of this study, identified from Figure 3.5, is the different rainfall patterns over the island, a question not discussed before about precipitation over the Madeira. This difference is summarized schematically in Figure 3.8. The maximums of accumulated precipitation are concentrated in different altitudes and slopes of the island. The accumulated precipitation is concentrated over the central peaks above a height of 1000 m (period 1, Figure 3.8a), or still in the highlands but more localized over the southern slopes (periods 2 and 4, Figure 3.8b). In opposition, the precipitation in the period 3 occurred in the northern slopes (Figures 3.8c and 3.8d). In PHASE 1 of this event, the localised precipitation occurred mainly in the NE coastal

plain below a height of 1000 m (Figure 3.8d), contrasting with the precipitation in the regions above 1000 m in PHASE 2 (Figure 3.8c).
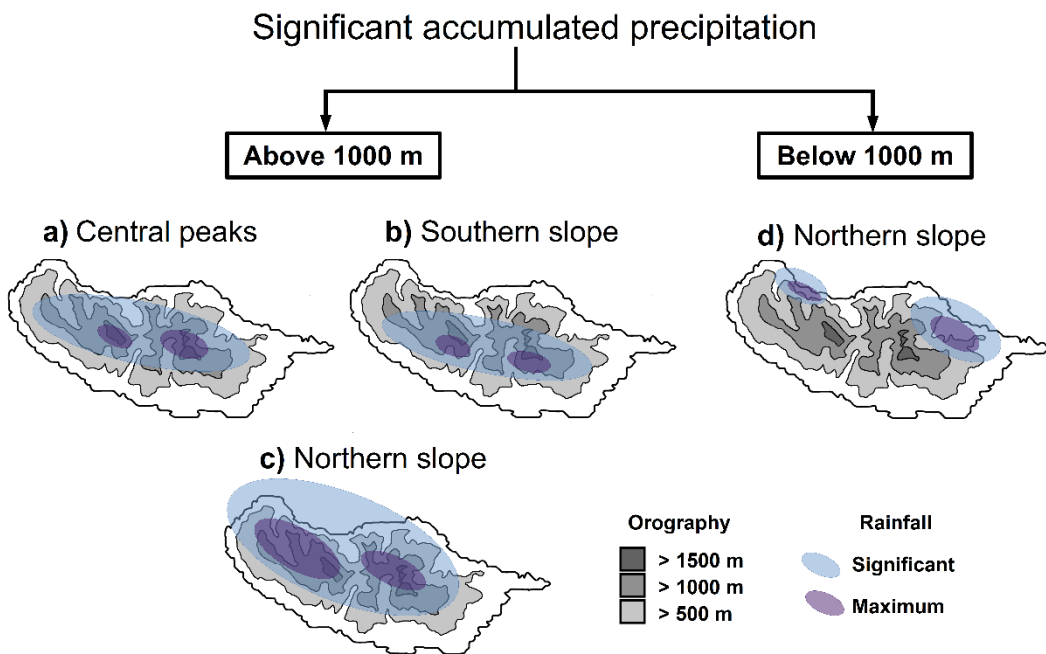
Figure 3.8 *Schematic representation of the rainfall patterns over the Madeira verified from the periods simulated. Maximums of accumulated precipitation occurred above a height of 1000 m and concentrated over (a) central peaks, (b) southern slope, and (c) northern slope; and (d) below a height of 1000 m in the northern slope. The solid lines represent the terrain in each 500 m.*

3.4. CONCLUSIONS

In this article, a set of eight numerical simulations for all significant rainfall periods in the Madeira island during the autumn 2012 were presented and evaluated for two different horizontal resolutions over large domain.

When confronted with the few observational data available, it was demonstrated the ability of the model to represent the ambient conditions near the island, and the main structure of the different cloudy weather systems over the surrounding ocean, and that for four distinct synoptic situations.

Regarding the accumulated precipitation results, the MESO-NH model was able to successfully capture the strong impact of the local mountains in the distribution and

volume of the rainfall over the Madeira at both horizontal resolutions. The simulations using 0.5 km grid spacing showed more realistic results when compared with the observations. The under or overestimation of the accumulated precipitation was considered acceptable taken into account the duration of the numerical experiments which is quite long as regard the predictability expected at this resolution and for convection.

Overall, beside the good representation of the events by the MESO-NH, the most important point underscored is the different rainfall patterns, which showed significant precipitation occurring in distinct regions over the island. The accumulated precipitation concentrated above or below a height of 1000 m. In the first case (above 1000 m), rainfall was observed in three regions, southern slopes, central peaks, and northern slopes, while in the second case (below 1000 m), localised precipitation occurred mainly in the NE coastal plain. Improving the knowledge about the spatial distribution of significant precipitation over the Madeira is an important issue, mainly because sometimes heavy rainfall events may induce floods, as occurred during the period 3, moreover, in a different region when comparing with the disaster on February 20, 2010. Also, it shows that the significant precipitation during the autumn 2012 was strongly related to the local orography, embedded or not within an extra-tropical weather system.

In the near future, the simulations will be used to investigate in detail the orographic mechanisms associated to these rainfall events that explain the various precipitation patterns over the island.

REFERENCES

Chaboureau J.-P., Söhne, N., Pinty, J.-P., Meirold-Mautner, I., Defer, E., Prigent, C., Pardo, J.R., Mech, M., Crewell, S., 2008. A Midlatitude Precipitating Cloud

Database Validated with Satellite Observations. *J. Appl. Meteor. Climatol.*, 47, 1337–1353. DOI: http://dx.doi.org/10.1175/2007JAMC1731.1.

Chen, C.-S., Lin, Y.-L., Peng, W.-C., Liu, C.-L., 2010. Investigation of a heavy rainfall event over southwestern Taiwan associated with a subsynoptic cyclone during the 2003 Mei-Yu season. *Atmos. Res.*, 95, 235–254. DOI: 10.1016/j.atmosres.2009.10.003.

Chen, C.-S., Lin, Y.-L., Hsu, N.-N., Liu, C.-L., Chen, C.-Y., 2011. Orographic effects on localized heavy rainfall events over southwestern Taiwan on 27 and 28 during the Post-Mei-Yu season. *Atmos. Res.*, 101, 595–610. DOI: 10.1016/j.atmosres.2012.10.008.

Cohuet, J.B., Romero, R., Homar, V., Ducrocq, V., Ramis, C., 2011. Initiation of a severe thunderstorm over the Mediterranean Sea, *Atmos. Res.*, 100, 603-620. DOI: http://dx.doi.org/10.1016/j.atmosres.2010.11.002.

Courtier, P., Freydier, C., Geleyn, J.-F., Rabier, F., Rochas, M., 1991. The Arpege project at Meteo France. In Numerical methods in atmospheric models, ECMWF Seminar Proceedings, 9-13 September 1991, ECMWF, Shinfield Park, Reading, UK, pp. 193-231.

Couto, F.T., Salgado, R., Costa, M.J., 2012. Analysis of intense rainfall events on Madeira Island during the 2009/2010 winter, *Nat. Hazards Earth Syst. Sci.*, 12, 2225-2240. DOI: 10.5194/nhess-12-2225-2012.

Couto, F.T., Salgado, R., Costa, M.J., Prior, V., 2015. Precipitation in the Madeira Island over a 10-year period and the meridional water vapour transport during the winter seasons. *Int. J. Climatol.*, In press. DOI: 10.1002/joc.4243.

Cuxart, J., Bougeault, P., Redelsperger, J.-L., 2000. A turbulence scheme allowing for mesoscale and large-eddy simulations. *Q. J. R. Meteorol. Soc.*, 126, 1-30. DOI: 10.1002/qj.49712656202.

Ducrocq, V., Nuissier, O., Ricard, D., Lebeaupin, C., Thouvenin, T., 2008. A numerical study of three catastrophic precipitating events over southern France. II: Mesoscale triggering and stationary factors. *Q. J. R. Meteorol. Soc.*, 134, 131-145. DOI: 10.1002/qj.199.

Ebert, E. E., 2008. Fuzzy verification of high-resolution gridded forecasts: a review and proposed framework. *Met. Apps*, 15, 51–64. DOI: 10.1002/met.25.

Lafore, J.P., Stein, J., Asencio, N., Bougeault, P., Ducrocq, V., Duron, J., Fischer, C., Héreil, P., Mascart, P., Masson, V., Pinty, J.P., Redelsperger, J.L., Richard, E.,

Vilà-Guerau de Arellano, J., 1998. The Meso-NH Atmospheric Simulation System. Part I: adiabatic formulation and control simulations, *Ann. Geophys.*, 16, 90-109. DOI: 10.1007/s00585-997-0090-6.

Lee, K.-O., Shimizu, S., Maki, M., You, C.-H., Uyeda, H., Lee, D.-I., 2010. Enhancement mechanism of the 30 June 2006 precipitation system observed over the northwestern slope of Mt. Halla, Jeju Island, Korea. *Atmos. Res.*, 97, 343–358. DOI: 10.1016/j.atmosres.2010.04.008.

Lee, K.-O., Uyeda, H., Lee, D.-I., 2014. Microphysical structures associated with enhancement of convective cells over Mt. Halla, Jeju Island, Korea on 6 July 2007. *Atmos. Res.*, 135–136, 76–90. DOI: 10.1016/j.atmosres.2013.08.012.

Levizzani, V., Laviola, S., Cattani, E., Costa, M.J., 2013. Extreme precipitation on the Island of Madeira on 20 February 2010 as seen by satellite passive microwave sounders. *Eur. J. Remote Sens.*, 46, 475-489. DOI: 10.5721/EuJRS20134628.

Lin, Y.-L., Chiao, S., Wang, T.-A., Kaplan M. L., Weglarz, R.P., 2001. Some Common Ingredients for Heavy Orographic Rainfall. *Wea. Forecasting*, 16, 633–660. DOI: http://dx.doi.org/10.1175/1520-0434(2001)016<0633:SCIFHO>2.0.CO;2.

Luna, T., Rocha, A., Carvalho, A.C., Ferreira, J.A., Sousa, J., 2011. Modelling the extreme precipitation event over Madeira Island on 20 February 2010, *Nat. Hazards Earth Syst. Sci.*, 11, 2437-2452. DOI: 10.5194/nhess-11-2437-2011.

Mittermaier, M.P., 2014. A strategy for verifying near-convection-resolving forecasts at observing sites. *Wea. Forecasting.* 29(2), 185-204. DOI: 10.1175/WAF-D-12-00075.1.

Mlawer, E.J., Taubman, S.J., Brown, P.D., Iacono, M.J., Clough, S.A., 1997. Radiative transfer for inhomogeneous atmospheres: RRTM, a validated correlated-k model for the longwave. *J. Geophys. Res.*, 102(D14), 16 663-16 682. DOI: 10.1029/97JD00237.

Pergaud, J., Masson, V., Malardel, S., Couvreux, F., 2009. A parameterization of dry thermals and shallow cumuli for mesoscale numerical weather prediction. *Bound-Lay Meteorol.*, 132, 83-106. DOI: 10.1007/s10546-009-9388-0.

Pinty, J.-P., Jabouille, P., 1998. A mixed-phase cloud parameterization for use in a mesoscale non hydrostatic model: Simulations of a squall line and of orographic precipitation. Proceedings of Conference on Clouds Physics, 17-21 August 1998, Everett, USA, 217-220.

Pujol, O., Lascaux, F., Georgis, J.F., 2011. Kinematics and microphysics of MAP-IOP3 event from radar observations and Meso-NH simulations, *Atmos. Res.*, 101, 124-142, DOI: http://dx.doi.org/10.1016/j.atmosres.2011.02.004.

Saunders, R., Matricardi, M., Brunel, P., English, S., Bauer, P., O'Keeffe, U., Francis, P., Rayer, P., 2005. RTTOV-8 science and validation report. NWP SAF Report, 41 pages, Tech. Rep.

Smith, R.B., Minder, J.R., Nugent, A.D., Storelvmo, T., Kirshbaum, D.J., Warren, R., Lareau, N., Palany, P., James, A., French, J., 2012. Orographic Precipitation in the Tropics: The Dominica Experiment. *Bull. Am. Meteorol. Soc.*, 93, 1567-1579. DOI: http://dx.doi.org/10.1175/BAMS-D-11-00194.1.

Verrelle, A., Ricard, D., Lac, C., 2015. Sensitivity of high-resolution idealized simulations of thunderstorms to horizontal resolution and turbulence parametrization. *Q.J.R. Meteorol. Soc.*, 141: 433–448. DOI: 10.1002/qj.2363.

Wang, C.-C., Hsu, J. C.-S., Chen, G. T.-J., Lee, D.-I., 2014a. A Study of Two Propagating Heavy-Rainfall Episodes near Taiwan during SoWMEX/TiMREX IOP-8 in June 2008. Part I: Synoptic Evolution, Episode Propagation, and Model Control Simulation. *Mon. Weather Rev.*, 142, 2619-2643. DOI: http://dx.doi.org/10.1175/MWR-D-13-00331.1.

Wang, C.-C., Hsu, J. C.-S., Chen, G. T.-J., Lee, D.-I., 2014b. A Study of Two Propagating Heavy-Rainfall Episodes near Taiwan during SoWMEX/TiMREX IOP-8 in June 2008. Part II: Sensitivity Tests on the Roles of Synoptic Conditions and Topographic Effects. *Mon. Weather Rev.*, 142, 2644-2664. DOI: http://dx.doi.org/10.1175/MWR-D-13-00330.1.

Wilks, D. S., 2006. Statistical Methods in the Atmospheric Sciences. International Geophysics Series, Volume 91 (2nd edition), Academic Press, 627 pp.

CHAPTER 4 – UNDERSTANDING SIGNIFICANT PRECIPITATION IN MADEIRA ISLAND USING HIGH-RESOLUTION NUMERICAL SIMULATIONS OF REAL CASES[‡]

Abstract

In order to advance the knowledge about precipitation development over the Madeira island, four rainfall patterns are investigated based on high resolution numerical simulations performed with the MESO-NH model. The main environmental conditions during these precipitation periods are examined, and important factors leading to significant accumulated precipitation in Madeira are shown. We found that the combination of orographic effect and atmospheric conditions is essential for the establishment of each situation. Under a moist and conditionally unstable atmosphere, convection over the island is triggered, and their location was determined mainly by variations of the ambient flow, which was also associated with different moist Froude number. Interestingly, our results showed some similarities with situations discussed in idealized studies, however, the real variations of the atmospheric configuration confirm the complexity of significant precipitation development in mountainous regions. In addition, precipitating systems initially formed over the ocean were simulated reaching the island. The four periods were characterised by different time duration, and the local terrain interacting with the mesoscale circulation was decisive to produce large part of the precipitation, which concentrated in distinct regions of the island induced by the airflow dynamic.

Keywords: Heavy precipitation; Orographic precipitating systems; Madeira island; MESO-NH model.

4.1. INTRODUCTION

The Madeira Archipelago is located in the Macaronesian region, which is formed by other volcanic archipelagos in the North Atlantic Ocean. Madeira (32°75'N and 17°00'W), a Portuguese island, is the largest of the archipelago with approximately 740 km² and 250 thousand inhabitants. The island has an east-west elongated form, and a central mountain chain with peaks from 1500 m up to above 1800 m in the eastern region, as well as deep valleys and cliffs. The mountains favour the development of orographic fogs throughout the year and dense vegetation. This vegetation is essential for the groundwater recharge, which is also dependent on precipitation and cloud water interception (see Prada et al., 2015, and references therein). Nowadays, these areas are maintained, however, strategies for a better preservation is still discussed (Fernandes et al., 2015). Once in a while, the island is affected by intense precipitation events, with two disastrous floods marking its history.

The first memorable event was on October 1803. According to the description of the disaster published by John Driver in 1838, the event was preceded by several months without precipitation. The torrential rain began in the evening and swept away the bridges, several houses, leading to an estimate of above 300 deaths (Driver, 1838). The second episode, the disaster on 20 February 2010, highlighted the vulnerability of the island to extreme precipitation events. It was marked by a huge economic damage estimated in millions of Euros, and more than 40 deaths. The greatest impact was observed in the southern region, where flash floods induced shallow, small, and numerous landslides (Lira et al., 2013). The catastrophe raised several questions about the occurrence of events with such socio-economic impact. For example, the episode altered the island's landscape and, in order to implement the capacity of the community to adapt to changes, some projects were developed improving landscape resilience (Bonati, 2014; Bonati and Mendes, 2014).

Before the disaster, there were not many studies about precipitation formation over the island, which were highly motivated after 2010. In general, the highest amounts of precipitation are recorded during the autumn and winter seasons. Extreme precipitation events with daily accumulated precipitation above 200 mm are not so frequent, and few events occurred on the highlands of Madeira in the last years (Couto et al., 2015). In addition, the summers are generally dry, influenced by the Azores anticyclone.

The atmospheric conditions during the disaster in 2010 have been well documented. These studies found that an anomalous wet winter and several rainfall events during the season probably contributed to the catastrophe by saturating the soils (e.g., Couto et al., 2012; Fragoso et al., 2012). More specifically, the high amount of moisture in the lower troposphere was associated with a frontal system that reached the island on 20 February 2010 (Luna et al., 2011). The tropical origin of this moisture was underscored by Couto et al. (2012) who identified a pattern denominated as "Atmospheric River", due to its filamentary structure and moisture amount. These structures contribute to the meridional transport of moisture from the Tropics and were present in other heavy precipitation events in Madeira during the 2009/2010 winter (Couto et al., 2012). Nevertheless, Couto et al. (2015) show that the impact of atmospheric rivers on the precipitation in Madeira is not so high when 10 winter seasons were considered [2002-2012], confirming the exceptional character of the 2009/2010 winter. According to Fragoso et al. (2012), the wet 2009/2010 winter was strongly connected to a negative North Atlantic Oscillation phase.

Besides large scale conditions propitious to precipitation formation, the local orography of the island plays an important role for the maximums of accumulated precipitation as shown by numerical simulations (Luna et al., 2011; Couto et al., 2012; Dasari and Salgado, 2015, among others), or by high resolution satellite observations (Levizzani et al., 2013). Recently, Couto et al. (2016) showed from very-high numerical simulations that high precipitation totals may occur in distinct regions over the island and may be produced under different synoptic situations.

The orographic mechanisms producing precipitation are well described in the literature (e.g., Houze, 2012), however, the initiation and development of convection over complex terrain remains still a challenge worldwide. From idealized numerical simulations of conditionally unstable flow affecting a two-dimensional mountain ridge, Chu and Lin (2000) identified three moist flow regimes associated with the formation and propagation of convective systems, controlled by the moist Froude number (Fr_w). These regimes are characterized by upstream propagating convective systems (low Fr_w; Regime I), quasi-stationary convective systems (moderate Fr_w; Regime II), and both quasi-stationary and downstream convective systems (large Fr_w; Regime III). A fourth regime was found by Chen and Lin (2005a), configured by an orographic stratiform precipitation system over the mountain. The authors also pointed out that the regime may change in

function of the Fr$_w$ and convective available potential energy (CAPE). For a three-dimensional mountain, Chen and Lin (2005b) identified the same regimes, calling attention for situations of strong winds, which induced large amount of precipitation on the windward slopes, instead over the mountain peak.

In the last years, more idealized simulations of uniform and conditionally unstable flow over mountain ridge have shown important features about precipitation regimes. For example, under weaker wind speeds (2.5 m s^{-1}), the cold pool produced by evaporation of precipitation propagates away from the ridge, inducing new convective cells upstream, but without stationary precipitation over the ridge. For larger wind speeds (10-20 m s^{-1}), quasi-stationary convective systems develop upstream side of the ridge with no cold pool present (Miglietta and Rotunno, 2009). On the other hand, for wind speeds of 20 m s^{-1}, the precipitation regime is quite independent of CAPE values, whereas for wind speeds of 10 m s^{-1} and low-CAPE, Miglietta and Rotunno (2010) proposed the analysis of two more parameters, which are related to a measure of the cold pool propagation and deceleration induced by the cold pool on the upstream flow. More recently, Miglietta and Rotunno (2012) showed that vertical variations of the wind field produced larger precipitation amounts from deeper and stronger convective cells, when considered those obtained from experiments with constant wind. The weak winds aloft favours the vertical development of these cells, producing stationary precipitation since they do not move with respect to the mountain. When a vertical wind shear is considered, Miglietta and Rotunno (2014) highlighted the quasi-stationary cold pool immediately upstream of the mountain peak. The uplifting induced by the cold pool reinforces the orographic forcing, producing deep and quasi-stationary convective cells, which present deep updraughts.

Numerical modelling is a good way to study precipitation development in Madeira, thanks to the improvements in the atmospheric models. Furthermore, a better representation of the physical and dynamical processes over the island is possible as resolution increases. In order to advance the knowledge about precipitation development on the island, the main goal of the present study is to investigate four distinct heavy rainfall patterns starting from the following questions: 1) What are the causes for the distinct rainfall patterns identified over the island? 2) What are the main atmospheric environments and factors involved in the periods of significant accumulated precipitation? 3) What is the microphysical structure of the clouds as seen from the

atmospheric model? These questions support the main goal and help us to better understand the occurrence of significant accumulated precipitation in Madeira.

The article is structured into five sections: Section 4.2 presents the rationale and methodology. Section 4.3 consists of the results for each situation considered, followed by discussion and summary in Section 4.4 and conclusions in Section 4.5.

4.2. RATIONALE AND METHODOLOGY

The autumn 2012 was the second wettest period identified by Couto et al. (2015) considering the seasonal accumulated precipitation on the highlands of Madeira over a 10-year period. In a subsequent study, all significant precipitation periods during the 2012 season were identified and simulated with very-high resolution by Couto et al. (2016). While Couto et al. (2012) showed maximums of accumulated precipitation only in highlands for the 2009/2010 winter season, Couto et al. (2016) highlighted the occurrence of significant accumulated precipitation in different regions over the island, either above or below the height of 1000 m (see Figure 8 of Couto et al., 2016). This finding is the starting point for the development of the present study, which is elaborated aiming to answer the questions raised in the introduction about the four distinct patterns of heavy precipitation over the island found by Couto et al. (2016).

The study is supported by the numerical experiments presented in Couto et al. (2016) using the MESO-NH model (Lafore et al., 1998). The simulations were configured with two large nested domains in order to obtain more realistic simulations (Figure 4.1a). The larger domain (D1; 1500 km x 1250 km) was set with a resolution of 2.5 km, whereas the inner domain with a 0.5 km (D2; 300 km x 300 km). The experiments were validated from comparison with the available observations and the authors pointed out the ability of the model to successfully reproduce the main ambient conditions associated with all periods considered. A more thorough description of the experiments can be found in Couto et al. (2016). The good performance of the model is underscored in several studies, for example, about precipitation over complex terrains (e.g., Nuissier et al., 2008; Ducrocq et al., 2008), or reproducing the main structure of convective systems (e.g., Couhet et al., 2011; Pujol et al., 2011).

To achieve the objectives of the study, we select four distinct situations that express the spatial variability of the accumulated precipitation over the island, all occurring during

the autumn 2012: maximum of accumulated precipitation over the central peaks above a height of 1000 m (Situation 1), maximum of accumulated precipitation still on the highlands but more localized over the southern slopes (Situation 2), or in the northern slopes (Situation 3), and maximum of accumulated precipitation in the north-eastern coastal plain below 1000 m (Situation 4).

Each situation is characterised in terms of the mesoscale environment affecting the island, for example, considering the CAPE (J kg^{-1}), the Thickness of Vapour Water (THVW; unit: mm) and the moist Froude number fields. The moist Froude number (Fr$_w$; Chen and Lin, 2005b, Bresson et al., 2012) have been computed as Fr$_w$ = U/N$_w$h, with U the wind speed, h the characteristic height of the mountain (1600 m in this case) and N$_w$ the Brunt-Väisälä frequency for moist air. When Fr$_w$ < 1, a "flow around" regime is favoured, whereas flow over the mountain is favoured when Fr$_w$ > 1. Dynamics and microphysics of the precipitating systems are characterized through vertical motions and the mixing ratios for cloud water (MRC), rain (MRR), graupel (MRG), snow (MRS), and ice (MRI) fields.

4.3. RESULTS

4.3.1 Situation 1: Precipitation maximums over the central peaks

This event had a duration of 33 hours, occurring between 0900 UTC on 22 Oct. and 1800 UTC on 23 Oct. 2012. The large mesoscale circulation is characterised by a predominant south-westerly flow affecting the island for almost all the period. In the second half of the period, the flow organizes into an elongated low level convergence line favouring the development of convective systems over the ocean. The convergent flow in the lower troposphere at 0800 UTC on 23 October is displayed in Figure 4.1a, at 850 hPa level, indicating that lifting along this convergence line was important for deep convection initiation over the ocean. A further examination of the wind field shows that the mesoscale flow had the same orientation at higher levels (not shown). The convergence zone is associated with a high THVW elongated zone, with values above 40 mm (Figure 4.1a) embedded within it. The flow brings moist air toward the island. In the beginning of the period, a more stable atmosphere marks the environment around the island (not shown), whereas from the late afternoon on 22 October, the island lies in a region more unstable

as evidenced by large CAPE values ahead of the convergence line, and greater than 1500 J kg^{-1} close to Madeira at 0800 UTC on 23 October (Figure 4.2a), particularly upstream. Figure 4.2a also shows the south-westerly flow at 100 m altitude directed toward the Madeira with speeds exceeding 10 m s^{-1}.
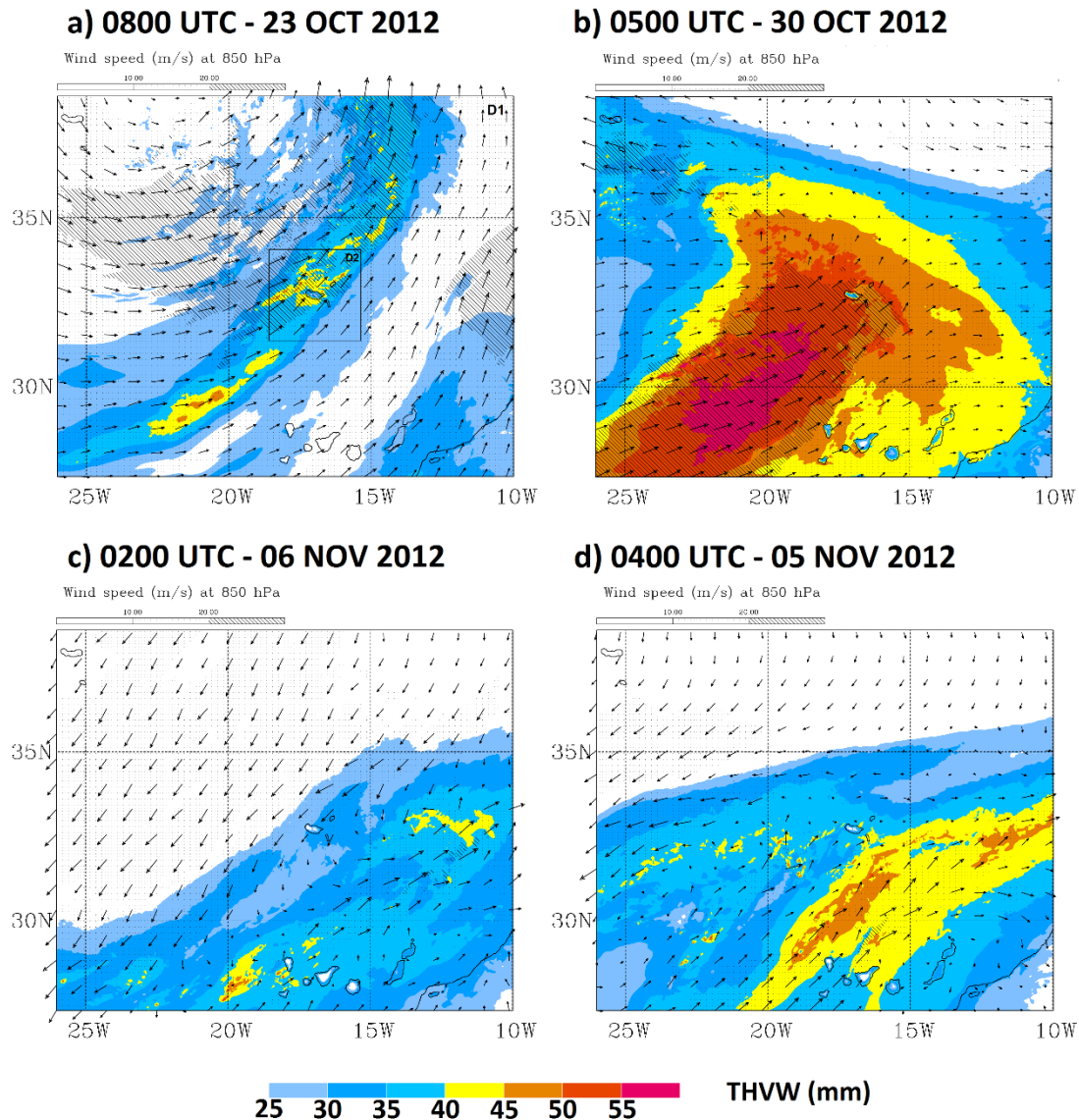
Figure 4.1 *Thickness of vapour water (coloured areas) simulated with 2.5 km resolution for a) Situation 1, b) Situation 2, c) Situation 3, and d) Situation 4. The arrows represent the horizontal wind vectors at 850 hPa level, whereas the hachured areas the wind speed at the same level.*
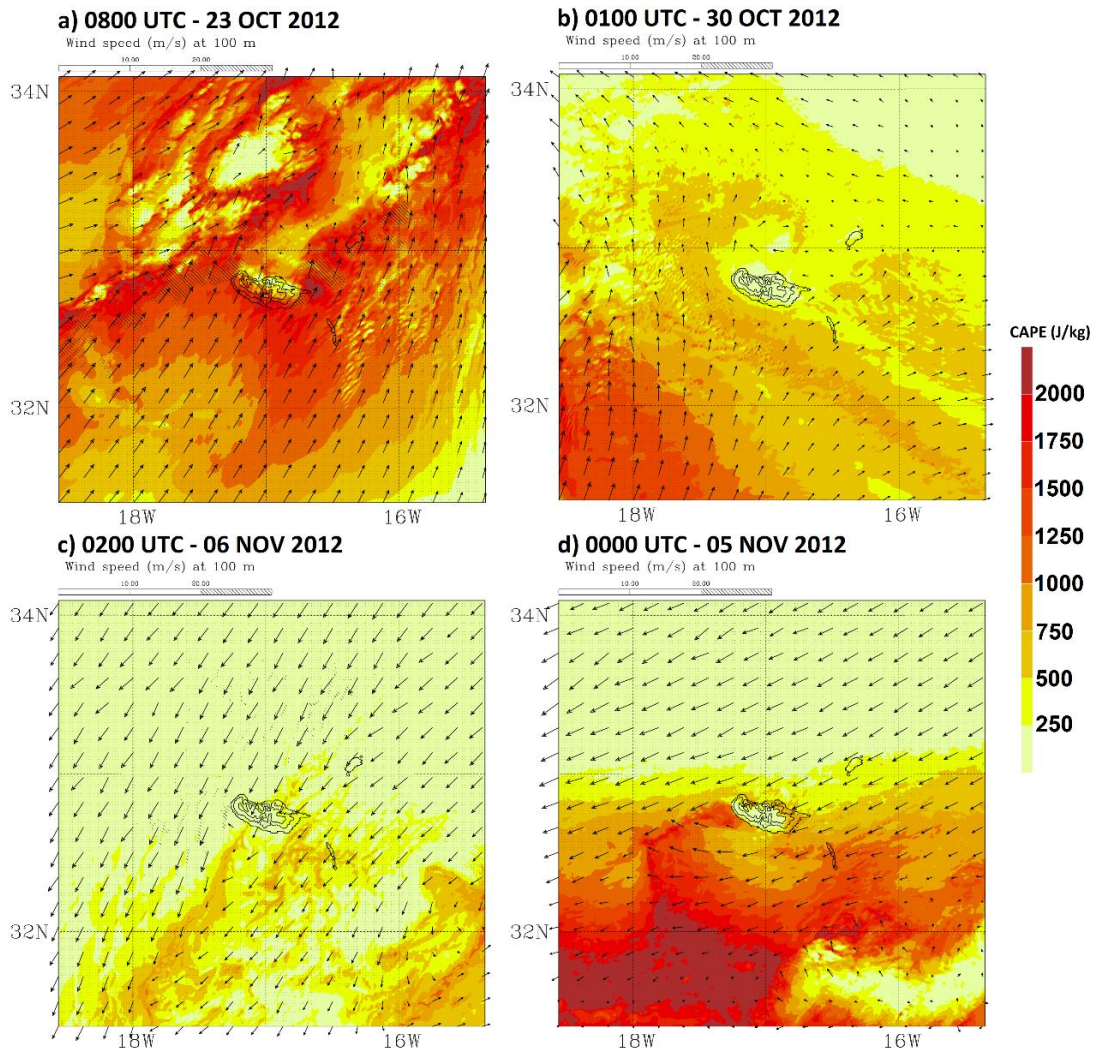
Figure 4.2 *Convective available potential energy (coloured areas) simulated with 0.5 km resolution for a) Situation 1, b) Situation 2, c) Situation 3, and d) Situation 4. The arrows represent the horizontal wind vectors at 100 m altitude, whereas the hachured areas the wind speed at the same level.*

Figures 4.3a and 4.3b show the vertical wind profiles in two instants for the "S" point located over the ocean, and displayed in the bottom of Figure 4.3. The almost prevailing south-westerly wind affecting the island is observed in the early period (1600 UTC on 22 Oct.; Figure 4.3a), with the flow near the surface veering slightly from southerly to south-westerly near the island top (around 1600 m), and speed lower than 15 m s^{-1} below 2 km altitude. The flow direction remains unchanged, while the speed increases with altitude. At 0100 UTC on 23 Oct. (Figure 4.3b), the south-westerly flow is also directed toward the island, but stronger winds are found at lower levels, close to 20 m s^{-1} at 800 m height.
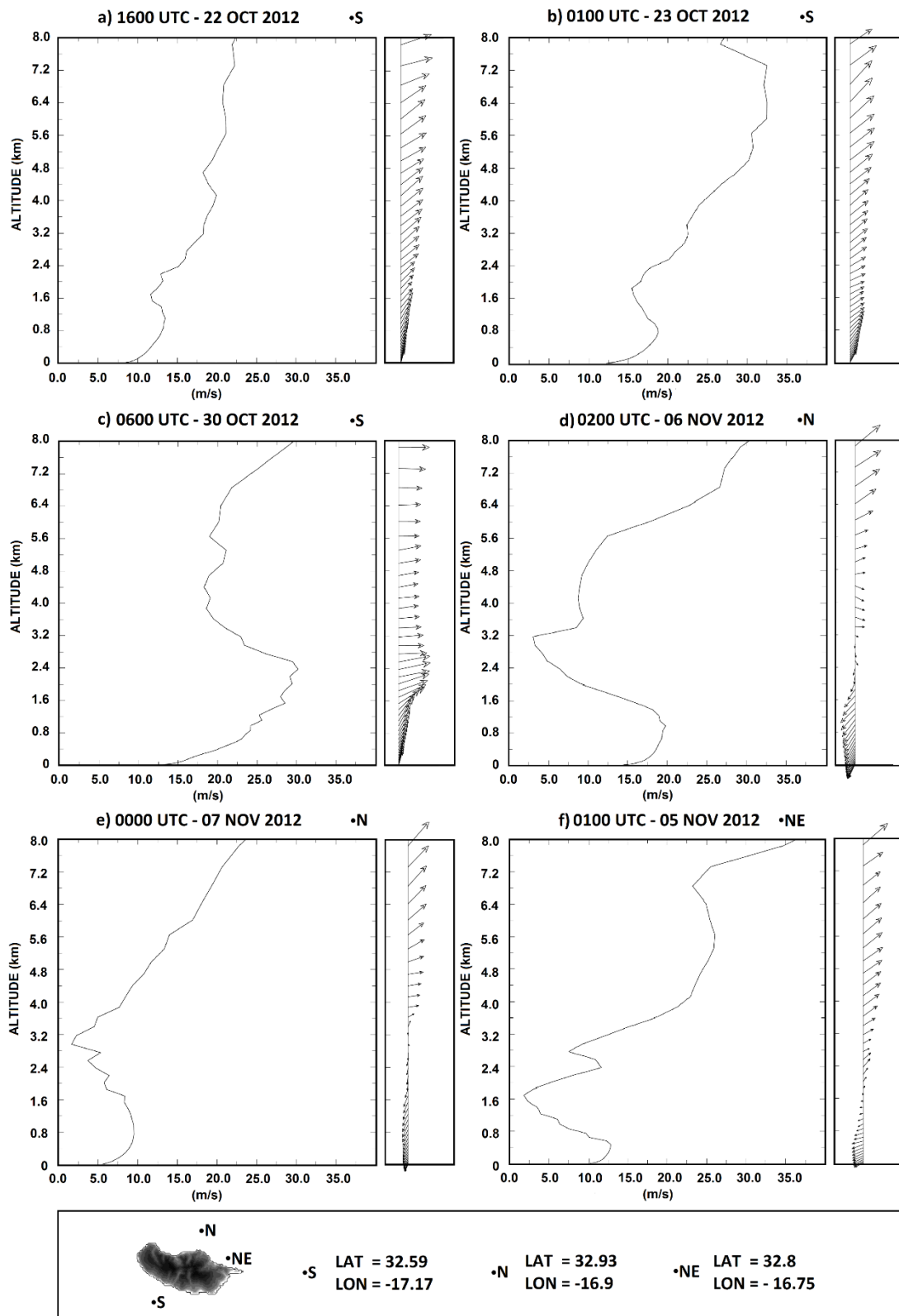
Figure 4.3 *Vertical profile of horizontal wind velocity and direction (arrows) simulated with 0.5 km resolution for: a) and b) Situation 1, c) Situation 2, d) and e) Situation 3, and f) Situation 4.*

The moist Froude number in the upstream is greater than 1 during large part of the period, in favour of a flow over the mountain. The SW-NE vertical cross-section (Figure 4.4a) confirms this "flow over" situation, with upward motion produced by local orography over the southern slope with vertical velocities above 1 m s^{-1} over the slope and 6 m s^{-1} on the highlands. The streamlines in the same figure show that the south-westerly flow is not blocked by the island orography, and that the mountains create a wave perturbation extending over the lee side, north-eastward of the Madeira. In the second half of the period, an enhancement of the orographic effect occurs, resulting in an intensification of the upward motion over the southern slope, and of the downward motion in the lee side (not shown).

SW-NE vertical cross-sections of vapour mixing ratio are shown from Figures 4.4b and 4.4c, whereas Figure 4.5 displays the total water mixing ratio for the liquid and ice hydrometeors (i.e., MRC+MRR+MRG+MRS+MRI). Over the island, the cloud formation is initiated by local processes related to orographic effect. At 1600 UTC on 22 October, the forced air ascension induces the lifting of water vapour, which is partially converted into liquid water and precipitation near the mountain peak (Figure 4.4b and 4.5a). Orographic clouds are simulated over the central mountain chain with bases around 1 km altitude and tops ranging between 2.5 and 3.5 km altitude, and not exceeding the freezing level (Figure 4.5ab). An increase of the depth of the moist layer is visible upstream the island, extending up to 3 km altitude (Figure 4.4b). The highest moisture contents are found in the southern slope above 10 g kg^{-1}, whereas lower values are present over the lee side.

Later, during the unstable period, deep convective systems developing over the ocean are reproduced by the model, extending throughout the troposphere with cloud tops above 10 km. When this band with embedded convection reaches the island, the orographic clouds are not easily identified, co-existing with the convective cells affecting the island (Figure 4.5c). The moist layer is identified extending up to 2.5-3 km, with values of 12 g kg^{-1} reaching 1 km altitude in the southern slope whereas high values associated with the moist band are also observed on the lee side (Figure 4.4c).

After the passage of the convective systems, the formation of vigorous orographic clouds with high concentration of liquid water, reaching the freezing level, are simulated by the model, as shown in Figure 4.5d.
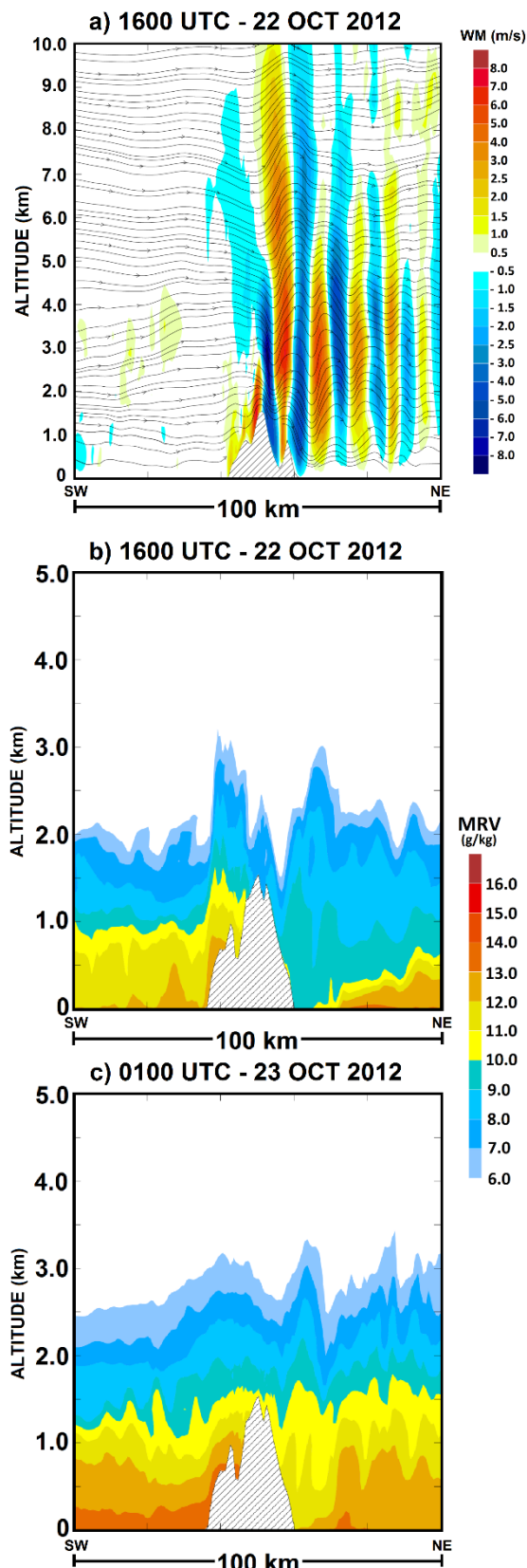
Figure 4.4 *SW-NE vertical cross-sections of a) vertical velocity (coloured areas) and streamlines, b) and c) mixing ratio of water vapour (coloured areas). Both fields simulated with 0.5 km resolution and for Situation 1.*
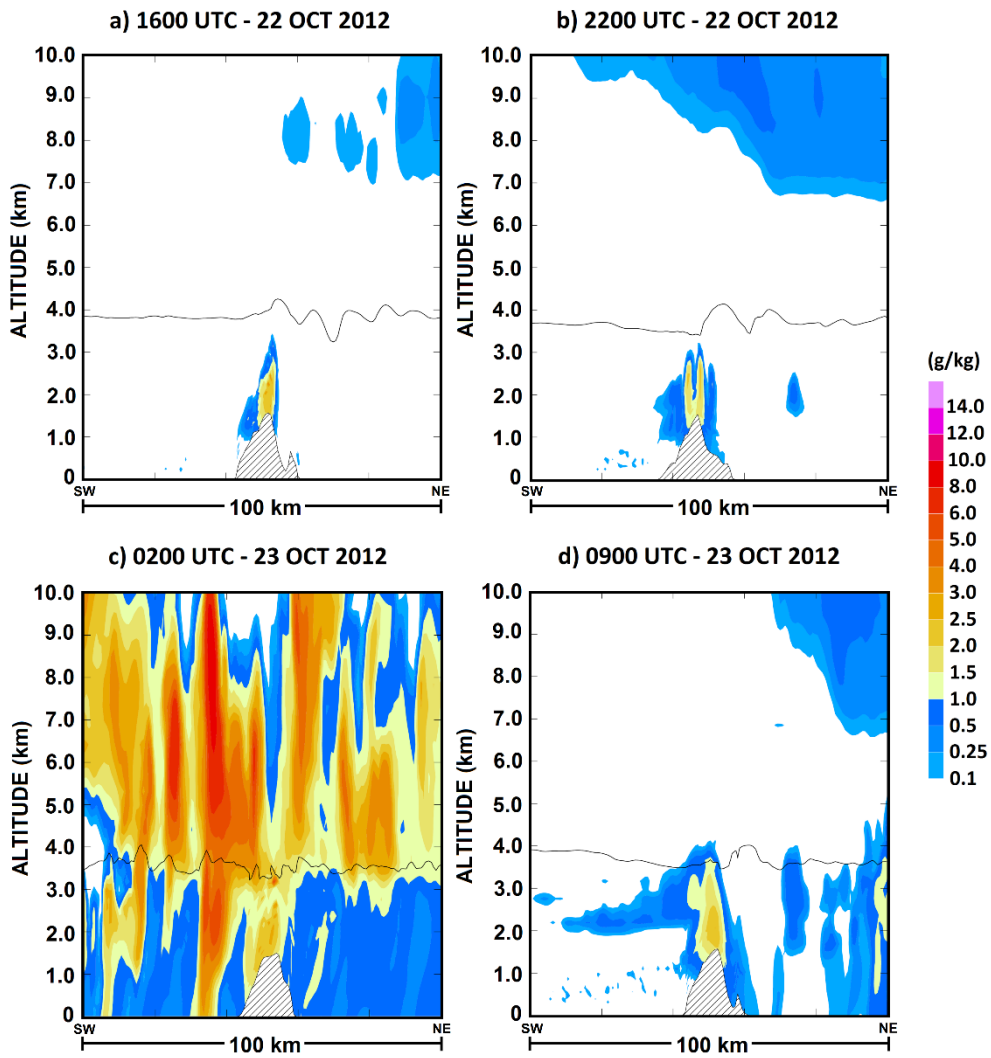
Figure 4.5 *SW-NE vertical cross-sections of liquid and frozen water mixing ratios (i.e., MRC+MRR+MRG+MRS+MRI) at some instants during the Situation 1, as simulated at 0.5 km resolution. The black line indicates the 0°C isotherm.*

4.3.2 Situation 2: Precipitation maximums above 1000 m in the southern slopes

This pattern was produced from an event of extreme precipitation occurring within 18 hours between 2100 UTC on 29 Oct. and 1500 UTC on 30 Oct. 2012. The mesoscale environment is characterized by a south-westerly flow at 850 hPa, and a tongue-shape band of moist air with THVW above 50 mm near the island at 0500 UTC on 30 Oct. (Figure 4.1b). The tongue shape moist flow is associated with conditionally unstable air with CAPE values above 1250 J kg^{-1} south-westward of the island few hours before the tongue reaches the Madeira (Figure 4.2b). This atmospheric configuration produced a shallow precipitating system over the ocean, accompanying the confluent flow at lower

levels (not shown). After the passage of this south-westerly confluent flow, a westerly flow affects the island (not shown).

The low-level jet signature is pointed out in Figure 4.3c from the vertical wind profile at "S" point, with wind speed increasing from below 20 m s^{-1} near the surface to about 30 m s^{-1} at 2.5 km. In the same figure it may be seen that the south to south-westerly flow at lower levels is replaced by a westerly flow as altitude increases. The Froude number Fr$_w$ is larger than 1 in the windward region. The impact of this intense flow crossing the central mountain chain on the vertical motion is evident on the vertical cross-section presented in Figure 4.6a, which shows a strong subsidence in the lee side (velocities of 6 m s^{-1}), whereas upward motions in the southern slope present velocities above 3 m s^{-1}. The orographic effect with a deep Foehn effect in the lee side is reproduced at several instants during the period.

The vertical distribution of the moisture content at 0600 UTC on 30 Oct. is displayed in Figure 4.6b, showing a deep moist layer, wherein the 6 g kg^{-1} isoline reaches a height of 4.5 km. Such moist layer remains throughout the event. In the windward region over the ocean, vapour mixing ratio above of 14 g kg^{-1} is found near the surface close to the island.

In the early morning (Figure 4.7a) a precipitating system associated with the larger scale environment affects the island. The region with higher concentration of hydrometeors extending up to 7 km altitude corresponds to a rain band with NW-SE orientation that moves quickly over the island to north-eastward. In addition, clouds extending up to upper levels are simulated, but without precipitation (weak hydrometeor content). The development of dense orographic clouds over the southern slope is simulated after the passage of the rain band, as seen in Figure 4.7b. These orographic clouds sometimes reach the mid-troposphere (Figure 4.7c), with high amounts of liquid water. The maximum concentration of hydrometeors was detected along the highlands and mostly in the southern slopes (Figure 4.7b-d). This area leans backwards, in agreement with the vertical wind shear associated with the jet. The cloud cover decreased in few hours, and scattered orographic clouds were simulated over the island (not shown).
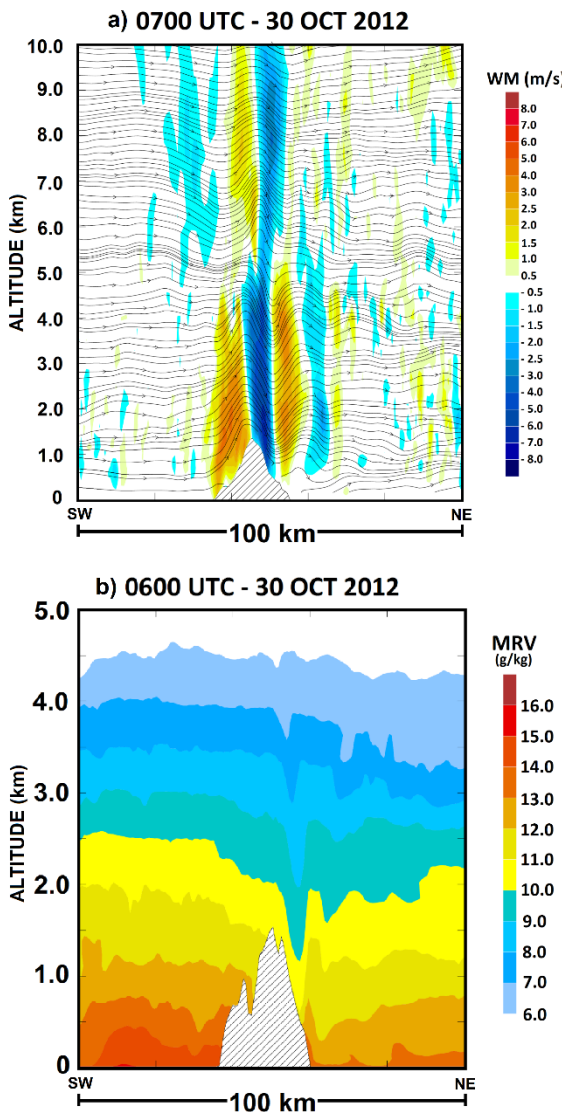
Figure 4.6 *SW-NE vertical cross-sections of a) vertical velocity (coloured areas) and streamlines, and b) mixing ratio of water vapour (coloured areas). Both fields simulated with 0.5 km resolution and for Situation 2.*

4.3.3 Situation 3: Precipitation maximums above 1000 m in the northern slopes

In this situation, precipitation occurred over a period of 54 hours between 1200 UTC on 05 Nov. and 1800 UTC 07 Nov. 2012. The airmass movement from north to south-westward characterises the mesoscale environment during this period. Under this configuration, the north-easterly flow affects the island with speeds above 10 m s^{-1} at low levels (Figures 4.1c and 4.2c). Figure 4.1c also provides the THVW distribution, showing a drier airmass north-westward of the island and a moist airmass to south-east associated with a south-westerly flow. The approaching airmass from north gradually decreases the moisture around the island. However, in the windward region, THVW above 30 mm is

still identified (Figure 4.1c), as well as conditionally unstable atmosphere along the period, with CAPE around 500 J kg^{-1} near and over the island (Figure 4.2c). During the early period, the flow affecting the island presents a moderate Fr_w number (between 0.5 and 1), and exceeding 1 as time passes.
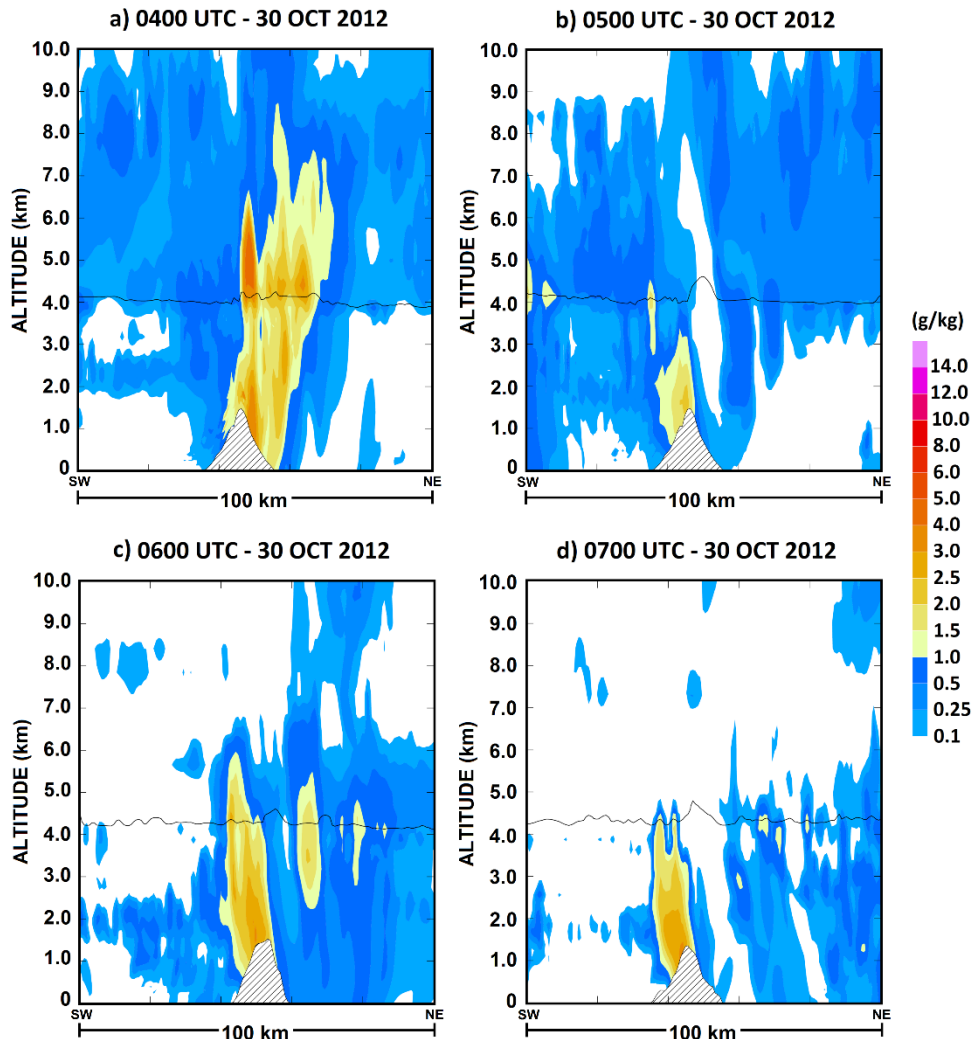
Figure 4.7 *The same as Fig. 4.5, but for Situation 2.*

The wind profile at point ("N") upstream the island is displayed at 0200 UTC on 06 Nov. (Figure 4.3d). The north-easterly flow in the lower tropospheric levels presents a maximum speed close to 20 m s^{-1} at 1 km altitude. It is topped by a layer of weak winds extending up to the mid-levels, where the flow veers 180° and reinforces, becoming a south-westerly flow. When considering a later moment (0000 UTC on 07 Nov.; Figure 4.3e), the wind speed at low levels decreases down to 10 m s^{-1}.

The vertical extent and associated maximum intensity of the upward motions produced in the northern slope are visible in Figure 4.8a. The air region with vertical upward movement extends vertically up to the middle levels over the northern slope, with velocities larger than 2 m s^{-1} close to the slope and above 8 m s^{-1} at around 4 km altitude. Also, the streamlines show the blocking effect created by the orography. At 0200 UTC on 06 Nov., the moist layer presents a height between 2.5 and 3 km, as seen for the 6 g kg^{-1} isoline (Figure 4.8b). Below 1 km altitude, vapour mixing ratio of 10 and 11 g kg^{-1} is found in the northern slope. Towards the end of the event, the air becomes drier, as may be seen in Figure 4.8c, at 1800 UTC on 06 Nov., when a thinner moist layer is located around the island, with the 6 g kg^{-1} isoline remaining below 2 km, and the maximum of mixing ratio is lower than 9 g kg^{-1}.
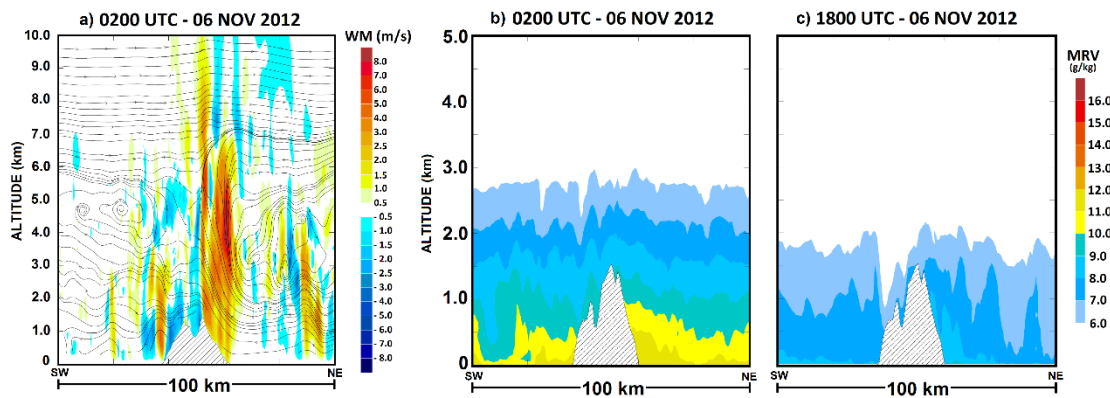
Figure 4.8 *The same as Fig. 4.4, but for Situation 3.*

Figures 4.9a-c shows the development of vigorous orographic clouds over the island. The cloud system, presenting tops around 7 km altitude, remains stationary over the island during the early hours on 06 November. The regions with higher concentration of hydrometeors are located over the central mountains and northern slope, however, the model indicates that the orographic cloud system also extends over the ocean. A near surface cooling of about 3 degrees (cold pool) developed beneath the system and extend over the near ocean. In Figure 4.9b-c, the hachured areas delineate the cold pool from the virtual potential temperature (THETAV) values lower than 292 K. During the afternoon of November 06, the system becomes less intense, however, orographic clouds are still present in the northern slope at 0100 UTC on 07 Nov. (Figure 4.9d).

a) 0200 UTC - 06 NOV 2012

b) 0700 UTC - 06 NOV 2012

c) 0900 UTC - 06 NOV 2012

d) 0100 UTC - 07 NOV 2012
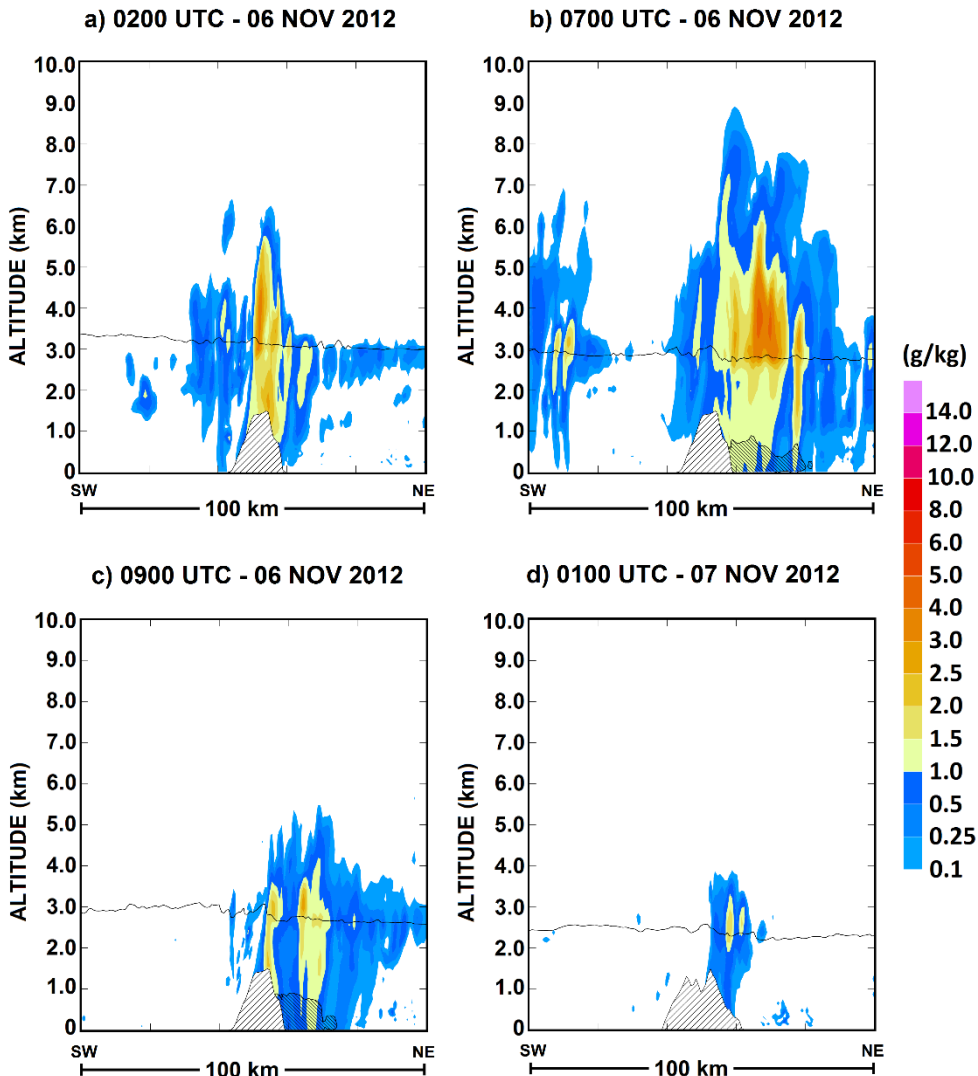
Figure 4.9 *The same as Fig. 4.5, but for Situation 3. The hachured areas represent the THETAV values lesser than 292 K.*

4.3.4 Situation 4: Precipitation maximum below 1000 m in the northern slope

This rainfall event was characterized by localised precipitation within 18 hours between 1800 UTC on 04 Nov. and 1200 UTC on 05 Nov. 2012. The circulation around the island at lower levels during the night is presented in Figures 4.1d and 4.2d. Note that the winds are weak near the island at 850 hPa level, without a predominant orientation (Figure 4.1d). In opposition, a strong north-easterly flow reaches the island at lowest levels, with a speed of 10 m s^{-1} at 100 m altitude, at 0000 UTC on 05 Nov. (Figure 4.2d). At that moment, it can be noted that the airflow goes around the island and converges over the ocean. The

island is found in a region marked by a strong horizontal moisture gradient, which separates a stable dry northward airmass from a moist airmass, strongly unstable to south (Figures 4.1d and 4.2d). Near the island, moist air in the north-eastward sector exhibit THVW values sometimes above 40 mm (Figure 4.1d). The conditionally unstable region to south-westward is marked by CAPE values above 2000 J kg^{-1}, however, over the north-eastern coastal zone, the model indicates lower values (around 750 J kg^{-1}; Figure 4.2d).

The vertical wind profile upstream ("NE" point, Figure 4.3 bottom), at 0100 UTC on 05 Nov. is shown in Figure 4.3f. Note the east to north-easterly flow reaching the island, stronger at lowest levels (first hundred meters), with speeds around 12 m s^{-1} at 400 m height. This flow present a veer of 180° as altitude increases, going from north-east at lowest levels to south-west above 3 km, and with a minimum speed around 1600 m height (Figure 4.3f). The simulation shows low Fr$_w$ during this precipitation period, with values lesser than 0.5 in favour of a "flow around" regime.

Some regions of the northern hillside are characterized by very steep slopes, which may act blocking the ambient flow creating localised ascending motion, such as displayed in Figure 4.10a, at midnight. The upward motion is just a result of the interaction of the stronger winds in the lowest levels with the local mountains, which produce ascending air. The SW-NE vertical cross-section presented in Figure 4.10b shows a moist layer exceeding 2.5 km altitude in the northern slope, as well as vapour mixing ratio above 13 g kg^{-1} very close to lowlands.

Under this environment, the model simulates the development of isolated orographic clouds concentrated in the north-eastern region, as shown in the vertical distribution of hydrometeors (Figure 4.11a-c). The model reveals a repeated development of new cloud cells, which remain quasi-stationary over the same region. Some of the clouds presented tops exceeding 5 km altitude, whereas others extended over the ocean (Figure 4.11d). The same feature was observed in the north-western part of the island, where a very rugged terrain is found as well (not shown). At the same time those orographic clouds occur in the northern slopes, the low level flow forced to go around the island induces cloud development over the ocean to south-westward of the island. After a few hours, these clouds merge with a mesoscale convective system (MCS). The system developed south-westward and moved north-eastward following the south-westerly flow at middle-levels. During its life cycle, the MCS passes quickly over the island (not shown).
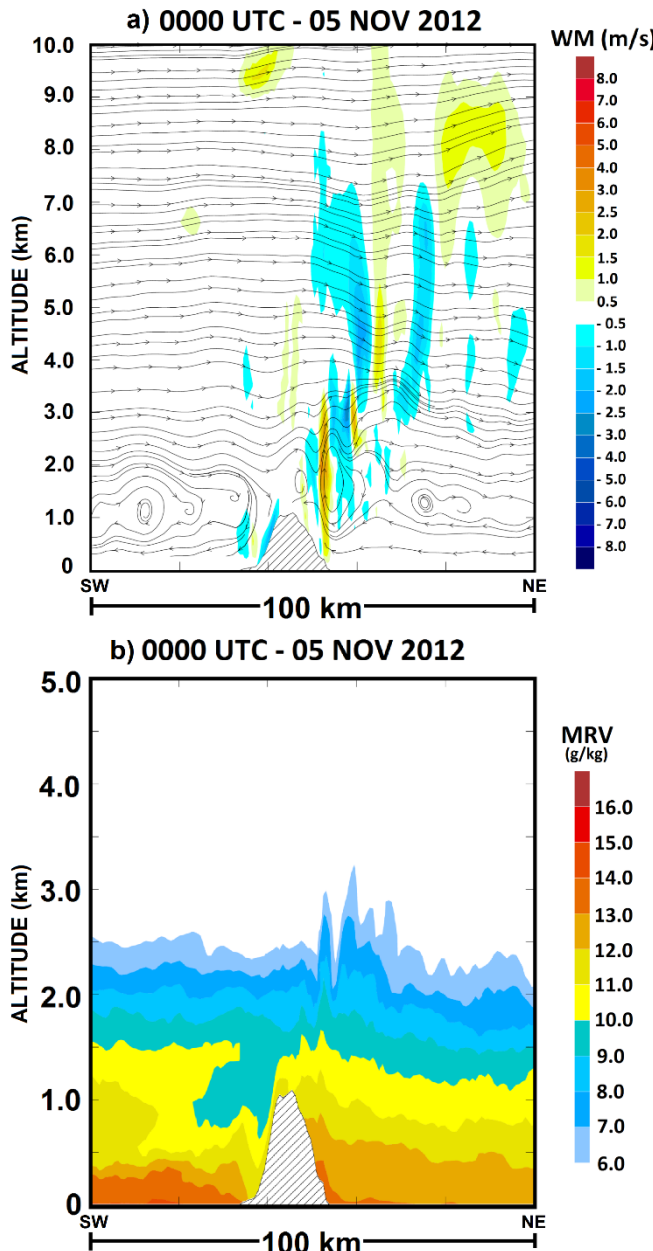
Figure 4.10 *The same as Fig. 4.6, but for Situation 4.*

4.4. DISCUSSION AND SUMMARY

The purpose of this section is to present a general discussion about the main factors that were responsible for significant accumulated precipitation in distinct regions of the island, such as presented above.

In order to understand the events, it should be kept in mind that Madeira represents a three-dimensional obstacle and the physical processes over there are initiated in function of the airflow dynamic, mainly because it may go around or above the island. The four

periods were characterised by a moist and conditionally unstable environment, however, in these real cases, the atmospheric conditions are not fixed, varying significantly in function of the time and space. For some of the situations convective systems develop over the Atlantic Ocean associated with these propitious larger-scale conditions and may pass over the island. The large difference between the periods is the airflow configuration affecting the local mountains, being connected to direction, intensity, and vertical profile. Figure 4.12 displays a schematic representation of the main environments involved in the four events of significant accumulated precipitation over the island. The vertical cross-sections have an approximately SW-NE orientation, and the elements drawn are the vertical wind profile over the windward region, as well as the orographic effects created in response to this flow.
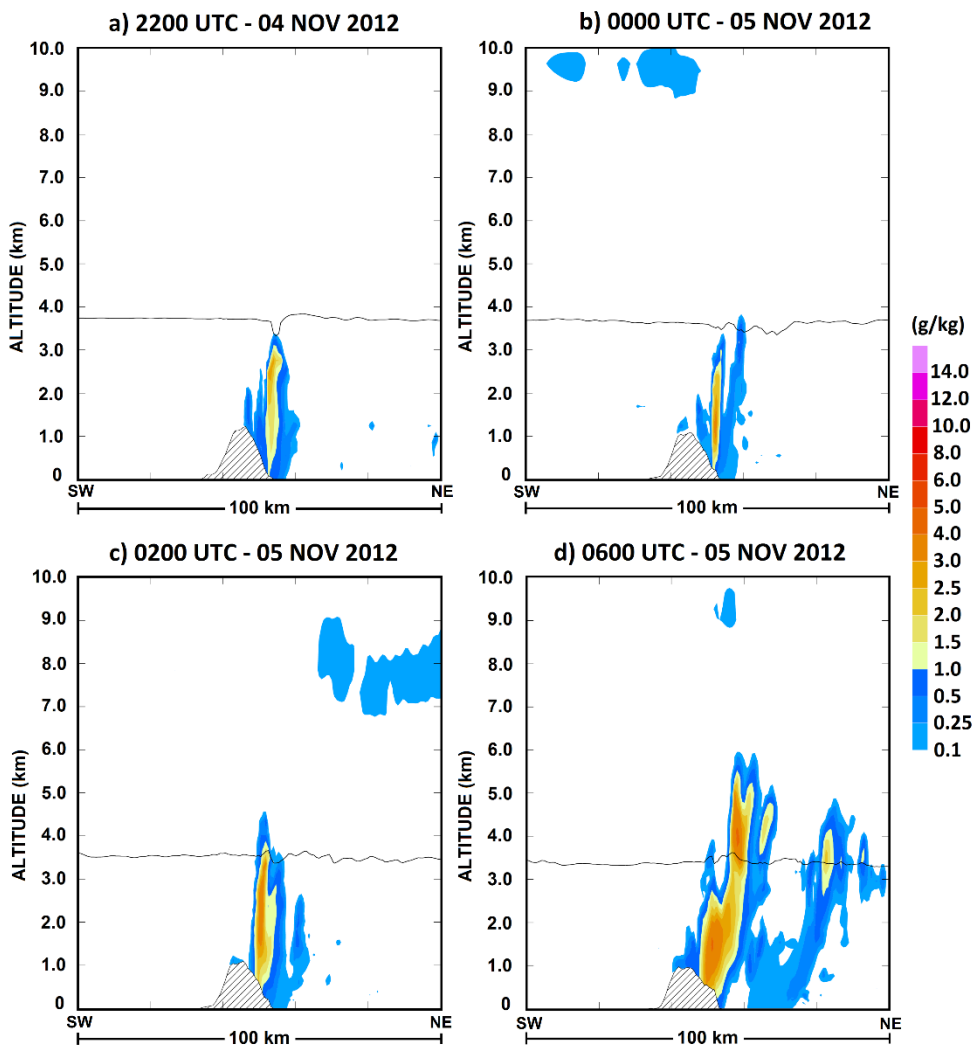
Figure 4.11 *The same as Fig. 4.5, but for Situation 4.*

In the first situation (Figure 4.12a), a south-westerly flow with wind speed stronger than 10 m s^{-1} at lower levels and presenting an almost unidirectional vertical wind profile, favoured shallow and quasi-stationary convective cells over the central mountains. Their characteristics are related to the flow intensity. For example, when this flow is reinforced, orographic shallow convection occurrence is more uniform along of the central mountain chain. When the wind speed reaches values close to 20 m s^{-1}, some clouds are simulated concentrating on the southern slope. In parallel, an increase in moisture content (above 10 mm of THVW), produces denser clouds with a larger concentration of liquid water. The Fr$_w$ number above 1 favours the upward motion in the southern slopes, inducing the repeated development of clouds and precipitation over the highlands. Some precipitating systems developing over the ocean along a south-west convergence line reach the island. An enhancement of the orographic precipitation through the seeder-feeder mechanism is suggested at that time, as well as for precipitation occurrence at lowlands. The significant accumulated precipitation over the central peaks is produced by warm-microphysics orographic clouds developing continuously over the central mountains during several hours. Their formation is favoured by the south-westerly flow crossing the island, which is forced to ascend along the southern slope. These orographic clouds have a chaotic distribution over the highlands, composed essentially by liquid water and extending few kilometres.

The important role of the wind intensity, as well as an enhancement in moisture content is confirmed in the second situation considered, also characterised by Fr$_w$ number above 1 in the windward region. The stronger winds in the lower troposphere (above 20 m s^{-1}) and an extremely moist environment (THVW above of 50 mm) produced stationary convective cells over the island, concentrating on the southern slope. In this case, the orographic clouds presented water contents larger than those simulated in the first situation and extending at some instants above the freezing level. These conditions persisting for few hours resulted in extreme amount of orographic precipitation. Although the complexities of real situations, we have considered these results coherent with those obtained from idealized simulations (e.g., Chu and Lin, 2000; Miglietta and Rotunno, 2009). The situation 2 shows that the orographic effect may be enhanced in response to an intensification of the south-westerly low level flow (Figure 4.12b). The upward motion created by orography produces condensation directly over the southern slope. In this case, a deep Foehn effect can be noted, and denser clouds concentrate over the windward

region, while the lee side is marked by strong downward motion. Such configuration, persisting for hours, may lead to significant accumulated precipitation on the highlands over the windward region.

In an environment marked by strong directional vertical wind shear, convection over the island occurred with different structures. In the first situation (i.e., NE flow at lower levels and SW upper levels), the orographic blocking produced deep orographic clouds over the island, that are more intense in the northern slope (windward region). Basically, the moist environment (THWV around 30 mm) was characterised by strong winds at lower troposphere (around 20 m s^{-1}), and a deep layer of weak winds aloft. The moderate to high Fr$_w$ number indicate that the impinging low-level flow tends to go over the mountainous island. Strong updraughts that extend up to the middle-levels are triggered over the northern slopes. The weak winds aloft may have helped to produce straight updraughts and a quasi-stationary convective system. In this case, the stationary convective system is more vigorous than those observed in the first two situations, extending over the ocean and presenting cloud tops over 7 km, well above the freezing level, as illustrated in Figure 4.12c. The deep convective system developed during several hours producing heavy and continuous precipitation over Madeira. This result is consistent with the results found by Miglietta and Rotunno (2014), since the system presents a cold pool upstream of the Madeira which favours convective cells triggering upwind. In addition, the system dissipation seems related to the weakening of the low level flow and the decrease of the moisture layer. As a result of the prevailing north-easterly flow at low levels and weak winds aloft, as well as of the associated stationary convective system, the maximum of accumulated precipitation is recorded in the highlands, but more localised over the northern slopes and extending also over the ocean.

Under a similar directional vertical wind shear, but occurring below the middle troposphere (i.e., NE flow at lowest levels and SW above 3 km), and in a low Fr$_w$ number environment, ascending air is created due the blocking effect caused by the steep orography at some regions of the northern slope in situation 4 (Figure 4.12d). The lifting of moist air (maximums of THVW larger than 40 mm) by the strong east to north-easterly flow at the lowest levels (above 10 m s^{-1}) favours clouds with high concentration of liquid water. The convective cells over the coastal zone in the NE slope remain quasi-stationary at their original region and, in general, do not extend above the freezing level. Consequently, the rainfall pattern was characterised by much localised accumulated

precipitation at lowlands in the northern slope coastal zone. This kind of situation has potential to cause local floods of short duration.
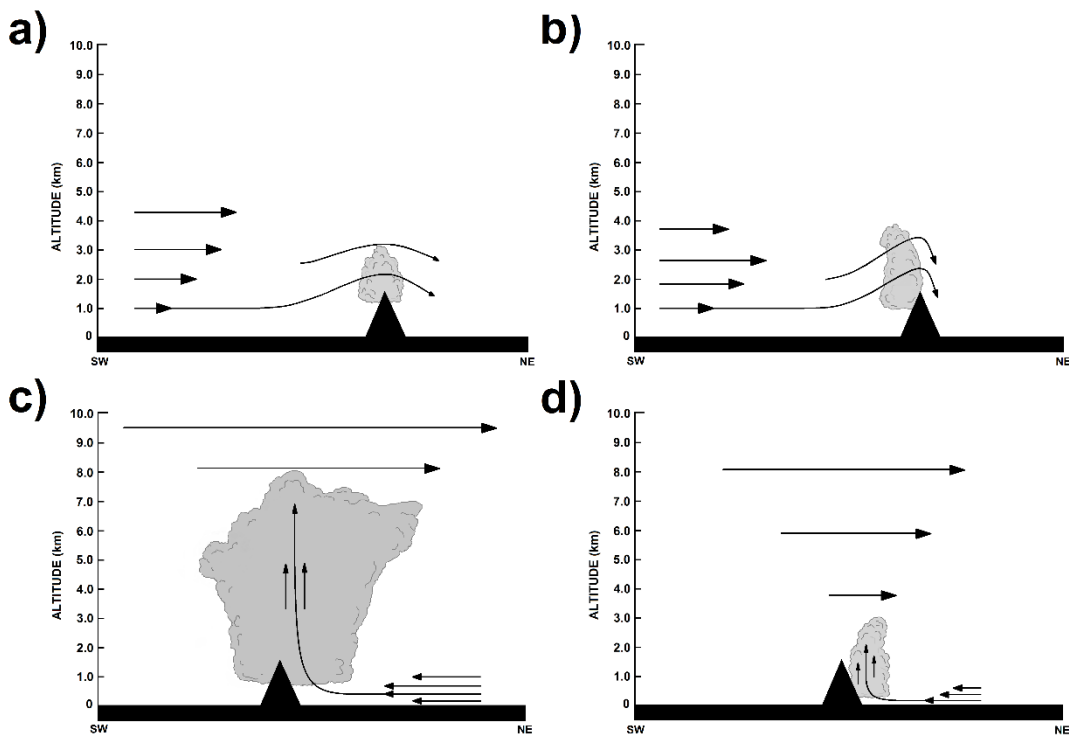
Figure 4.12 *Schematic representation of some features identified in the four situations examined. The vertical cross-sections have a SW-NE orientation, and the elements drawn are the vertical wind profile over the windward region, and the orographic effects created in response to this flow, namely producing convection over the island.*

In some situations, precipitating systems initially formed over the ocean are simulated by the model, sometimes passing over the island. These systems play an important role in the enhancement of pre-existing precipitation. However, the results show that these systems represent a minor contribution to the accumulated precipitation in Madeira over the whole periods. The largest contribution to the surface precipitation amount over the island is due to quasi-stationary and long-lasting orography-induced precipitation systems affecting the island during almost all the periods.

Therefore, the major difference among the patterns of high precipitation over the island is connected with the airflow characteristics. The variations of the airflow affecting the local mountains is the main factor influencing precipitation over different regions of the island.

4.5. CONCLUSIONS

A set of numerical simulations have been used to investigate in detail the atmospheric environments of four different rainfall patterns identified over the Madeira island.

The four real situations considered produced significant accumulated precipitation in the island. The examination of the main features associated with them, allow for concluding that variations of the ambient flow (direction and intensity) is the first factor that determines the distinct rainfall patterns over Madeira. Considering the situations studied, when a moist and conditionally unstable flow affects the island in such manner that it is forced to ascend, i.e., crossing the central mountain chain with an orientation between S-SW or N-NE, the ascending air reaches sufficiently high altitudes to trigger convection. An almost unidirectional flow was identified throughout the troposphere, and slight or strong veer with altitude. Furthermore, the vertical wind profile favoured different kinds of convection over the island, with shallow and deep structure.

Precipitation maximums over the highlands of the Madeira occurred under environments characterised by high Fr_w number (> 1), whereas at lowlands, precipitation maximums happened under low Fr_w values (< 0.5). In the first case, the flow is favoured to go above the island producing quasi-stationary and shallow convective systems over the central mountains (Situation 1), and the concentration of these cells on the windward was determined by the speed of the flow (Situation 2). When a deep layer of weak winds is identified above an intense low level flow, deep convective clouds exceeding the middle troposphere produce stationary and heavy precipitation over the island (Situation 3). Under these conditions, the maximums of accumulated precipitation occur above 1000 m height over the central peaks, or more concentrated to southern/northern slopes. In the second case, when Madeira lies in an environment marked by low Fr_w number, a blocking effect is created at local scale, inducing the development of much localised quasi-stationary systems in the northern slope. Such environment produces maximums of precipitation in the coastal zone (Situation 4).

Moisture availability, jointly with the upward motion produced by local orography is crucial to trigger convection over the island. For example, high moisture content is necessary for dense orographic clouds to form, which will produce high amounts of liquid water. However, if the wind field is not favourable to create upward motion over the island and thus lift water vapour, a moist atmosphere does not result in cloud

development. For dense orographic clouds to form, these two elements must act together, if not, the orographic precipitation efficiency is reduced.

The study provides useful guidelines for interpreting the impact of different mesoscale environments that may trigger convection over the island inducing significant precipitation in Madeira. It is also concluded that large part of the precipitation was connected with orographic effects and, a minor quota is due to precipitating systems that moved quickly over the island. The simulations were very useful in representing both the cloud systems formed over the island and those initially formed over the ocean.

Essentially, the results show that the combination of airflow dynamics, moist content, and orography is the major mechanism that produces precipitation in different regions of the island. These factors together with the event duration act to define the regions of excessive precipitation. The schematic representation presented summarizes the differences (e.g., airflow configuration and convection structure) and similarities (e.g., orographic lifting) associated with the periods. Moreover, this can help understanding the main characteristics of favourable environments producing clouds and precipitation over the island.

Finally, the results may constitute helpful information to improve the forecast of significant precipitation events over the island, mainly by identification of similar situations. On the other hand, although the study provides useful results from the description of real case simulations linked to significant precipitation events, some points are underscored for future studies, which fall out of the scope of the current study. The analysis was unable to quantify the impact of the seeder-feeder mechanism in the precipitation enhancement over the island. Furthermore, the distinct environments inducing significant accumulated precipitation indicate that sensitivity tests through an idealized framework may be very useful for a better characterization of specific situations, in order to identify processes controlling the development of orographic precipitation over the island.

REFERENCES

Bonati S. 2014. Resilientscapes: Perception and Resilience to Reduce Vulnerability in the Island of Madeira. *Procedia Economics and Finance*. 18: 513-520. DOI: 10.1016/S2212-5671(14)00970-8.

Bonati S, Mendes MP. 2014. Building Participation to Reduce Vulnerability: How Can Local Educational Strategies Promote Global Resilience? A Case Study in Funchal – Madeira Island. *Procedia Economics and Finance*. 18: 165-172. DOI: 10.1016/S2212-5671(14)00927-7.

Bresson E, Ducrocq V, Nuissier O, Ricard D, de Saint-Aubin C. 2012. Idealized numerical simulations of quasi-stationary convective systems over the Northwestern Mediterranean complex terrain. *Quarterly Journal of the Royal Meteorological Society*. 138: 1751–1763. DOI: 10.1002/qj.1911.

Chen S-H, Lin Y-L, 2005a: Effects of moist Froude number and CAPE on a conditionally unstable flow over a mesoscale mountain ridge. *Journal of the Atmospheric Sciences*. 62: 331–350. DOI: http://dx.doi.org/10.1175/JAS-3380.1.

Chen S-H, Lin Y-L, 2005b: Orographic effects on a conditionally unstable flow over an idealized three-dimensional mesoscale mountain. *Meteorology and Atmospheric Physics*. 88: 1-21. DOI: 10.1007/s00703-003-0047-6.

Chu CM, Lin Y-L, 2000: Effects of orography on the generation and propagation of mesoscale convective systems in a two-dimensional conditionally unstable flow. *Journal of the Atmospheric Sciences*. 57: 3817–3837. DOI: http://dx.doi.org/10.1175/1520-0469(2001)057<3817:EOOOTG>2.0.CO;2.

Cohuet JB, Romero R, Homar V, Ducrocq V, Ramis C. 2011. Initiation of a severe thunderstorm over the Mediterranean Sea. *Atmospheric Research*. 100: 603-620. DOI: http://dx.doi.org/10.1016/j.atmosres.2010.11.002.

Couto FT, Salgado R, Costa MJ. 2012. Analysis of intense rainfall events on Madeira Island during the 2009/2010 winter. *Natural Hazards and Earth System Sciences*. 12: 2225-2240. DOI: 10.5194/nhess-12-2225-2012.

Couto FT, Salgado R, Costa MJ, Prior V. 2015. Precipitation in the Madeira Island over a 10-year period and the meridional water vapour transport during the winter seasons. *International Journal of Climatology*. 35: 3748-3759. DOI: 10.1002/joc.4243.

Couto FT, Ducrocq V, Salgado R, Costa MJ. 2016. Numerical simulations of significant orographic precipitation in Madeira Island. *Atmospheric Research*. 169: 102-112. DOI: 10.1016/j.atmosres.2015.10.002.

Dasari HP, Salgado R. 2015. Numerical modelling of heavy rainfall event over Madeira Island in Portugal: sensitivity to different micro physical processes. *Meteorological Applications*. 22: 113-127. DOI: 10.1002/met.1375.

Ducrocq V, Nuissier O, Ricard D, Lebeaupin C, Thouvenin T. 2008. A numerical study of three catastrophic precipitating events over southern France. II: Mesoscale triggering and stationary factors. *Quarterly Journal of the Royal Meteorological Society*. 134: 131-145. DOI: 10.1002/qj.199.

Driver J. 1838. Letters from Madeira in 1834: with an appendix, illustrative of the history of the island, climate, wines, and other information up to the year 1838. By John Driver, London: Longman & Co. Liverpool; J. F. Cannell, Castle street. Available on 22 March 2016: http://purl.pt/17099.

Fernandes JP, Guiomar N, Gil A. 2015. Strategies for conservation planning and management of terrestrial ecosystems in small islands (exemplified for the Macaronesian islands). *Environmental Science & Policy*. 51: 1-22. DOI: 10.1016/j.envsci.2015.03.006.

Fragoso M, Trigo RM, Pinto JG, Lopes S, Lopes A, Ulbrich S, Magro C. 2012. The 20 February 2010 Madeira flash-floods: synoptic analysis and extreme rainfall assessment. *Natural Hazards and Earth System Sciences*. 12: 715-730. DOI: 10.5194/nhess-12-715-2012.

Houze RA Jr. 2012. Orographic effects on precipitating clouds. *Reviews of Geophysics*. 50: RG1001. DOI: 10.1029/2011RG000365.

Lafore JP, Stein J, Asencio N, Bougeault P, Ducrocq V, Duron J, Fischer C, Héreil P, Mascart P, Masson V, Pinty JP, Redelsperger JL, Richard E, Vilà-Guerau de Arellano J. 1998. The Meso-NH Atmospheric Simulation System. Part I: adiabatic formulation and control simulations. *Annales Geophysicae*. 16: 90-109. DOI: 10.1007/s00585-997-0090-6.

Levizzani V, Laviola S, Cattani E, Costa MJ. 2013. Extreme precipitation on the Island of Madeira on 20 February 2010 as seen by satellite passive microwave sounders. *European Journal of Remote Sensing*. 46: 475-489. DOI: 10.5721/EuJRS20134628.

Lira C, Lousada M, Falcão AP, Gonçalves AB, Heleno S, Matias M, Pereira MJ, Pina P, Sousa AJ, Oliveira R, Almeida AB. 2013. The 20 February 2010 Madeira Island flash-floods: VHR satellite imagery processing in support of landslide inventory and sediment budget assessment. *Natural Hazards and Earth System Sciences*. 13: 709-719. DOI: 10.5194/nhess-13-709-2013.

Luna T, Rocha A, Carvalho AC, Ferreira JA, Sousa J. 2011. Modelling the extreme precipitation event over Madeira Island on 20 February 2010. *Natural Hazards and Earth System Sciences*. 11: 2437-2452. DOI: 10.5194/nhess-11-2437-2011.

Miglietta MM, Rotunno R, 2009: Numerical simulations of conditionally unstable flows over a ridge. *Journal of the Atmospheric Sciences*. 66: 1865–1885. DOI: 10.1175/2009JAS2902.1.

Miglietta MM, Rotunno R, 2010: Numerical simulations of low-CAPE flows over a mountain ridge. *Journal of the Atmospheric Sciences*. 67: 2391–2401. DOI: 10.1175/2010JAS3378.1.

Miglietta MM, Rotunno R, 2012: Application of theory to observed cases of orographically forced convective rainfall. *Monthly Weather Review*. 140: 3039–3053. DOI:10.1175/MWR-D-11-00253.1.

Miglietta MM, Rotunno R, 2014: Numerical Simulations of Sheared Conditionally Unstable Flows over a Mountain Ridge. *Journal of the Atmospheric Sciences*. 71: 1747–1762. DOI: http://dx.doi.org/10.1175/JAS-D-13-0297.1.

Nuissier O, Ducrocq V, Ricard D, Lebeaupin C, Anquetin S. 2008. A numerical study of three catastrophic precipitating events over Southern France. I: Numerical framework and synoptic ingredients. Qua*rterly Journal of the Royal Meteorological Society*. 134: 111–130. DOI: 10.1002/qj. 200.

Prada S, Figueira C, Aguiar N, Cruz JV. 2015. Stable isotopes in rain and cloud water in Madeira: contribution for the hydrogeologic framework of a volcanic island. *Environmental Earth Sciences*. 73: 2733-2747. DOI: 10.1007/s12665-014-3270-1.

Pujol O, Lascaux F, Georgis JF. 2011. Kinematics and microphysics of MAP-IOP3 event from radar observations and Meso-NH simulations. *Atmospheric Research*. 101: 124-142. DOI: http://dx.doi.org/10.1016/j.atmosres.2011.02.004.

CHAPTER 5 – BRIEF NOTES ON THE WEATHER FORECAST OF HPE IN MADEIRA

5.1 MERIDIONAL WATER VAPOUR TRANSPORT

Among the conclusions of the studies gathered in this thesis, there are some useful findings for the operational forecast of heavy precipitation events in Madeira. For example, the satellite data may support the monitoring of water vapour transport over the Atlantic Ocean. From an operational point of view, this information may help the forecast of HPE in Madeira. As discussed in Chapter 2, the meridional transport of water vapour is easily identified from satellite data, becoming possible its identification over the ocean several hours before it reaches the island.

Taking as example the event on February 20, 2010, Figure 5.1 shows a sequence of satellite image from 16 to 21 February 2010. Four days before the HPE event, on February 16 (Figure 5.1a) a high amount of precipitable water with values greater than 40 kg/m^2 is visible over the Caribbean region. In the next day (Figure 5.1b), precipitable water above 60 kg/m^2 and already configuring a long and narrow band is located in the western part of the Subtropical Atlantic Ocean.
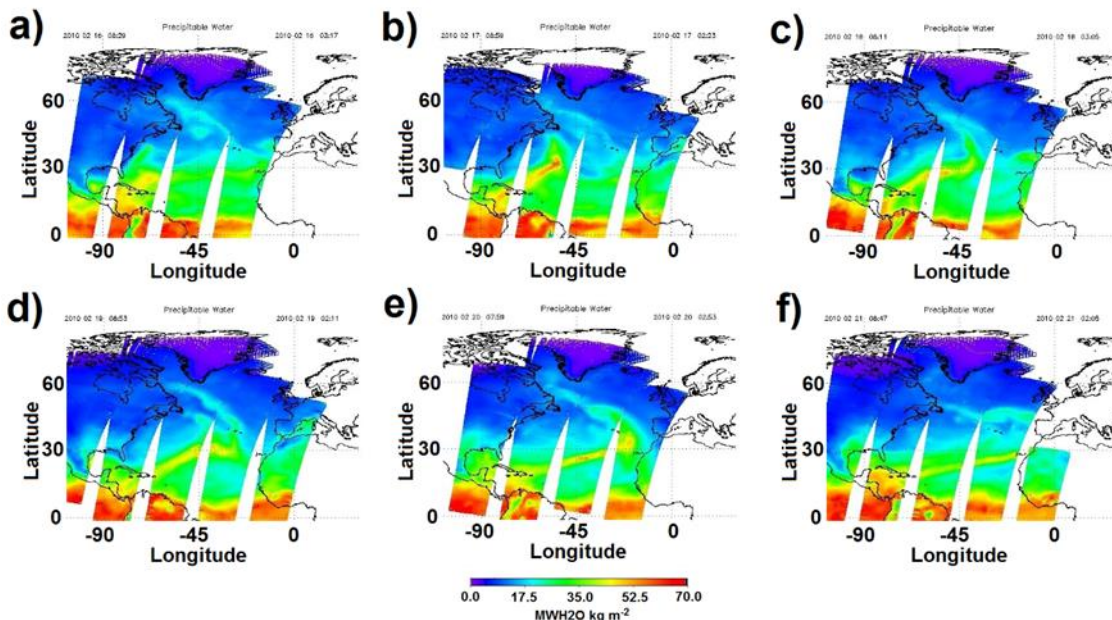
Figure 5.1 *Aqua-AIRS satellite images of precipitable water vapour on a) 16 FEB 2010 – 08:29 UTC; b) 17 FEB 2010 – 08:59 UTC; c) 18 FEB 2010 – 08:11 UTC; d) 19 FEB 2010 – 08:53 UTC; e) 20 FEB 2010 – 07:59 UTC; and f) 21 FEB 2010 – 08:47 UTC.*

The transport reaches a latitude of 30°N and becomes more meridional in the following days (Figures 5.1c-d). On 20 February (Figure 5.1e), the atmospheric river is easily identified over the North Atlantic Ocean. The Madeira is directly affected by its passage, which maintains the filamentary structure with a southwest-northeast orientation. On 21 February (Figure 5.1f), the atmospheric river does not affects the Madeira, reaching the Canary Islands located southeast of the Madeira's archipelago. In short, the image sequence show that the high amount of moisture linked to the atmospheric river could be identified over the Atlantic a few days before February 20, 2010.

The meridional water vapour transport is also successfully represented by the ECMWF analysis for the precipitable water vapour field. Figure 5.2 displays the evolution of the field for the same period considered in Figure 5.1, showing high amount of tropical moisture transported to the east of the North Atlantic Ocean by the atmospheric river.
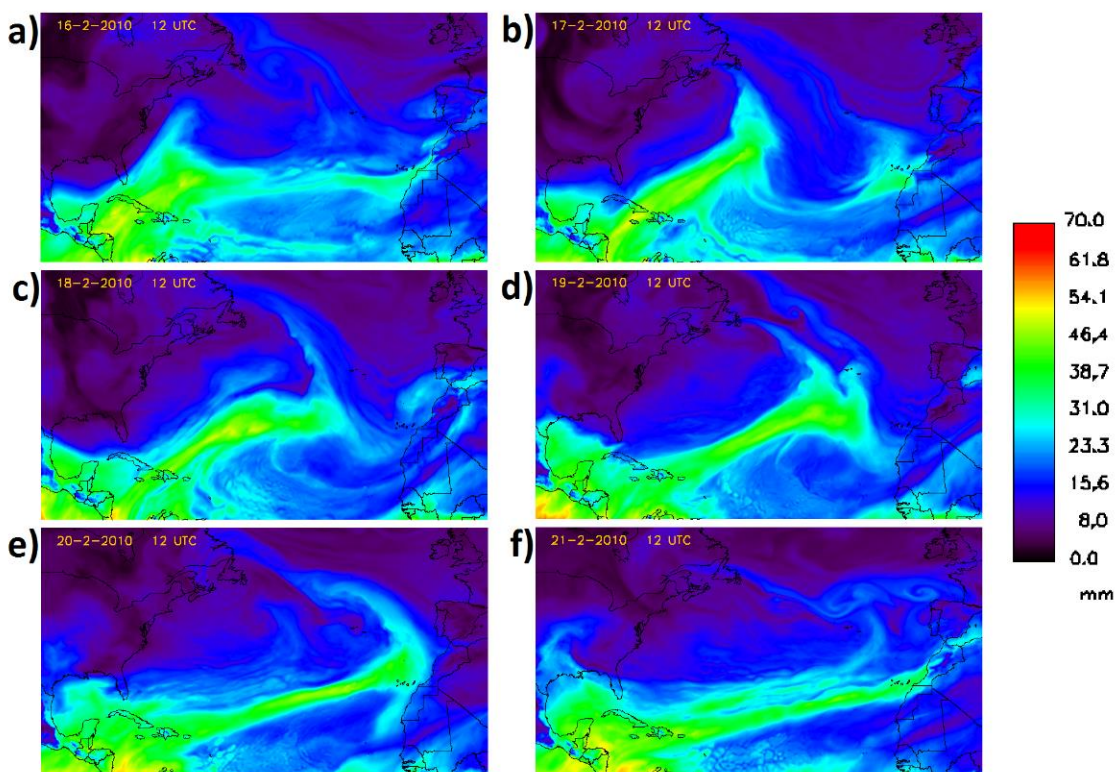
Figure 5.2 *Precipitable water vapour field for the ECMWF Analysis (unit: mm) at 1200 UTC. a) 16 FEB 2010; b) 17 FEB 2010; c) 18 FEB 2010; d) 19 FEB 2010; e) 20 FEB 2010; and f) 21 FEB 2010.*

In summary, during the passage of this structure over the island, the local orography was the main factor converting the high atmospheric water content into rain, and inducing the extreme precipitation, which was enough to trigger flash floods and landslides in many spots on the southern region.

5.2 LOCAL EFFECTS

In this part, the local effects for the accumulated precipitation over the island is highlighted, and supported by an operational forecast model. Hitherto, most of the studies about precipitation over Madeira have been concentrated in case studies using high resolution numerical models. Some of these, also showed the performance of these models in forecast mode (e.g., Couto et al., 2012; Dasari and Salgado, 2015). In Chapter 3, it was shown maximums of accumulated precipitation occurring above 1000 m height over the central peaks, or more concentrated to southern/northern slopes, as well as in the north-eastern coastal plain below 1000 m. Here, the precipitation events showed in Figure 3.2bcd are considered, aiming to verify if they are captured by the current operational model responsible for the precipitation forecast over the island. Besides the spatial distribution of the precipitation, another important question associated with precipitation forecast is related to the amount of precipitation given by the model, i.e., the Quantitative Precipitation Forecast (QPF). However, the detailed analysis about the performance of the model falls out of the scope of the current study.

The Application of Research to Operations at Mesoscale (AROME) model (Seity et al., 2011) at 2.5 km resolution is currently operational at the Portuguese Sea and Atmosphere Institute, IPMA. For the Madeira domain, it is running twice per day, at 0000 UTC and 1200 UTC. The results for the two run starting before each accumulated precipitation period are shown in Figure 5.3.

For the first situation (Figure 5.3ab), the model well represents the orographic effect in the 33 hour accumulated precipitation for the run started at 1200 UTC on 21 October 2012 (Figure 5.3a). The same characteristic is predicted by the run started at 0000 UTC on 22 October 2012, however, the precipitation amount is higher and more coherent with the results obtained by the MESO-NH at 2.5 km resolution showed in Chapter 3 (see Figure 3.5ab), with rainfall maximums above 100 mm over the central mountains.
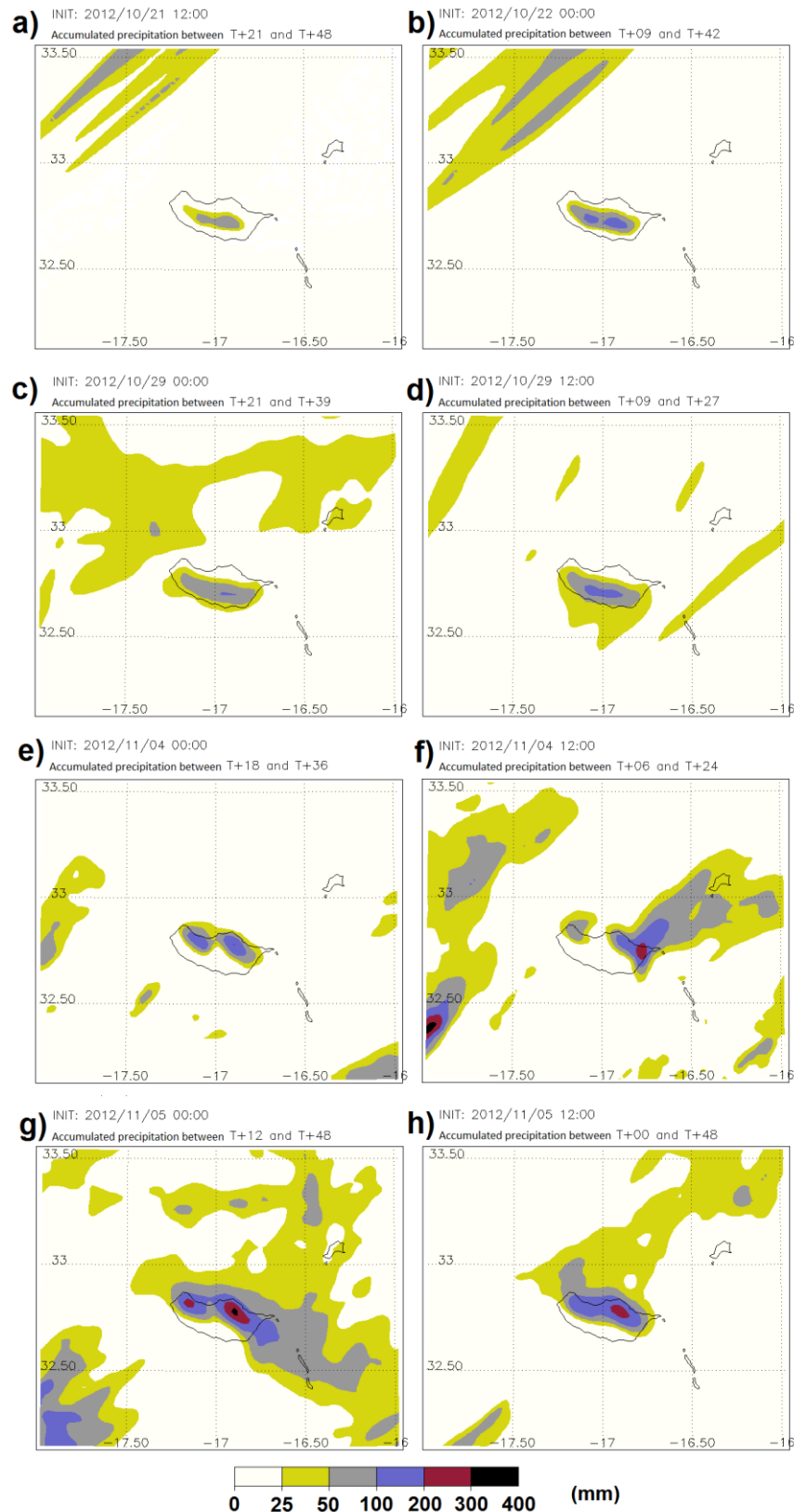
Figure 5.3 *Accumulated precipitation from AROME model at 2.5km resolution. For each situation, the two run before each accumulated precipitation period are considered, starting at 0000 UTC or 1200 UTC.*

In the second situation, the AROME also captures the orographic precipitation concentrating over the southern slope (Figure 5.3cd), and in higher amount for the run started at 1200 UTC (Figure 5.3d). However, in this case, the two AROME forecasts underestimate the precipitation amount, since the maximum accumulated precipitation recorded at Areeiro station was almost 300 mm on 30 October 2012 (see Figure 3.2a). It should be noted that this is a short precipitation event (lesser than 18 hours), in opposition to the first case, when the accumulated precipitation was recorded in 33 hours.

The third period was characterised essentially by localised precipitation at some regions over the northern slope (see Figure 3.2d – PHASE I). However, in some occasions convective systems initially formed over the ocean reach the island along the period. For the run starting at 0000 UTC on 04 November 2012 (Figure 5.3e), the orographic effect in the establishment of the rainfall maximums is clear, and well captured by the model. The maximums of accumulated precipitation between 100 and 200 mm are coherent with the values simulated by the MESO-NH (see Figure 3.5gh). In the second run, started at 1200 UTC on 04 November 2012 (Figure 5.3f), the maximums of orographic precipitation are not easily identified, and a large precipitation region with significant precipitation is simulated extending over the ocean, probably associated with the convective systems.

The last precipitation event considered had a duration of 54 hours, with more intense precipitation in the early hours of November 06 (see Figure 3.2d – PHASE II). Since the AROME model is run operationally only up to 48 hours, none of the runs can encompass the entire period, however, the runs started at 0000 UTC and at 1200 UTC on 05 November 2012 were considered. For the run started at 0000 UTC 05 November 2012 (Figure 5.3g), the 36 hours accumulated precipitation period evidences the orographic effect, with the rainfall maximums occurring over the northern slope. Significant precipitation was also predicted to occur over the ocean to south-eastward. For the run started at 1200 UTC (Figure 5.3h), the accumulated precipitation for 48 hours showed results more consistent with the results obtained from the MESO-NH (Figure 3.5jkl), with precipitation extending over the ocean northward. Since the different time period used for the accumulated precipitation with the AROME, the precipitation amount is not quantitatively compared with the results found in Chapter 3.

For all the four events, the orographic effect in the spatial distribution of the accumulated precipitation was well captured by the AROME. This result is coherent with

those from the MESO-NH model, i.e., maximums of accumulated precipitation occurring over the central mountains or in the southern/northern slopes. From this brief and subjective analysis, it can be concluded that, at least for the heavy precipitation events studied here, when the precipitation was controlled by the local orography, the AROME was able to reproduce satisfactorily the regions of significant accumulated precipitation in a short-range forecast. On the other hand, a more detailed analysis of the AROME performance is suggested for future works, also considering other situations.

REFERENCES

Couto FT, Salgado R, Costa MJ. 2012. Analysis of intense rainfall events on Madeira Island during the 2009/2010 winter. *Natural Hazards and Earth System Sciences*. **12**: 2225-2240. DOI: 10.5194/nhess-12-2225-2012.

Dasari HP, Salgado R. 2015. Numerical modelling of heavy rainfall event over Madeira Island in Portugal: sensitivity to different micro physical processes. *Meteorological Applications*. **22**: 113-127. DOI: 10.1002/met.1375.

Seity Y, Brosseau P, Malardel S, Hello G, Bénard P, Bouttier F, Lac C, Masson V. 2011: The AROME France convective-scale operational model. *Monthly Weather Review*. **139**: 976–991. DOI: 10.1175/2010MWR3425.1.

CHAPTER 6 – CONCLUSIONS

6.1 CONCLUSIONS

In the first part of the study (Chapter 2), the main aspects associated with precipitation on the highlands of Madeira over a 10 year period were analysed. At the same time, the features related to the meridional water vapour transport from the atmospheric rivers affecting the island, and their impact on the precipitation recorded in Madeira during 10 winter periods were presented, concluding that:

- ➤ The summers are generally dry, while the highest accumulated precipitation are recorded mainly during the winter, although some significant events may occur in the spring and autumn.

- ➤ The 2009-2010 winter was the wettest season during the study period, and the wettest autumn was in 2012, both showing seasonal accumulated precipitation over 2000 mm, higher than the seasonal average.

- ➤ Although most atmospheric rivers (ARs) reach the island in a stage of dissipation, showing low precipitable water vapour values, some are strong enough to reach Madeira, configured as filamentary structures presenting a large amount of precipitable water vapour. Two main types of AR were observed carrying a significant amount of water vapour to the island from the tropics. These two types were classified as narrow corridors, Type 1 (and according to their orientation over the island they were sub-classified as Type 1a, 1b, and 1c), and Type 2, reminiscent of warm conveyor belt structures. The source region of high amounts of precipitable water vapour was identified as being the Caribbean Sea region (Type 1), and the central part of the Tropical Atlantic (Type 2).

- ➤ From a comparison of daily accumulated precipitation measurements and the presence of atmospheric rivers over the island, it is clear that the larger the amount of water vapour transported by atmospheric rivers, the greater the likelihood of the occurrence of intense to extreme precipitation events over the island.

- ➤ In the 2009-2010 winter, moisture transport over Madeira associated with atmospheric rivers was more intense and frequent, and was of crucial importance for the occurrence of significant precipitation over the island, as concluded in a previous study (Couto et al., 2012). However, the high frequency and intensity of

this transport affecting the precipitation in Madeira was not observed when 10 winter seasons were considered, between 2002 and 2012.

Therefore, the first part of this study shows that atmospheric rivers, when associated with large amounts of precipitable water vapour over the island of Madeira may provide favourable conditions for the development of precipitation, and are sometimes associated with high levels of rainfall. However, they are not the sole factor affecting the intense precipitation events in Madeira.

In the second part (Chapter 3), a set of eight numerical simulations for all significant rainfall periods in the Madeira during the autumn 2012 were presented and evaluated for two different horizontal resolutions over large domain. The conclusions are summarized below.

➢ The MESO-NH model was able to represent the ambient conditions near the island, and the main structure of the different cloudy weather systems over the surrounding ocean, and that for four distinct synoptic situations.

➢ The model has successfully captured the strong impact of the local mountains in the distribution and volume of the rainfall over the Madeira at 2.5 km and 0.5 km horizontal resolutions. The simulations using 0.5 km grid spacing showed more realistic results when compared with the observations.

➢ It was possible to identify different rainfall patterns, showing significant precipitation occurring in distinct regions over the island. The accumulated precipitation can concentrate above and below a height of 1000 m. In the first case (above 1000 m), rainfall was observed in three regions, southern slopes, central peaks, and northern slopes, while in the second case (below 1000 m), localised precipitation occurred mainly in the NE coastal plain.

In general, the significant precipitation during the autumn 2012 was strongly related to the local orography, embedded or not within an extra-tropical weather system.

Concerning the results presented in Chapter 4, the same set of numerical simulations was used to investigate in detail four different rainfall patterns identified in Chapter 3 and the following points are highlighted:

➢ The variation of the ambient flow (direction and intensity) is the first factor that determines the distinct rainfall patterns over Madeira. Considering the situations

studied, when a moist and conditionally unstable flow affects the island in such manner that it is forced to ascend, the ascending air reaches sufficiently high altitudes to trigger convection. It was identified an almost unidirectional flow throughout the troposphere, and slight or strong veer with altitude. Furthermore, the vertical wind profile favoured different kinds of convection over the island, with shallow and deep structure.

➢ Precipitation maximums over the highlands of the Madeira occurred under environments characterised by high Fr_w number (> 1), whereas at lowlands, precipitation maximums happened under low Fr_w values (< 0.5). In the first case, the flow is favoured to go above the island producing quasi-stationary and shallow convective systems over the central mountains (Situation 1), or on the windward region (Situation 2), depending on the speed of the flow. In situations characterized by the existence of a deep layer of weak winds above an intense low level flow, deep convection is favoured and the clouds, whose tops exceed the middle troposphere, produce stationary and heavy precipitation over the island (Situation 3). Under these conditions, the maximums of accumulated precipitation may occur above 1000 m height over the central peaks, or more concentrated to southern/northern slopes. In the second case, when Madeira lies in an environment marked by low Fr_w number, a blocking effect is created at local scale, inducing the development of much localised quasi-stationary systems in the northern slope. Such environment produces maximums of precipitation in the coastal zone (Situation 4).

➢ Moisture availability, jointly with the upward motion produced by local orography is crucial to trigger convection over the island. However, if the wind field is not favourable to create upward motion over the island and thus lift water vapour, a moist atmosphere does not result in cloud development. For dense orographic clouds to form, these two elements must act together, if not, the orographic precipitation efficiency is reduced.

➢ Large part of the precipitation was connected with orographic effects and, a minor quota is due to precipitating systems that moved quickly over the island.

Essentially, Chapter 4 shows that the combination of airflow dynamics, moist content, and orography is the major mechanism that produces precipitation in different regions of the island. These factors together with the event duration act to define the

regions of excessive precipitation. Finally, the Chapter 5 briefly presented two useful points for the operational sector, regarding the meridional water vapour transport, and local effects in the accumulated precipitation over the island. The latter was supported by simulations with the AROME model, the current operational model responsible for the precipitation forecast over the island.

6.2 SUGGESTIONS FOR FUTURE WORKS

In accordance with the results found in this study, it is suggested that an objective analysis of the atmospheric rivers structures should be made using an automatic method, as well as detailed case studies. Concerning the numerical modelling, the MESO-NH model provided useful results linked to significant precipitation events in Madeira. Furthermore, the distinct environments inducing significant accumulated precipitation indicate that idealised studies may be very useful for a better characterization of specific situations, in order to identify processes controlling the development of orographic precipitation over the island. Finally, it is recommended for future studies a better discussion about these results in an operational context, in order to improve the predictability of HPE in Madeira island.

REFERENCE

Couto FT, Salgado R, Costa MJ. 2012. Analysis of intense rainfall events on Madeira Island during the 2009/2010 winter. *Natural Hazards and Earth System Sciences*. **12**: 2225-2240. DOI: 10.5194/nhess-12-2225-2012.